Norwegian University
of Life Sciences

Master's Thesis 2024   30 ECTS
Faculty of Science and Technology

Load Shifting Potential of Local Energy Communities with Seasonal Thermal Energy Storage

Lastflyttingspotensialet til lokale energisamfunn med

termisk sesonglagring

Lill Mari Engan
Environmental Physics and Renewable Energy

PREFACE

This Master's thesis marks the end of my degree in Environmental Physics and Renewable Energy at the Norwegian University of Life Sciences, NMBU. These years have given me an interest in and insight into challenges the power system will need to overcome in order to ensure security of supply in the future.

I would like to thank my supervisor, Heidi S. Nygård, for great feedback on multiple drafts, and thorough discussions along the way.

Finally, I would like to thank my partner, Håvard R. Krogstie, for great discussions, proofreading, and support throughout this semester, and my sister, Hilde Kristine Engan, for proofreading the final draft.

Ås, Norway 11 May 2024

Lill Mari Engan

ABSTRACT

One of the most efficient initiatives for reaching Norway's 2030 emission reduction targets is electrification. This electrification will increase the need for power transmission capacity, which in turn will require grid reinforcements in several areas. Grid reinforcements are time-consuming, costly, and often involve nature encroachments. The electricity grid must have sufficient transmission capacity to cover peak power demand, even if the demand is significantly lower most of the time. The capacity demand in Norway has high seasonal variations, as space heating during winter makes up a large share of residential power consumption. This means that there is a lot of unused capacity in the summer. The principle behind a seasonal thermal energy storage (STES) is to store surplus energy from the summer as thermal energy, and use it to meet thermal demand during winter. This thesis investigates how a community with a STES system can reduce the seasonal variation in its grid use, to see if STES systems can contribute to a more socioeconomically efficient development of the grid in the future. This is investigated through a linear optimization model representing a community with 100 households, and by using the results from the optimization model as an aggregated load in a reference distribution grid. The community can invest in a STES and a photovoltaic (PV) system, and aim to minimize grid rent, electricity cost, and investment costs. The result is compared to two reference cases, one of which can only invest in PV, and uses panel ovens, while the other may also invest in individual heat pumps. The model of the community with a STES showed a somewhat lower capacity demand and installed a larger PV system than the community with heat pumps. Even though the STES case installed more PV, the peak export of surplus power was lower, which indicates that having a STES system can make it easier to increase local energy production in a grid friendly manner. When the load profile of the three cases was added to the reference grid, the STES case increased the grid's peak load the least, even though the total yearly load was about the same as in the heat pump case. This means that the grid's transmission capacity was used more efficiently. A 2030-scenario, with greater seasonal variations in electricity prices, and a separate export tariff was also implemented. In this scenario, the STES was used to cover more of the community's thermal demand, which decreased peak import and seasonal variations further. A larger share of the local energy production was also used locally, which lowers the risk of voltage violations elsewhere in the grid. The results indicate that STES can become a useful tool to enable more socioeconomically efficient grid development, especially in grids with limited transmission capacity.

SAMMENDRAG

Et av de mest effektive tiltakene Norge kan gjøre for å nå klimamålene inn mot 2030, er elektrifisering. Denne elektrifiseringen krever at strømnettet tåler den økte belastningen, og den største begrensningen i mange deler av strømnettet vil være at overføringskapasiteten er for lav. Øking av overføringskapasiteten krever utbedring av strømnettet, noe som krever tid, penger og naturinngrep. Nettet må tåle timene med høyest kapasitetsbehov, kjent som nettets topplast, selv om kapasitetsbehovet er betraktelig lavere store deler av året. Norge har store sesongvariasjoner i kapasitetsbehov, som i stor grad skyldes at elektrisitet brukes til romoppvarming om vinteren, og fører til at nettet er overdimensjonert for kapasitetsbehovet på sommeren. Hovedprinsippet bak et termisk sesonglager er å lagre overskuddsenergi fra sommeren i form av varme, for å dekke termisk behov om vinteren. Denne oppgaven undersøker i hvor stor grad et nabolag med et termisk sesonglager kan redusere sesongvariasjonen i forbruket sitt, og om bruk av termiske sesonglager dermed kan bidra til en mer samfunnsøkonomisk utbygging av nettet i framtiden. Dette undersøkes gjennom å representere et nabolag på 100 husstander med en lineær optimeringmodell, og ved å bruke resultatene fra optimeringsmodellen som last i et referansenett. Nabolaget kan investere i et termisk sesonglager og solceller for å minimere årlige kostnader knyttet til nettleie, strøm og investeringer. Resultatene sammenlignes med to referansecaser, hvor den ene kun kan investere i solceller, og bruker panelovner til oppvarming, mens den andre også kan investere i private varmepumper. Modellen av et nabolag med termisk sesonglagring hadde et noe lavere kapasitetsbehov i forhold til et nabolag med individuelle varmepumper. I tillegg ble det installert flere solceller i nabolaget med sesonglagring enn i nabolaget med kun varmepumper. Likevel hadde førstnevnte lavere toppeksport, som tyder på at et termisk sesonglager kan gjøre det enklere å utnytte lokal energiproduksjon på en nettvennlig måte. Når lastprofilen til de ulike casene ble satt inn i referansenettet, bidro nabolaget med det termiske sesonglageret minst til nettets totale topplast, selv om det totale energibehovet gjennom året var omtrent like stort. Det betyr at nettets overføringskapasitet ble bedre utnyttet. Et 2030-scenario, med større sesongvariasjoner i strømpris, samt en separat eksporttariff, ble også implementert. I dette scenariet ble sesonglageret brukt mer, som reduserte topplast og sesongvariasjon ytterligere. En større andel av den lokale energiproduksjonen ble også brukt lokalt, som senker risikoen for spenningsproblemer andre steder i nettet. Resultatene tyder på at bruk av termisk sesonglagring kan være et nyttig verktøy for samfunnsøkonomisk utvikling av strømnettet, spesielt der tilgjengelig overføringskapasitet er begrenset.

CONTENTS

FIGURES

TABLES

Abbreviations

BTES	Borehole thermal energy storage
COP	Coefficient of performance
DSO	Distribution system operator
HP	Heat pump
NVE	The Norwegian Water Resources and Energy Directorate
PV	Photovoltaic
RME	The Norwegian Energy Regulatory Authority
STES	Seasonal thermal energy storage
TSO	Transmission system operator

Symbols

r_h	Electric-thermal-demand-ratio of a load profile in hour h [1]
L_h^{el}	Electric demand in hour h [kWh/h]
L_h^{DHW}	Domestic hot water demand in hour h [kWh/h]
L_h^{th}	Thermal demand in hour h [kWh/h]
EAC	Equivalent annual cost [€/year]
I	Investment cost [€]
r	Interest rate [%]
n	Lifetime of a given asset [years]
Q_h	Thermal energy supplied to hot reservoir [J]
Q_c	Thermal energy taken from the cold reservoir [J]
E_{el}	Electric energy used to transport thermal energy from cold reservoir to hot reservoir [J]

Sets

$h \in [1, \ldots, H]$	Hours
$n \in [1, \ldots, N]$	Consumers in the community

Parameters

$D_{n,h}^{el}$	Electric demand of consumer n at hour h [kWh]
$D_{n,h}^{th}$	Thermal demand of consumer n at hour h [kWh]
g_h	PV generation per installed capacity at hour h [kWh/kW$_p$]
vnt	Volumetric grid tariff [€/kWh]
snt	Volumetric grid tariff for selling surplus power [€/kWh]
cnt	Capacity based grid tariff [€/kWh]
cnt_i	Capacity based grid tariff for individual peak [€/kW$_{peak}$]
cnt_{agg}	Capacity based grid tariff for aggregated peak [€/kW$_{peak}$]
tax	Electricity tax [€/kWh]
λ_h^{SP}	Electricity spot price for hour h [€/kWh]
I_a^{PV}	Annualized capacity specific PV investment cost [€/kW$_p$]
I_a^{HP}	Annualized capacity specific heat pump investment cost [€/kW$_{\text{th}}$]
$I_a^{\text{STES,c}}$	Annualized capacity specific STES investment cost [€/kWh]
$I_a^{\text{STES,b}}$	Annualized base cost of STES investment cost [€]
$I_{\text{STES, a}}^{\text{HP}}$	Annualized capacity specific cost of STES pumps [€/kW$_p$]
η^{STES}	The fraction of heat retained from one hour to the next [1]
T^{max}	Maximum operating temperature of the STES [°C]
T^{min}	Minimum operating temperature of the STES [°C]
δT^{max}	Maximum temperature increase/decrease per hour [°C]
T^{water}	Temperature of the water used to charge the STES [°C]
T^{BASE}	Temperature of the ground surrounding the STES [°C]
c_v	Volumetric heat capacity of the ground [kWh/m^{3}K]
η^{Δ}	STES charging efficiency [1]
η^{∇}	STES discharge efficiency [1]
COP^{HP}	COP of STES heat pump [1]
COP^{∇}	COP of STES discharging pump [1]
$H_{\text{m,start}}$	First hour of month m [1]
$H_{\text{m,end}}$	Last hour of month m [1]

Variables

C^{tot}	Total annual cost of the community [€]
C^{SP}	Total annual electricity cost of the community [€]
C^V	Total annual volumetric grid cost of the community [€]
C^C	Sum of monthly capacity grid cost of the community [€]

C^T	Total annual electricity tax cost of the community [€]
C^{PV}	Annualized cost of the community's total PV investment [€]
C^{HP_i}	Annualized total cost of individual heat pump investments [€]
C^{STES}	Annualized cost of the community's STES investment [€]
c_n^{PV}	Installed PV capacity of consumer n [kW$_p$]
c_n^{HP}	Installed heat pump capacity of consumer n [kW]
$P_{n,m}^{\mathrm{max,i}}$	Monthly peak of consumer n in month m [kWh/h]
$P_{\mathrm{imp,\ m}}^{\mathrm{max,\ agg}}$	Aggregated monthly import peak of the community in month m [kWh/h]
$P_{\mathrm{exp,\ m}}^{\mathrm{max,\ agg}}$	Aggregated monthly export peak of the community in month m [kWh/h]
$c_{\mathrm{STES}}^{\mathrm{HP}}$	Capacity of STES pumps [kW]
$Q_{n,h}^{J}$	Electricity used for / heat produced by joule heating of consumer n at hour h [kWh]
$Q_{n,h}^{\mathrm{HP}_i}$	Thermal energy from the house heat pump to consumer n at hour h [kWh]
$d_{n,h}^{\mathrm{HP}_i}$	Electricity used to run the house heat pumps of consumer n at hour h [kWh]
$d_{n,h}^{\mathrm{STES}}$	Electricity used to run the STES pumps coming from consumer n at hour h [kWh]
$imp_{n,h}$	Energy imported from the power market to consumer n at hour h [kWh]
$exp_{n,h}$	Energy exported to the power market from consumer n at hour h [kWh]
$Q_{n,h}^{\mathrm{STES}}$	Thermal energy from STES supplied to consumer n at hour h [kWh]
$Q_h^{\mathrm{HP}_{\mathrm{dir}}}$	Energy from STES heat pump going directly to district heating loop at hour h [kWh]
$Q_h^{\mathrm{HP}_{\mathrm{s}}}$	Total energy delivered by the STES heat pump at hour h [kWh]
Δ_h	Charging of STES at hour h [kWh]
∇_h	Discharging of STES at hour h [kWh]
SOC_h	State of charge of STES at the end of hour h [kWh]
V	Volume of STES [m^3]
T_h	Mean temperature of STES at hour h [°C]

ONE

INTRODUCTION

1.1 Background

Norway has ambitious climate goals for the reduction of global greenhouse gas emissions, through national and international commitments. Some of these goals have already been achieved, such as the goal of reducing emissions by 30% compared to Norway's 1990 emissions by 2020 [1]. However, these commitments have mostly been achieved through the purchase of carbon credits from other countries, and participation in the EU Emissions Trading System. Although Norway has met its international climate obligations so far, national emissions were only reduced by 4.7% from 1990 to 2021 [2]. In 2022, Norway updated its Climate Change Act, and committed to a 55% reduction in national greenhouse gas emissions by 2030, compared to 1990 levels. The reduction must be obtained through national emission cuts, and can not be compensated for through the purchase of carbon credits. By 2050, Norway has committed to becoming completely carbon-neutral [3].

Electrification has been identified as the single most important initiative for reaching the 2030 emission reduction targets, by the Norwegian Environment Agency. In their report "Klimakur 2030", electrification is estimated to make up 34% of Norway's potential for emission reduction [4]. Electrification refers to the phasing out of fossil fuels in transportation and industry, in favor of electrically powered vehicles, machines, and heating. This increases the total demand for electric energy, as well as increasing peak power transmission in the electricity grid.

Every component in the electricity grid has a maximum power transmission capacity, limiting the peak power that can be delivered at any given time. New consumers can not be connected unless the grid has sufficient capacity. However, increasing these limits, through grid enhancements, is costly and time-consuming. In recent years, the number of requests for electric capacity has been increasing, to enable the electrification of existing, and development of new, industry [5]. Limited grid capacity slows this process, and several regions have long queues [6]. Grid operators are expecting to invest between 10% to 37% more into grid reinforcement and development in the period 2021-2030, compared to the previous

decade [5].

An alternative to grid expansion is to implement methods for reducing consumers' peak power demands, which in turn can reduce the needed transmission capacity. One method of reducing power demand is through the installation of local energy production systems. The main source of local energy production in many countries is solar energy. Photovoltaic (PV) systems have seen an increase in popularity as investment costs have decreased substantially. From 2010 to 2020, the average cost of a residential PV system decreased by 64% [7]. PV systems have the added benefit of being easy to install on rooftops and façades, making small scale PV systems suitable for residential buildings. During sunny periods, local production can cover parts of the prosumer's[1] demand, which reduces the needed power import. In periods of high production and low demand, the prosumer can also sell surplus solar energy to the power market [8].

However, the intermittent nature of solar irradiation makes PV generation difficult to control, which often leads to a mismatch between production and demand. The production-demand-mismatch can be especially challenging in high latitude countries, such as Norway [9]. Cold winters lead to high demand when solar irradiation is at its lowest, and high production in the summer when demand is low. This not only means that solar energy is poorly suited for reducing peak demands, additional problems can occur when surplus production is fed to the power grid, which may lead to voltage violations. In other words, seasonal weather variations work against increasing local energy production and consumption, and instead imposes new challenges [10].

These challenges can potentially be mitigated by storing excess solar energy produced in the summer, for use in the winter. Batteries can store electric energy for long periods of time, but would be prohibitively expensive to implement on the scale required to cover a significant part of winter demand [11]. An alternative to batteries is storing thermal energy. The average Norwegian household uses about two thirds of its yearly electricity consumption for space heating [2], and peaks in electricity demand occur on cold winter days. The introduction of seasonal thermal energy storage allows surplus energy from the summer to supplement electric space heating in the winter, lowering the peak electricity demand [5].

The Norwegian Climate Change Committee emphasizes that measures to reduce electricity demands are necessary, and that seasonal thermal energy storage technologies can help to reach this goal [12]. In a capacity constrained power grid, the introduction of seasonal thermal energy storage may reduce peak electricity demand in winter. If this is the case, grid enhancements may be deferred, enabling a more socioeconomically efficient use of existing power grid infrastructure.

1.2   Motivation

Since the 1970s, different thermal energy storage technologies have been conceptualized and developed. In the 70s, research focused on short-term thermal energy storage, also known as diurnal storage [13]. Shortly after, increasing attention was

---

[1]A prosumer is defined as a grid consumer that also produces energy locally [8]

given to long-term storage technologies, known as seasonal thermal energy storage (STES). By the beginning of the 21st century, several thermal energy storage systems were in operation in Germany, the Netherlands, Sweden, and Denmark [14].

A review of existing systems conducted in 1998 concluded that solar energy could cover 50-70% of the annual thermal demand of communities that used seasonal storage systems. For comparison, communities with diurnal systems would only have 10-20% of their thermal demand covered, due to seasonal variation in solar irradiation [15]. Seasonal storage solutions are especially useful in high latitude regions, where the seasonal variation is greater [9].

This highlights the potential of STES to increase the use of renewable solar energy. However, challenges surrounding high heat losses and economic feasibility have been a barrier. For the last decades, research has therefore mainly focused on addressing these issues through choice of materials and insulation, intelligent system controllers and the development of simulation tools for optimizing designs [16].

Several technologies, mainly based on sensible heat storage, are now at the point of commercialization [14]. Despite this, few studies have investigated the potential benefits STES can have on the electric power system. In a 2020 report by DNV on energy storage for power system flexibility, only short term thermal energy storage is mentioned [17]. The potential STES has for load shifting and deferral of grid enhancements has seen little research.

One exception is a case study conducted by Kauko et al., who found that the implementation of a STES resulted in a peak load reduction of 31% in a neighborhood in Oslo, Norway. The paper suggests that the impact widespread use of STES can have on grid enhancement savings should be analyzed further [18]. In addition, Lyden et al. analyzed how the use of STES in smart energy systems can be used for electrical network balancing [19]. Both papers argue that comprehensive studies on the synergy between the power system and STES should be conducted to find optimal solutions for meeting climate goals.

1.3 Research question and scope

The aim of this thesis is to investigate the load shifting potential of an energy community with a STES system, and evaluate the socioeconomic utility from an electric power grid perspective. The socioeconomic utility will be evaluated based on reducing the need for grid reinforcements and reducing yearly line losses, when developing residential communities.

To investigate this, the thesis will consider the following research questions:

1. Will the inclusion of a STES be valuable to the distribution grid through enabling load shifting?

2. Does the inclusion of a STES in a residential community increase the use of local energy production, which in turn reduces line losses?

3. How will alternative grid tariff models affect the utility of installing a STES?

To answer these questions, a model consisting of a linear optimization model and power flow analysis in a reference distribution grid has been developed. The optimization model represents a synthetic community in Oslo, Norway. The community consists of 100 households, where each household is represented by a real load profile. The load profiles consist of one year of hourly electric and thermal demand, that will be covered by a combination of a power grid, local PV production, and STES. The objective of the optimization model is to minimize the yearly costs of the community by determining how much it will invest into PV systems and STES.

The optimization model results in an aggregated load profile of the community's net power import, as seen by the surrounding distribution grid. The load profile will be connected to CINELDI's reference distribution grid to study peak loads and transmission losses for the entire system. The results will be compared to two identical communities without the option of investing in a STES, where one has the option of investing in individual heat pumps and the other one has to use joule heating to cover thermal demand.

A 2030-scenario has also been developed to explore how a different grid tariff model influences the optimization model's investments and operation of the STES.

1.4   Model limitations

The optimization model has a single objective, which is to minimize the total costs among all households in the community. It ignores how the costs are divided among them, and assumes perfect collaboration between the households. In a real world scenario, it is more likely that each household would attempt to minimize its own costs, without considering how neighbors' costs could be minimized.

The model will not attempt to calculate how much grid reinforcement costs are reduced by using a STES, as the need for reinforcements, and the associated costs, depend on a multitude of factors, such as available capacity, voltage levels, and the load profiles of all connected consumers. The aim of this thesis is instead to give a general idea of the load shifting potential of local energy production. This knowledge can be used to evaluate the potential socioeconomic benefits of future STES projects, on a case by case basis.

Another limitation is the modeling of the STES. The model uses a borehole storage system, with generalized parameters and simplified operation. In the real world, each STES system needs to consider the exact conditions in the area, such as how well the ground conducts heat. In addition, losses in the system will be affected by the temperature gradient within and outside the STES. In the simplified model, there is no temperature gradient. In the model, a single value represents the average temperature, and losses are calculated as a fixed ratio.

THEORY

2.1   The Norwegian power system

The electric power system refers to all infrastructure involved in the production, transportation, and consumption of electric energy. Electricity is produced continuously at power plants, such as hydroelectric plants and windmill parks, and the total production has to match the simultaneous consumption at all times in order to maintain balance. Consumers are often located far away from the production sites, making an electricity grid necessary to transport the electric energy from producers to consumers [5]. Figure 2.1 shows the main components of the power system: production, transportation and consumption. The rest of this section will cover the different components of the electricity grid in more detail.
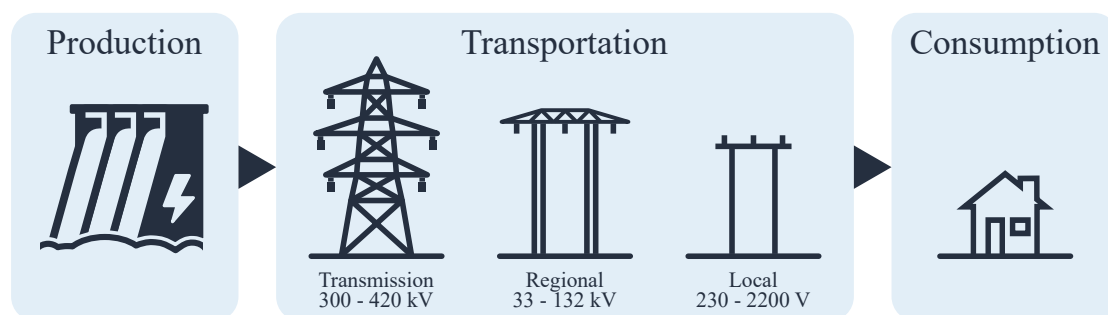
Figure 2.1: Overview over the main components of the electric power system: production, transportation, and consumption.

2.1.1   The electricity grid

The electricity grid is responsible for transporting electric energy from producers to consumers. It is divided into three levels: the transmission grid, the regional distribution grid, and the local distribution grid. The electricity grid is categorized by its nominal voltage level, and transformers are used to step the voltage up and down between different levels.

The transmission grid has the highest voltage level, with a nominal voltage level of 300 kV or 420 kV. It is used to transport large amounts of power across different regions. Large power plants are usually connected directly to the transmission grid [5].

The regional distribution grid usually operates with voltages ranging from 33 kV to 132 kV. Medium-sized power plants and energy-intensive industries, such as concrete manufacturing, are usually connected to this grid level. Like the name implies, regional distribution grids transport power within a region [5].

The local distribution grid, with voltage levels between 230 V and 22 kV, is the lowest level of the electricity grid. Consumers in residential and commercial buildings, as well as less energy-intensive industries, are connected to this level [5].

2.1.2 Regulatory and operational roles

The electricity grid is operated by one transmission system operator (TSO) and many distribution system operators (DSOs). They are responsible for maintaining the security of electricity supply in their operating region [20].

The TSO in Norway is Statnett SF, who owns and operates the national transmission grid. One of their most important roles is to provide frequency stability by balancing simultaneous production and consumption at all times. They are also responsible for the operational security of the transmission grid [21].

The regional and local distribution grid is operated by different DSOs. Each region of the distribution grid is owned by one DSO, giving them a natural monopoly in that area. Consumers pay grid rent to their local DSO to get access to the distribution grid. The DSO is responsible for making sure the consumers have reliable access to electricity, by operating, maintaining, and developing the electricity grid in their area. When faults occur, or the supply quality is unsatisfactory, they are required to take the necessary actions to rectify the issues [20, 5].

Since the electricity grid operators are natural monopolies, the TSO and DSOs are heavily regulated by national regulators. The Norwegian Energy Regulatory Authority (RME) is a unit within the Norwegian Water Resources and Energy Directorate (NVE), often referred to as NVE-RME. They are responsible for monitoring the TSO and DSOs, ensuring that consumers have access to electricity, supplied with adequate quality. RME also regulates how much DSOs can charge in grid rent, to ensure that the distribution grid development is socioeconomically efficient [5].

2.1.3 Grid investment outlook

The need for grid investments is expected to increase in the following years as a consequence of old infrastructure and electrification, which leads to higher capacity demands. The life expectancy of power lines is typically between 40 and 70 years, but depending on the strain it has been put under during operation, it can last longer or shorter. Seeing as most of the existing grid was built between 1950 and 1990, it is assumed that many lines will need to be renewed in the near future [5].

The power demand is also higher than when most of the existing electricity grid was built, and it is expected to keep increasing as a consequence of electrification. This means that on top of maintaining the existing grid, new infrastructure has to be built, and existing infrastructure must be upgraded to increase the transmission capacity. Grid development is, however, resource intensive in terms of time, money, and nature encroachments, which makes it lucrative to find ways of lowering the need for grid development. [5].

2.2 Grid capacity

Each power line and transformer in the electricity grid will have some transmission losses, that turn electric energy into heat. To avoid damage, each component has a rated maximum transmission capacity. To ensure security of supply in the event of disturbances, additional limitations are imposed on the maximum transmission capacity [21]. The aggregated power delivered to consumers through a given power line has to stay within the line's rated capacity. Transmission losses also cause voltage drops, which can lead to voltage quality issues for consumers [10]. It is the responsibility of the grid operators to rectify these issues, for example through grid reinforcement [5].

2.2.1 Seasonal load variations

Load profiles

Consumer demand varies throughout the day, and between seasons. The demand of residential consumers usually peaks in the morning, when most people wake up, make breakfast and shower. After regular working hours there is another peak due to consumers making dinner, showering and charging electric vehicles. The aggregated demand during these hours is significantly higher than during the middle of the day and at night [22]. The supplying power lines need to have a rated capacity higher than the aggregated peak power of the consumers, even though the demand is lower most of the time [5].

In addition, cold climate countries, like Norway, have higher power demands during winter. Cold days increase the space heating demand, and Norwegian households predominantly use electricity for space heating. This leads to an increase in the electricity demand in the winter [5]. The seasonal variation can be seen in Figure 2.2, which shows Norway's aggregated load profile from 2023. The difference is especially prominent for households that use joule heating.
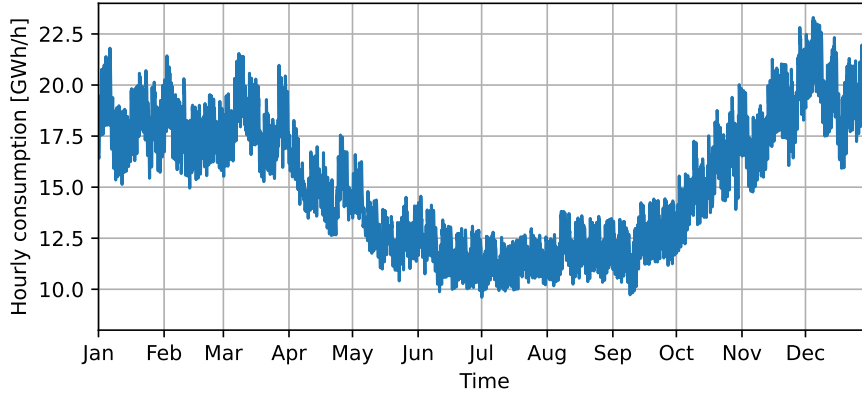
Figure 2.2: Norway's hourly load profile in 2023, based on data from Statnett [23].

Joule heating

Joule heating, also known as resistive heating, is the heat produced from running current through a resistor. This converts electric energy to thermal energy, and is the principle used by panel heaters [24]. It is the least efficient method of space heating, with a 1:1 ratio between supplied electric energy and delivered thermal energy, when ignoring losses. Use of joule heating contributes to the high seasonal variation that can be seen in Figure 2.2.

Heat pumps

An alternative to joule heating is heat pumps, that produce more thermal energy than the electric energy they consume [25]. Heat pumps work by using electric energy to transport thermal energy from a cold reservoir to a hot reservoir. The cold reservoir can be the air outside a house, and the warm reservoir can be the air inside the house. Since both reservoirs are air, this would be an air-air heat pump. Examples of other types of pumps are water-air, air-water, and water-water, where the first word describes the cold reservoir, and the second word describes the hot reservoir [26].

The total amount of thermal energy Q_h delivered to the hot reservoir is given by

$$Q_h = Q_c + E_{\text{el}}, \tag{2.1}$$

where Q_c is the amount of thermal energy taken from the cold reservoir, and E_{el} is the electric energy supplied for running the heat pump.

The heat pump's coefficient of performance (COP) describes the ratio between thermal energy delivered to the hot reservoir, and electric energy consumed by the heat pump, defined as

$$COP = \frac{Q_h}{E_{\text{el}}}. \tag{2.2}$$

Normal COP values for residential air-air heat pumps are $3 - 5$, which means that for each unit of electric energy consumed, $3 - 5$ times as much thermal energy is delivered [27]. Using heat pumps for space heating can therefore reduce the seasonal variation in electric demand. However, the COP of a heat pump is

dependent on the temperature of the cold reservoir, because more electric energy is required to deliver the same amount of thermal energy if the cold reservoir is colder [26]. This means that when it is cold outside, more electric energy is needed to deliver the same amount of thermal energy, than when it is warmer.

Load duration curves

Load profiles can also be represented as load duration curves, that show what proportion of time a given capacity is required. Figure 2.3 shows the duration curve of the load profile in Figure 2.2. The peak on the left-hand side indicates that the full capacity of the is rarely required. However, grid operators are required to maintain security of electricity supply. This involves having adequate transmission capacity, to meet the instantaneous power demand at all times. The grid therefore has to be dimensioned for peak demand, even if the demand usually is a lot lower. This means there will be unused capacity most of the time, such as in the summer [21].

For the specific load profile shown in Figure 2.3, it would be sufficient to have a transmission capacity of 20 GWh/h 90% of the time. However, due to the peak load, the electricity grid has to be dimensioned for at least 23 GWh/h.
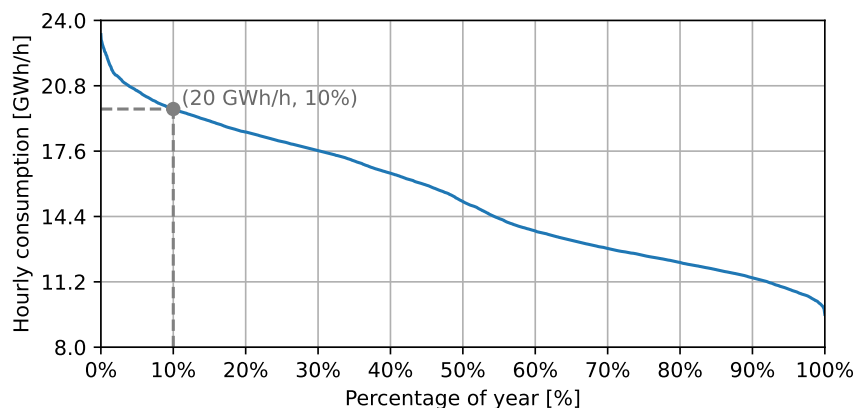
Figure 2.3: Norway's duration curve in 2023, based on data from Statnett [23].

2.2.2   Coincidence factor

Being able to estimate the aggregated peak load is fundamental for grid planning [28]. The aggregated peak in a given grid is usually lower than the sum of each consumer's individual peak, and the grid capacity is usually dimensioned accordingly. To estimate what the peak load will be after introducing a new consumer, the estimated coincidence factor of that consumer type can be used. The coincidence factor describes the load of a consumer at the time of the aggregated peak load of all consumers [28], and is defined as

$$\text{Coincidence factor} = \frac{\text{A consumer's load during the grid's peak load}}{\text{The consumer's individual peak load}}. \quad (2.3)$$

Having a low coincidence factor means that the consumer contributes little to the aggregated peak in a given part of the electricity grid. Having a coincidence factor

of 1 means the consumer's peak and the aggregated peak coincides. A study from 2018 found that the coincidence factor of apartment complexes usually is around 0.3 – 0.4 [10]. If a consumer can shift some of its load away from the aggregated peak load, the required grid capacity will be reduced.

2.2.3   Load shifting

Load shifting describes moving a load from a period of high demand to a period of low demand, thus evening out the load profile [29], as illustrated in Figure 2.4. Some loads can relatively easily be shifted to a period where there is more available grid capacity. Electric vehicles are one example of flexible load. The electric vehicle can be charged at any time, as long as it is sufficiently charged when the consumer wants to use it. This means that it can be charged during periods of low load, instead of when the consumer comes home from work, as long as the consumer can drive to work or other activities when needed. This way, the load of the electric vehicle is shifted from the afternoon peak described in Section 2.2.1, to off-peak periods, for example at night.

However, in Norway, predominantly electric heating means that the peak load is strongly correlated to the outside temperature [4]. Peak load therefore occurs during winter, while in the summer, when thermal demand is low, there is usually a lot of available capacity. If the consumer is able to reduce the electricity required for space heating in cold periods, it would reduce the consumer's contribution to the grid's peak load.
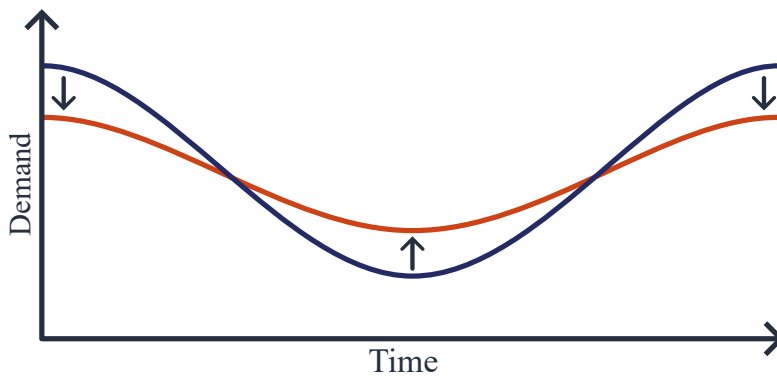
Figure 2.4: Illustration of load shifting. The original load (blue) has been shifted by moving some load from peak demand hours, to hours of lower demand (red).

2.3   Transition to decentralized power system

Traditionally, the electric power system has followed a hierarchical, centralized structure. Few, large power plants have delivered power to the transmission grid, that transports the power to the end-users, who are mostly connected to the distribution grid. The centralized model makes the power system relatively easy to operate, as the TSO can communicate with the power plants to coordinate power balancing. A large share of power production in Norway comes from controllable hydropower, allowing power production to be regulated according to demand [21].

The power system is currently transitioning to a more decentralized model, motivated by the transition to renewable energy sources, such as solar and wind power [30]. The new model requires several technological developments, such as communication channels between producers, consumers, and the DSO, as well as between DSOs and the TSO. Communication and various control mechanisms are necessary because the TSO is still responsible for balancing demand and production at all times. In a decentralized power system, the consumers are given a more active role, for example by offering load flexibility, or through local energy production [31].

2.3.1   Local energy production

Local energy production allows consumers to meet part of their own electric demand. If the system produces more electricity than the consumer needs, the surplus can be sent to the distribution grid, and imported by neighbors. This electricity travels a short distance, leading to low losses [31]. The distribution grid's feeder also needs to supply less electricity, as the demand for imported electricity has been reduced. If local energy production covers parts of the peak load, it also reduces the needed grid capacity, which in turn may lower the need for grid reinforcement over time.

A common and increasingly popular form of local energy production is residential PV systems [32]. The number of residential PV systems has seen an exponential growth the last few years. In 2023, the total installed PV capacity in Norway was doubled, from 300 MW_p the year prior, to 600 MW_p [33]. Advantages of local PV systems are that they require little land degradation, as they can be installed on rooftops and façades [34]. PV systems have also seen a price reduction [35], making them more lucrative, especially when electricity prices increase, like they did during the European energy crisis [36].

The intermittent nature of solar energy causes PV systems to have some disadvantages as well. PV production does not coincide with the peak demand in the Norwegian power system, as solar irradiation peaks in summer, while demand peaks in winter [34], as shown in Figure 2.5. This means that PV systems are unlikely to decrease the grid's peak usage. In addition, there may be periods of high production and low demand during the summer, where excess power will be delivered to the external grid. This can lead to power flow reversal, which can cause regional challenges like overvoltage [10].

To prevent overvoltage from occurring during sunny hours, PV curtailment can be used. Curtailment refers to cutting off production during periods with high surplus production, to prevent voltage issues. The cut-off limit can either be a hard limit, or dynamically set based on the current state of the power grid [39]. Curtailment would allow consumers to have larger PV systems without causing voltage violations, at the cost of decreasing the total amount of energy produced and sold to the power market. If overvoltage is expected to occur only a few hours every year, curtailment can be an effective countermeasure. Regulations do not allow DSOs to enforce prosumers to curtail, however, without entering special agreements with the prosumer [40].
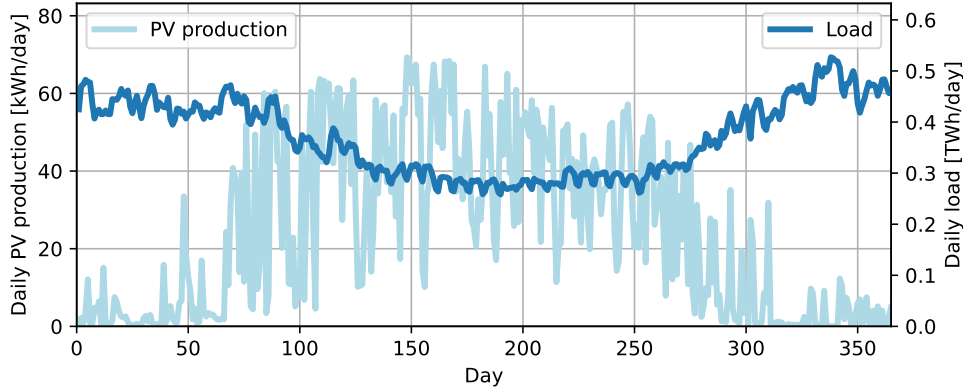
Figure 2.5: Example profiles showing daily load and PV production in Norway. The load profile (light blue) shows Norway's total consumption in 2023 [23], and the PV profile shows the simulated production of a 10 kW$_p$ PV system in Oslo, Norway [37, 38].

As an alternative to curtailment, local energy storage systems allow surplus production to be stored for later use, or exported at a later time, when the grid has more capacity, and the electricity price might be higher.

2.3.2 Local flexibility markets

Flexibility will become more important in a decentralized power system with more renewable energy sources. Today, Norway has mostly flexible production through hydropower, which makes it possible to preserve instantaneous balance between power production and consumption [21]. However, as more of the power production comes from intermittent energy sources, like solar and wind power, utilizing flexible loads will become important tools for aiding power balance, grid congestions, and peak reduction [41, 42].

In a decentralized power system, consumers may participate in local flexibility markets to ensure security of supply, and avoid unnecessary grid reinforcements. Consumers can offer flexibility by, for example, charging electric vehicles at a favorable time, or by avoiding simultaneous use of multiple electric appliances, such as dishwashers and washing machines. Consumers with local production can also have batteries, or other means of energy storage, to store surplus production, if feeding it to the distribution system would cause overvoltage. Flexibility markets allow customers to receive compensation for providing flexibility, which system operators can use [42].

Consumers could also get together and form aggregators, selling more flexibility by coordinating within the group, or purchasing shared energy storage systems. This can make it easier for consumers to participate, and for system operators to obtain enough flexibility to resolve grid issues. How future local flexibility markets should operate is still in the research stage, but the idea is to directly incentivize consumers to adjust both short- and long-term load and production through a market solution [42].

2.3.3 Energy sharing in Norway

On October 1st 2023, a regulatory framework for energy sharing was enacted in Norway. The framework allows consumers to share surplus energy production from a shared small scale power plant. This is done by connecting the power plant, for example a rooftop PV system, to its own power meter with its own meter ID, and informing the DSO about the arrangement. Each consumer gets a share of the plant, and the owners are free to decide what percentage share each consumer has. The plant can either be shared equally, or based on other factors, such as the investment cost or floor area of each consumer. The share of each consumer, combined with the power plant's hourly production, is used to adjust the consumers' electricity bills. The consumers are billed as if their share of the power plant was installed behind their own power meter. This reduces apparent imported power when the power plant is active, leading to a reduction in power market costs, taxes, and power grid fees [43].

Before the introduction of this framework, surplus power generated behind one power meter, could not be shared with consumers behind different power meters. The surplus would have to be sold to the power market, and bought back again by the other meter [44]. This round-trip would incur taxes and grid tariffs, despite the electricity itself not traveling any significant distance.

In order to qualify for the energy sharing arrangement, the involved consumers have to meet requirements on geography and capacity. Geographically, the consumers must be within the same municipality, and share cadastral and property unit numbers. The capacity criterion limits the installed capacity of the shared plant to 1000 kW_p. As a point of comparison, a residential rooftop PV system in Norway usually has an installed capacity in the order of 10 kW_p [43].

The stated goal of the energy sharing framework is to allow consumers in apartment buildings to invest in local power production to reduce their electricity bill, in the same way owners of freestanding houses can [44]. This can in turn increase the integration of distributed renewable energy production, giving more consumers access to their own locally produced electricity.

However, in a follow-up report on the framework, RME points out that the effect energy sharing has on operational cost are minimal. This is mainly due to the mismatch between solar production and the consumers' peak load, which usually occur in the summer and winter respectively. The consequence of this is that the energy sharing consumers will have the same capacity requirements as regular consumers. Some costs can be reduced due to lower line losses in the summer, but these savings are low compared to expenses related to grid capacity demand. The framework is thus unlikely to lower operational costs considerably [43].

2.3.4 Local energy communities

Local energy community is a term used to describe communities where participants share local energy production, coordinate local demands or share energy storage. The coordination may allow trading within the community, or participation in flexibility markets as an aggregated load [45]. The concept of energy communities is not well-defined, and may be organized differently depending on regulatory

frameworks, end-user engagement, and technological development [46]. In general, energy communities are legal entities where the citizens involved can share and manage their own energy production, storage, and consumption [47].

The current energy sharing framework is not comprehensive enough to enable local energy communities, as the consumers involved are not taking an active role in grid congestion management. For example, the current energy sharing framework does not allow local coordination through peer-to-peer trading. The participants have no incentive, and no means of collaborating, to reduce peaks in aggregated load. The advantage of full-blown local energy communities would be that consumers get the tools needed to coordinate local demands [48].

Different energy communities may have different goals, depending on the local energy and capacity situation. Some communities would aim to lower their over all energy consumption, while others would take capacity reduction initiatives. Most of the existing pilot projects in Norway, that come close to being full-blown local energy communities, focus on energy reduction, for example by installing local PV systems to become more self-sufficient. However, given that capacity limitations are expected to be the main cost drivers in the Norwegian power system, it would be more socioeconomic to have local energy communities that focus on capacity demand reduction initiatives [48].

2.4 Electricity prices and grid rent

This section will give a description of the three components of the electricity bill in Norway: retail electricity price, grid rent, and taxes, and discuss the aim of the new grid rent model. Table 2.1 gives an overview of the different components, after splitting the grid rent into volumetric and capacity based grid tariff.

Table 2.1: Overview of electricity bill components.

Component	Description
Retail electricity price	Variable cost paid per kWh to the electricity supplier based on spot price or a fixed cost.
Volumetric grid tariff	Variable cost paid per kWh to the DSO for transportation of the electricity used.
Capacity grid tariff (fixed tariff)	Fixed cost based on the peak capacity demand.
Public taxes	A set of public taxes paid per kWh

2.4.1 Retail electricity prices

The retail electricity price is the price a consumer pays for the electric energy they have used. The price is determined by the electricity supplier, either at a fixed rate, or based on an hourly spot price. Spot prices are calculated the day before, after the day-ahead market has closed. The hourly electricity price reflects the energy availability in that hour. Norway is divided into 5 price regions, and

spot prices can differ between them, depending on availability in each region. Regions with surplus can sell energy to other regions, but capacity constraints in the transmission network can create bottlenecks. This can cause large differences in spot prices between regions [49].

Traditionally, electricity prices have been relatively stable, because the main energy sources, such as hydropower in Norway, and fossil fuels in other parts of Europe, are controllable to a large extent. The transition to more renewable energy sources in Europe involves increased usage of uncontrollable energy production, such as solar and wind power. This is expected to lead to higher price variations, as it becomes harder to match production with demand [50].

Electricity prices in 2030

In 2030, it is expected that increased amount of solar power will be the driving force behind the price variations. Solar power leads to seasonal price variations, with low prices during the summer, when production is high, and high prices during the winter, when production is low. NVE expects the seasonal production, combined with seasonal variation in demand, to give price profiles with more seasonal variations, as the one in Figure 2.6, in 2030 [50].

Solar power has already led to negative electricity prices in Norway, and is expected to continue to do so in hours of high production, as more PV systems are installed. This also increases the price variations between daytime and nighttime. However, negative electricity prices have not been included in NVE's analysis [50].
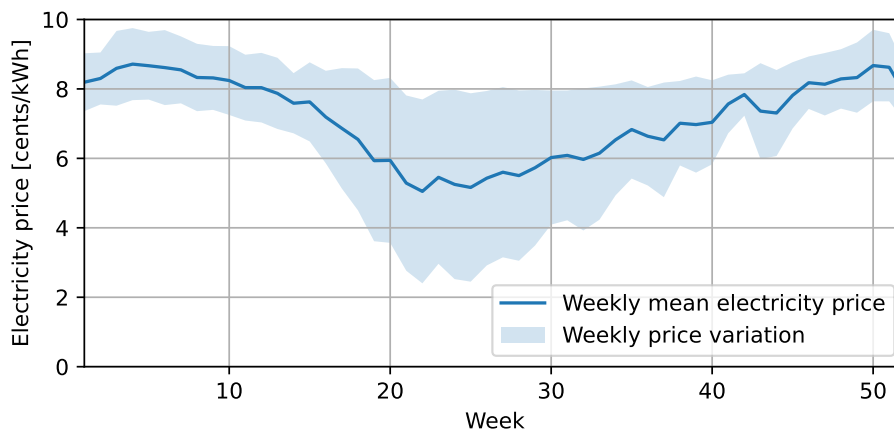
Figure 2.6: Mean weekly electricity prices in 2030 in Norway (dark blue), based on NVE's long term market analysis [50]. Variation within the week is represented by standard deviation (light blue)

2.4.2   Grid rent

Every house and commercial building connected to the distribution grid pays grid rent to the local DSO. It consists of two parts: the volumetric grid tariff, and the capacity grid tariff.

The volumetric grid tariff is the rent a consumer pays for each unit of energy transported to their meter. This means that energy produced behind the meter is ignored. The tariff is fixed, or has a fixed pattern, to incentivize load shifting to periods of low grid usage, such as during the night [51].

The consumer also pays for the grid capacity they use, which is the capacity grid tariff [51]. The DSOs have different pricing models, but a stepped model is common, and is used by Norway's largest DSO, Elvia [52]. Each step represents a capacity interval, such as 2 kWh/h — 5 kWh/h, and has an associated fixed monthly cost. Which step a consumer falls into each month is determined by calculating the average power demand in the three hours with the highest consumption each month. The hours must also be on three distinct days [52].

2.4.3   Public taxes

In addition to grid rent and electricity price, energy consumption is also taxed. The public taxes consist of three parts [52]:

- A value-added tax of 25%

- A statutory payment to Enova of 0.087 cents/kWh

- An electricity tax per kWh

2.4.4   Aim of new grid rent model

The new grid rent model, presented in Section 2.4.2, was introduced in July 2022. The old model had a fixed monthly grid tariff, independent of the consumer's grid use. In the new model, the fixed grid tariff is replaced by the capacity based tariff, that charges consumers with large spikes in demand more than consumers with steady energy consumption. The volumetric grid tariff was also changed to charge consumers more for using energy during hours of high demand, such as weekdays between 06:00 and 22:00. With the new model, the volumetric grid tariff should make up a smaller part of the total grid rent than previously, reflecting the fact that only 10% of grid costs are due to line losses [53].

The aim of the new grid rent model is to incentivize stable energy use, and reduce peak demand. Higher instantaneous demands lead to higher transmission losses, and increase the likelihood of needing grid reinforcements. This increases operational costs, which are covered by the grid rent. Evening out energy use reduces peaks, which means that unnecessary grid reinforcements can be avoided, thus reducing the grid rent. In the old model, a much larger share of the DSO's income came from the energy tariff, incentivizing energy reduction more than peak reduction [53].

Another aim of the new model is fairer distribution of costs between consumers. Consumers with high peaks, or high demand during peak hours, increase the need for grid reinforcements more than consumers who contribute less to the grid's capacity peaks. Since the DSO uses grid tariffs to cover grid investment expenses, the new model makes consumers who drive up the need for grid investments, pay a larger share of the costs [53].

2.5   Seasonal thermal energy storage

Seasonal thermal energy storage (STES) is an umbrella term for energy storage technologies designed to store thermal energy across seasons. Seasonal variations increase with latitude, making STES ideal for high latitude countries, such as Norway [15]. In these cold climate areas, a STES system can store solar energy produced in the summer, and deliver the energy as space heating during winter, thus helping to combat the seasonal mismatch in available solar energy and thermal demand.

Most existing STES systems use solar thermal collectors as their main energy source, but waste heat is also a popular alternative when it is available [14, 13]. Some storage systems use heat pumps driven by PV systems [54], or hybrid PV-/solar thermal systems [55].

STES technologies can be divided into three categories based on how energy is stored:

- **Sensible heat storage** stores energy by increasing the temperature of a storage medium, such as water or gravel.

- **Latent heat storage** stores latent energy by changing the phase of the storage medium from solid to liquid state, or from liquid to gas.

- **Thermochemical heat storage** stores energy through reversible endothermic chemical reactions.

The concepts are at different stages of maturity, with sensible heat storage being the only concept at the commercialization stage. Latent heat storage is currently at a stage of demonstration, while thermochemical heat storage is only at the research and development stage [14]. This thesis will take a closer look at sensible heat storage technologies, since these are the only ones that are considered market ready.

2.5.1   Sensible thermal energy storage

Compared to latent and thermochemical systems, sensible heat storage systems are based on simple and well understood technologies, and can be made from low-cost materials. However, they also have lower energy densities and higher heat losses than the other categories [14]. In order to keep losses at a minimum, the systems should be large-scale, as losses decrease with higher volume-to-surface ratio [11].

Sensible heat storage concepts can be divided into four subcategories, based on the vessel energy is stored in:

- **Pit thermal energy storage** is made by creating a pit in the ground, which can be insulated if necessary, and use water as the storage medium [56].

- **Aquifer thermal energy storage** stores energy in subsurface geological layers capable of holding on to a lot of water, called aquifers [56].

- **Tank thermal energy storage** is a large, insulated tank with water as the

storage medium. Small-scale tanks have commonly been used for short-time storage, and they can work as buffer storage when used in combination with any of the other technologies [14].

- **Borehole thermal energy storage** consists of long pipes, called borehole heat exchangers, buried in the ground. The ground surrounding the pipes works as storage medium and insulation [14].

Choice of technology is case specific, and depends on a number of factors. One determining factor is the geological characteristics of the area. The ground must be stable and have little to no groundwater flow to prevent further heat loss in order for either of these technologies to be suitable. Pit and tank have the fewest geological requirements, while aquifer requires the presence of a natural aquifer layer, and borehole requires drillable ground [14]. In return, both aquifer and borehole systems have lower capacity specific investment costs than pit and tank systems [57].

Borehole thermal energy storage seems to be the most suitable option for community-scale systems, based on experience from existing STES systems [58]. The reason for this is mainly that community-scale systems require large amounts of energy to be stored. Storing the energy directly into the ground, instead of building a finite storage vessel, has proven to be cost-efficient for systems of this size [58, 11]. Existing and planned STES projects in Norway have for the most part used borehole thermal energy storage [54, 59, 60]. Due to these factors, this thesis will be focusing on borehole thermal energy storage.

2.5.2 Borehole thermal energy storage

Technical description of system

A borehole thermal energy storage system (BTES) consists of an energy source, borehole heat exchangers, a district heating loop, and buffer tanks for short-term storage if needed [61], as shown in Figure 2.7. A working fluid is used to transport heat between the components through a set of loops, and pumps are used to transport the fluid around in the loops.
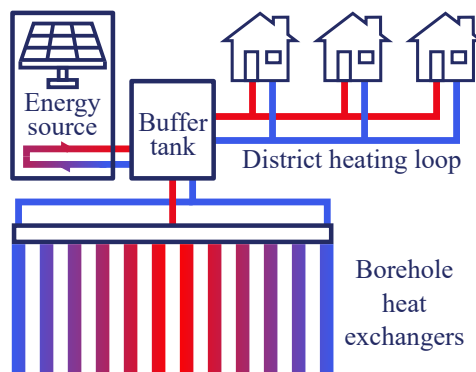

Figure 2.7: Overview of a general BTES system with a buffer tank.

In most cases, the energy source is either solar thermal collectors or waste heat, with solar collectors being the most common [14, 62]. If the energy source is a PV

system, the electric energy produced can be used to run a heat pump that delivers thermal energy to the working fluid [63].

To deliver energy to the storage, hot working fluid is run through borehole heat exchangers. The borehole heat exchangers are a set of pipes in boreholes drilled into the ground. When the working fluid is pumped through the pipes, it will exchange heat with the surrounding ground. It is the ground itself that works as the storage medium of the thermal energy, which means it has no defined boundary or isolation, but rather a gradual temperature gradient. Because there is no form of isolation, BTES has the highest heat losses among the sensible heat storage technologies [11].

A district heating loop is used to deliver thermal energy to the community, normally used for space heating. If the storage temperature is high enough, the working fluid can be used directly. Otherwise, a heat pump is used to increase the temperature of the working fluid before it enters the district heating loop [64].

Buffer tanks can be used to handle short-term peaks in thermal energy production or demand, as they have higher charging and discharging rates than borehole heat exchangers [57]. This can for example be useful on sunny days, if thermal energy is produced faster than the ground can absorb it. Excess heat can be stored in the buffer quickly, while slowly charging the BTES. A buffer tank can also be useful for reducing electricity use when satisfying short-term demand. This is done by running the pumps on low speed for a few hours in advance to charge the buffer tank from the BTES [65]. On the other hand, buffer tanks have a high investment cost [57], and may not be necessary if the system has sufficient pumping power, and electricity used for this purpose is not a concern.

System operation – charging and discharging

When there is a thermal demand in the community, the heat from the energy source can be delivered directly to the district heating loop. Otherwise, the energy can be used to charge the BTES. Heating the ground creates an underground temperature gradient, leading to heat loss. In order to minimize these losses, it is common practice to use cylindrical BTES arrays divided into concentric thermal zones. A set of boreholes heat exchangers are then connected in series, moving the working fluid from the center to the edge of the cylinder, as shown in Figure 2.8. This keeps the core at the highest temperature, with temperatures gradually decreasing towards the outermost zone. This design allows for better heat retainment [66].

The BTES is discharged by pumping colder working fluid through the borehole heat exchangers in the opposite direction. The fluid enters the outer boreholes first, and heats up as it moves towards the center, absorbing thermal energy from the storage medium. The hot working fluid can then be delivered to the district heating loop. Extracting heat in the opposite direction ensures that the core of the BTES remains the warmest zone [66].
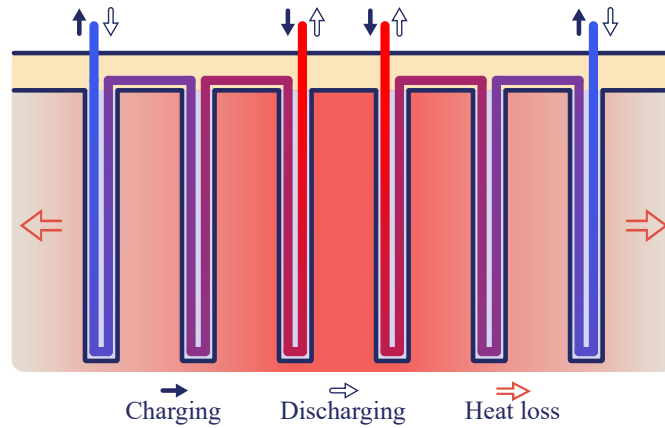
Figure 2.8: Cross-section of a borehole thermal energy storage system, showing borehole heat exchangers. The arrows indicate the direction the working fluid is pumped during charging and discharging.

Design considerations

The pipes are connected in a combination of series and in parallel, as shown in Figure 2.9. To optimize the heat injection rate of the system, a variety of geometric parameters should be optimized, such as the depth and spacing between the pipes. Other characteristics, such as the heat capacity and conductivity of the ground, will also determine the operational properties of the BTES. A BTES system also has an initial charging period that lasts 3 – 6 years, where heat losses as very high due to low ground temperatures and steep temperature gradients [13]. After some years of operation, the ground surrounding the BTES will stabilize at a higher temperature, and losses will decrease. The initial charging period must be considered when planning a BTES system.
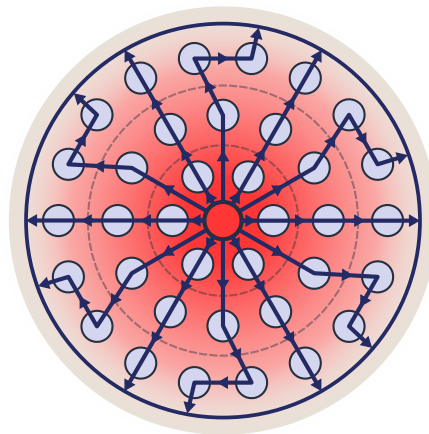
Figure 2.9: Example of how boreholes heat exchangers can be connected in a combination of series and parallel to minimize heat loss.

Thermodynamic properties will not be investigated further in this thesis, as the overall aim is to compare the strain a STES-based community will have on the distribution grid, compared to a community with no STES. Designing a system requires knowledge of the specific location to determine the type of system that should be used, what material will be best suited, and other design factors.

2.5.3   Seasonal thermal energy storage and the power grid

Implementing seasonal thermal energy storage systems may contribute to lowering the need for grid reinforcements. The different sensible storage systems, described in Section 2.5.1, can store large amounts of energy using relatively inexpensive materials, compared to batteries. This means that a system that has been charged during the summer can cover a large share of the thermal demand during winter, which shifts the load from winter to summer. Existing systems are usually designed to cover about 50% of the total thermal demand [62], with some systems aiming to supply 90% of annual thermal demands [54, 67]. This means the systems could decrease the seasonal variations of a community's electric demand significantly.

The storage systems can also be a way of implementing more renewable energy. The core idea of STES is to harvest and store surplus energy in the summer, and use it to cover thermal demands in the winter [62]. This means that the charging window is long, and that the charging pattern can be adapted to charge when energy is readily available, for example from a PV system on sunny days.

However, the systems need to be large to be efficient, as relative heat losses decrease with increased storage size. This means STES systems are best suited for larger communities, and existing STES projects usually supply energy to 100 households or more [13, 62]. Large communities, sharing a commodity like a STES, require some form of coordination, which is challenging without a suitable legal framework.

For the remainder of this thesis, BTES will be referred to as STES.

THREE

METHOD

3.1 Overview of cases

The aim of this thesis is to compare the grid impact of a new residential development, with and without a seasonal thermal energy storage system (STES). This will be done by simulating the yearly grid import of a residential community in three cases. In case 1, the community's thermal demand can only be met by joule heating. In case 2, households may invest in individual heat pumps, while case 3 makes the community invest in a shared STES. In all cases, the community may also invest in a shared PV system. A simplified overview of the cases is shown in Figure 3.1, and each case will be described in greater detail in Section 3.1.1.
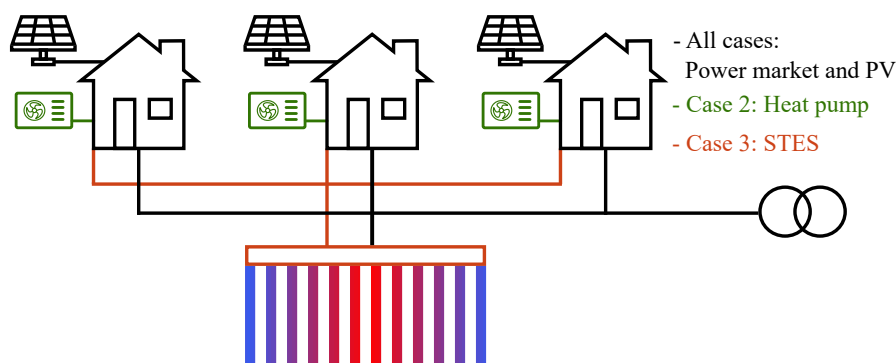
Figure 3.1: Overview of the three cases. All cases model the same community with 100 households. In case 1, they can only invest in a shared PV system, case 2 allows consumers to invest in individual heat pumps, and in case 3 they invest in a shared STES.

The community consists of 100 households with an hourly thermal and electric demand for the simulated year. The demand profiles are described in Section 3.3.1. The load profiles are identical across the three cases, only investment options differ. Given the investment options, energy demands, and hourly electricity prices, the model will optimize the community's collective investments and operation to minimize total costs. This results in an aggregated load profile for the entire

community, which will be connected to a reference distribution grid to study the community's effect on the distribution grid in each case.

The three cases will each be evaluated in two different scenarios. The first scenario, called the 2020-scenario, represents the current regulatory framework for energy sharing, with current day grid tariffs and power market prices. The second scenario uses a synthetic 2030 electricity price profile, and has a different regulatory framework for energy sharing. The 2030-scenario will be described in Section 3.1.2.

3.1.1 Case descriptions

Case 1

Case 1 represents traditional electric heating, with panel heaters being the only space heating source. This will be used as a reference, to evaluate the impact of STES against using only joule heating. The community is allowed to invest in a shared PV system, and the PV production is shared among the households according to the current energy sharing framework. Each household has a share of the PV system based on their individual investment cost.

Case 2

Case 2 is similar to case 1, except each household may now also invest in a heat pump to meet thermal demand more efficiently than using panel heaters alone. This case will be used to evaluate the STES compared to modern houses where heat pumps are common. Like in case 1, households may also invest in a share of the PV system.

Case 3

In case 3, the community forms a local energy community that invests in a shared STES. Like in case 1 and 2, households may invest in a share of the PV system. PV production can be used to cover consumer demand, or to charge the STES. The STES may also be charged by electricity purchased on the power market.

3.1.2 2030-scenario

In the 2030-scenario, an electricity price profile with greater seasonal variation is used. It is assumed that the current energy sharing framework has been developed in order to incentivize local consumption over export. In this thesis, the new framework introduces a separate capacity grid tariff for export, instead of having one capacity tariff that applies to both export and import, whichever is highest that month. Capacity based export tariffs have been identified as one way to mitigate problems that arise from distributed power export [68]. It should be noted that the aim of the 2030-scenario is only to investigate how the model responds to excess export being disincentivized, and not to recommend or find the best grid tariff model to reach that goal.

In addition, the community will pay for its aggregated import and export instead of paying individually. The capacity tariff is modified accordingly, so the community will pay the same as they would have otherwise, as long as the load profile remains unchanged. Calculation of the new capacity tariff is explained in Section 3.3.6.

3.2   Model

Investigation of the grid impact will be done by first using an optimization model to minimize the total costs of the community in the cases described above. This will result in an aggregated load profile for each case. The load profiles will then be added to CINELDI's reference distribution grid [69], where power flow analysis can be conducted, to compare the strain the different communities put on the grid. Figure 3.2 shows an overview of the input data, the model, and the produced outputs. The source code is available at [70].
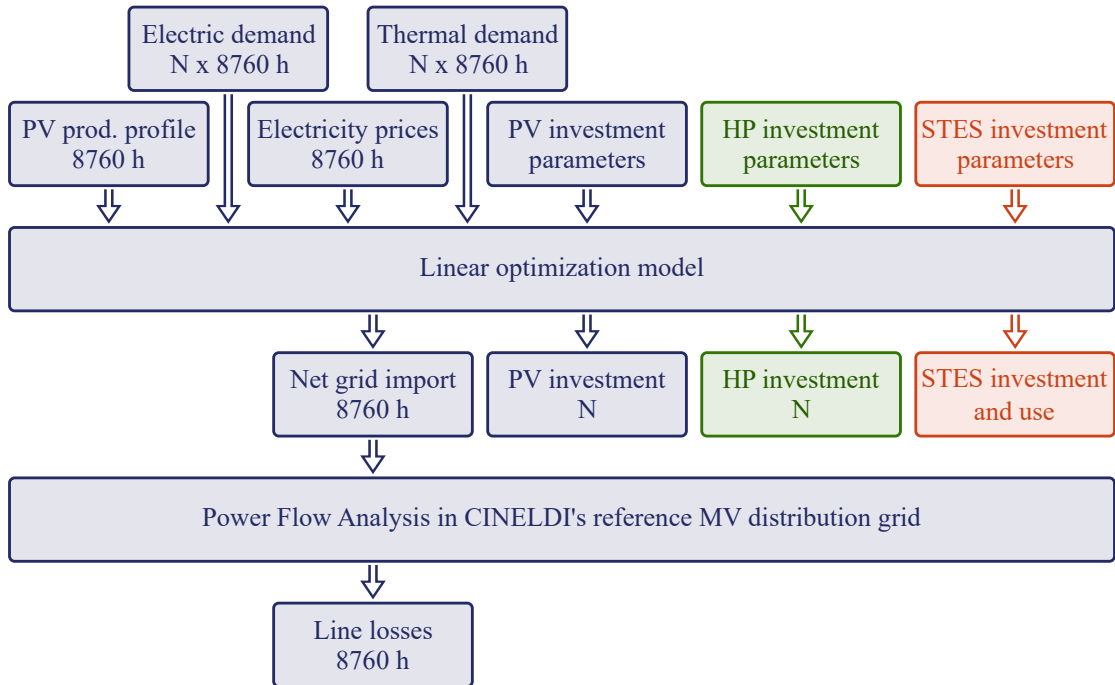
Figure 3.2: High level overview of the data passed into the linear optimization model, and the power flow analysis. N is the number of houses in the community, and 8760 is the number of hours per year. HP and STES are only included in case 2 and 3, respectively.

3.2.1   Architecture of optimization model

The electric and thermal demands of the community, the power market, local PV generation and the use of STES, are all modeled as a linear optimization problem. The problem consists of a set of variables, and a set of constraints on those variables. A solution is an assignment of each variable that satisfies all constraints. The objective function describes the utility of a given solution mathematically, and the solver attempts to find the solution maximizing this utility. In linear optimization, the objective function and constraints are all linear combinations of variables, and all variables are real numbers. Constant values that are known beforehand and used in the definition of the problem are known as parameters.

To create the linear optimization problem described below in a format suitable for a solver, the model was written as a python program, run in Python 3.11 [71]. The program defines the variables, the constraints and the objective function using Gurobi's Python API, gurobipy, version 11.0. To solve the linear optimization problem, the Gurobi solver version 11.0 was used [72].

Objective function

The goal of the community is to minimize its total annual cost, C^{tot}. The cost consists of electricity price, grid rent, and the annualized investment cost of PV, heat pumps, and STES. The community can invest in PV, heat pumps, and STES to lower the imported power, thus reducing electricity and grid rent cost. The STES can also be charged by imported grid power, which can be used to even out the seasonal load variations. For a description of all parameters and variables, see the nomenclature. The objective of the optimization model is to minimize the total costs of the community. The complete objective function is given as

$$Min : C^{\text{tot}} = C^{SP} + C^V + C^C + C^T + C^{\text{PV}} + C^{\text{HP}} + C^{\text{STES}}. \tag{3.1}$$

Equations (3.2) to (3.8) give a detailed description of the individual cost components.

C^{SP} is the community's total electricity cost, which is the sum of the net imported hourly power each hour h for each consumer n, multiplied by the hourly spot price λ_h^{SP}

$$C^{SP} = \sum_{n=1}^{N} \sum_{h=1}^{H} \lambda_h^{SP} \cdot (imp_{n,h} - exp_{n,h}). \tag{3.2}$$

It is assumed that each consumer in the community pays for electricity based on spot price, instead of a fixed cost.

The volumetric grid cost C^V is the sum of hourly imported power times the volumetric grid tariff vnt and the hourly exported power times the volumetric grid tariff for selling surplus power snt

$$C^V = \sum_{n=1}^{N} \sum_{h=1}^{H} (imp_{n,h} \cdot vnt + exp_{n,h} \cdot snt). \tag{3.3}$$

The capacity part of the grid tariff C^C is the capacity grid tariff cnt times the peak power import or export each month, and is given by

$$C^C = \sum_{n=1}^{N} \sum_{m=1}^{M} \left(cnt_i \cdot P_{n,m}^{max,i} + cnt_{agg} \cdot (P_{\text{m, imp}}^{\text{max, agg}} + P_{\text{m, exp}}^{\text{max, agg}}) \right). \tag{3.4}$$

Notice that there is one term for individual peak, and two for aggregated peak, one for import and one for export. In the 2020-scenario cnt_{agg} is set to 0, and in the 2030-scenario cnt_i is set to 0. Only the 2030-scenario incentivizes reducing peak import and peak export separately.

C^T is the electricity tax, and is applied to power imported from the power market

$$C^T = \sum_{n=1}^{N} \sum_{h=1}^{H} tax \cdot imp_{n,h}. \tag{3.5}$$

The only local energy production the community can invest in is a shared PV system. The PV investment cost C^{PV} is given by the capacity specific investment cost times the sum of each consumer's share of the installed PV capacity, and is given by

$$C^{PV} = I_a^{PV} \cdot \sum_{n=1}^{N} c_n^{PV}. \tag{3.6}$$

In case 2, the consumers can invest in individual heat pumps to meet parts of their thermal demand. The investment cost of the heat pumps C^{HP} is the sum of each consumer's installed heat pump capacity times the capacity specific heat pump cost:

$$C^{HP} = I_a^{HP} \cdot \sum_{n=1}^{N} c_n^{HP}. \tag{3.7}$$

The community will invest in a STES system in case 3. The total cost of the STES C^{STES} is the sum of the base cost, volume cost, and the cost of the STES heat pump, and is described as

$$C^{STES} = I_a^{\text{STES,V}} \cdot V + I_a^{\text{STES,b}} + I_{\text{STES,a}}^{\text{HP}} \cdot c_{\text{STES}}^{\text{HP}}. \tag{3.8}$$

The investment costs for PV, heat pumps, and STES are annualized.

Normally, the goal of consumers would be to minimize their individual cost. This would require solving a complementarity problem, where an equilibrium is found such that all consumers minimize their own cost. Optimizing such a model efficiently requires using Karush-Kuhn-Tucker (KKT) conditions. This would make the model more complex, and is outside the scope of this thesis. In this thesis, consumers are thought to cooperate to minimize the total cost. How the cost would be divided internally is also outside of scope. The simplified model used to solve this optimization problem is viewed as sufficient to investigate the impact STES systems can have on the electricity grid.

Decision variables

The decision variables in the objective function are either associated with power import and export, space heating sources, or investment in energy production, heat pumps, and STES. When STES is available, a set of variables describing the operation and state of the STES is also added. Table 3.1 describes each decision variable, and which cases the variable is relevant for. If nothing else is specified, the variable applies to both the 2020-scenario and the 2030-scenario.

All decision variables, except from the STES volume V, have a lower bound of 0.

Table 3.1: Decision variables for all cases

Symbol	Description	Cases
Grid		
$imp_{n,h}$	Energy imported from the power market to consumer n at hour h [kWh]	All
$exp_{n,h}$	Energy exported to the power market from consumer n at hour h [kWh]	All
$P_{n,m}^{\max,\mathrm{i}}$	Monthly peak of consumer n in month m [kWh/h]	All (2020)
$P_{\mathrm{m,\,imp}}^{\max,\,\mathrm{agg}}$	Aggregated monthly import peak of the community in month m [kWh/h]	All (2030)
$P_{\mathrm{m,\,exp}}^{\max,\,\mathrm{agg}}$	Aggregated monthly export peak of the community in month m [kWh/h]	All (2030)
Heating		
$Q_{n,h}^{J}$	Thermal energy from joule heating of consumer n at hour h [kWh]	All
$Q_{n,h}^{\mathrm{HP}_i}$	Thermal energy from the individual heat pump to consumer n at hour h [kWh]	Case 2
$Q_{n,h}^{\mathrm{STES}}$	Thermal energy from STES supplied to consumer n at hour h [kWh]	Case 3
Investment		
c_n^{PV}	Installed PV capacity of consumer n [kW$_p$]	All
$c_n^{\mathrm{HP}_i}$	Installed heat pump capacity of consumer n [kW]	Case 2
$c_{\mathrm{STES}}^{\mathrm{HP}}$	Installed capacity of STES heat pump [kW]	Case 3
V	Volume of STES [m^3]	Case 3
STES		
SOC_h	State of charge of STES at hour h [kWh]	Case 3
$d_{n,h}^{\mathrm{STES}}$	Electricity used to run the STES pumps coming from consumer n at hour h [kWh]	Case 3
$Q_h^{\mathrm{HP,\,STES}}$	Energy from heat pump to STES at hour h [kWh]	Case 3
Δ_h	Charging of STES at hour h [kWh]	Case 3
∇_h	Discharging of STES at hour h [kWh]	Case 3

Constraints

In order for the model to produce a feasible result, a set of constraints have to be implemented. This ensures that physical limitations are followed. An overview of the constraints used in the model will be given in this section, and Figure 3.3 gives a visual representation of the constraints related to energy.
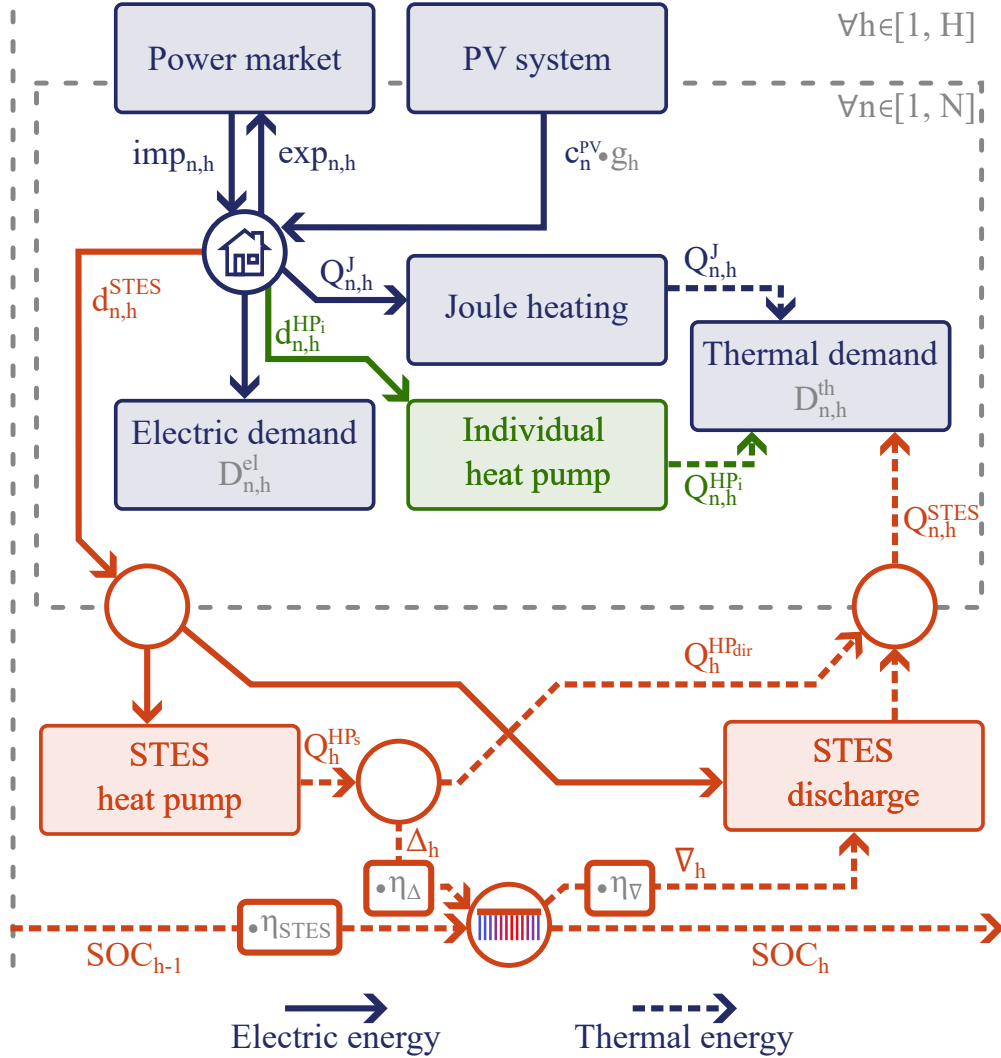
Figure 3.3: Overview of the electric and thermal energy flow in the optimization model each hour. The inner gray outline represents a single house, and the energy equations within. The amount of energy flowing into each circle, is equal to the energy leaving the circle. Edges are labeled when they represent a specific variable in the model. Parameters are written in gray. Variables related to costs are not included, neither are the constraints limiting the maximum output of heat pumps and the boreholes.

1. Energy balance

The electric demand of a household must be met using the household's own power production, and power imported from the power market:

$$D_{n,h}^{el} + Q_{n,h}^{J} + d_{n,h}^{\text{HP}_i} + d_{n,h}^{\text{STES}} = imp_{n,h} - exp_{n,h} + g_h \cdot c_n^{PV} \quad \forall n, h. \qquad (3.9)$$

A household's total electric demand consists of electricity used to power appliances, electricity used to power panel heaters, the electric demand of the house heat

pumps, and any contribution to the electric demand of the STES system. The PV generation is only indexed by hour, since the same generation profile is used for all households, while installed PV capacity is indexed by consumer.

Each consumer's thermal demand also has to be met:

$$D_{n,h}^{th} = Q_{n,h}^{J} + Q_{n,h}^{\mathrm{HP}i} + Q_{n,h}^{\mathrm{STES}} \quad \forall n, h. \tag{3.10}$$

Thermal energy can either come from joule heating, from individually owned heat pumps, or from the district heating loop connected to the STES. It is assumed that there are no losses in the panel ovens, which means that joule heating converts electric energy into thermal energy directly. A single variable is therefore used to represent both the electricity consumption and delivered thermal energy.

In case 2, each consumer can invest in an individual heat pump, with thermal power output given as

$$Q_{n,h}^{\mathrm{HP}i} = d_{n,h}^{\mathrm{HP}i} \cdot \mathrm{COP}^{\mathrm{HP}}, \tag{3.11}$$

and with maximum thermal power output being restricted by the installed capacity of that heat pump:

$$Q_{n,h}^{\mathrm{HP}i} \leq c_n^{\mathrm{HP}i} \quad \forall n, h. \tag{3.12}$$

The total amount of thermal energy extracted from the district heating loop, will at all times be equal to the amount of energy the STES system pushes into the district heating loop. This includes both thermal energy from the storage, and thermal energy delivered directly to the district heating loop by the STES heat pump:

$$\sum_{n=1}^{N} Q_{n,h}^{\mathrm{STES}} = \frac{\nabla_h \cdot \mathrm{COP}^{\nabla}}{\mathrm{COP}^{\nabla} - 1} + Q_h^{\mathrm{HP}s} \quad \forall h. \tag{3.13}$$

STES discharging is performed by pumping cold water into the boreholes to heat it up, and sending the hot water to the district heating loop. Some electricity is needed to run the pump, so just like for heat pumps, the parameter COP^{∇} describes how much thermal energy the pump outputs per unit of electric energy. The pump is, however, not a heat pump. The first term in Equation (3.13) is derived in Appendix A.

2. Power grid

Part of the grid tariff is calculated based on the hours with the highest power import or highest export each month. It is common to calculate peak capacity usage by taking the average of the top three days each month. The model simplifies this by only considering the single hour with the highest import or export.

In the 2020-scenario, peak monthly power draw is calculated for each consumer:

$$|imp_{n,h} - exp_{n,h}| \leq P_{n,m}^{max,i} \quad \forall n, m, \forall h \in [H_{\mathrm{start,m}}, H_{\mathrm{end,m}}]. \tag{3.14}$$

In the 2030-scenario, the peak hourly power import, used for capacity tariff calculations, is the collective peak of the community each month. The aggregated net

power import is equal to every consumer's import minus every consumer's export, in a given hour:

$$\sum_{n=1}^{N}(imp_{n,h} - exp_{n,h}) \leq P_{imp,m}^{max,agg} \quad \forall m, \; \forall h \in [H_{\text{start,m}}, H_{\text{end,m}}]. \tag{3.15}$$

In addition, capacity tariffs for peak hourly import and export are now paid for separately, giving a separate constraint for peak net power export each month:

$$\sum_{n=1}^{N}(exp_{n,h} - imp_{n,h}) \leq P_{exp,m}^{max,agg} \quad \forall m, \forall h \in [H_{\text{start,m}}, H_{\text{end,m}}]. \tag{3.16}$$

3. STES

To model the STES, it is assumed that the STES has reached steady state operation before the simulated year, so the STES should begin and end the year with the same state of charge. Losses are assumed to be linear, and do not depend on the chosen STES volume. Temperature differences within the STES are not represented in the model, which only considers the average temperature of the thermal storage medium. The average temperature of the storage volume is used to limit charging and discharging.

The STES system consists of two units: the shared air-to-water heat pump, and the borehole heat exchangers. Electricity going from house n at hour h to power the system is denoted $d_{n,h}^{\text{STES}}$. Electricity must either go to the heat pump, or to the STES discharging pump:

$$\sum_{n=1}^{N} d_{n,h}^{\text{STES}} = \frac{Q_h^{\text{HP}_s}}{\text{COP}^{\text{HP}}} + \frac{\nabla_h}{\text{COP}^{\nabla} - 1} \quad \forall h. \tag{3.17}$$

The amount of electricity needed by each pump is calculated based on its output and its COP. See full calculations in Appendix A.

The shared heat pump's output is restricted by its maximum capacity:

$$Q_h^{\text{HP}_s} \leq c_{\text{STES}}^{\text{HP}} \quad \forall h. \tag{3.18}$$

The thermal output of the shared heat pump either goes to the boreholes for storage, or directly to the space heating loop:

$$Q_h^{\text{HP}_s} = \Delta_h + Q_h^{\text{HP}_{\text{dir}}} \quad \forall h. \tag{3.19}$$

The state of charge of the STES each hour is the sum of charge and discharge that hour, added to the state of charge from the previous hour after accounting for transmission losses and borehole heat losses. The latter is modeled as a factor η^{STES}, known as heat retainment, that describes how much of the energy stored last hour has been retained:

$$\text{SOC}_h = \eta^{\Delta}\Delta_h - \frac{\nabla_h}{\eta^{\nabla}} + \eta^{\text{STES}} SOC_{h-1} \quad \forall h. \tag{3.20}$$

Since the STES is operating in steady state, the $h - 1$ wraps around to the last hour of the year when $h = 0$.

The variable SOC_h describes the amount of energy stored in the STES, with 0 energy being defined as the level where the STES and the ground are at thermal equilibrium, with the ground having an average temperature of T^{BASE}. As the amount of stored energy changes, the average temperature of the STES in a given hour T_h is calculated as

$$T_h = T^{BASE} + \frac{SOC_h}{c_v V},$$ (3.21)

where c_v is the volumetric heat capacity of the ground around the boreholes, and V is the volume of the STES. Note that T_h is not a variable, only an expression that can be calculated from the other parameters and variables available.

The STES can only be charged as fast as thermal energy from the circulating hot water can be transferred to the surrounding ground. As the average temperature of the STES approaches the temperature of the working fluid, the maximum possible transfer of heat decreases. Figure 3.4 shows how this is modeled linearly.
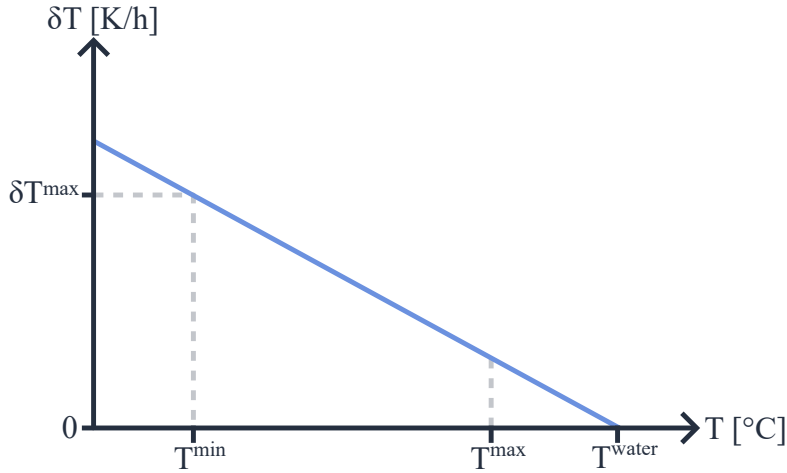
Figure 3.4: Constraint (3.22) shown in a plot where the x-axis is the current temperature, and the y-axis is the maximum possible increase in temperature this hour. The constraint forces the rate of charging to be below the blue line. T^{min} and T^{max} is the operating range of the STES. T^{water} is the temperature of the water used to heat the STES.

Expressing the constraint in Figure 3.4 as a linear combination of variables requires some algebra, shown in Appendix B. The final constraint becomes:

$$A^{\Delta} = \frac{\delta T^{max}}{T^{water} - T^{min}}$$
$$B^{\Delta} = A^{\Delta} T^{water}$$
$$\frac{\eta^{\Delta} \Delta_h}{c_v} \leq -A^{\Delta} \cdot V \cdot T_h + B^{\Delta} \cdot V \quad \forall h$$ (3.22)

The same idea applies when discharging the STES. The water used to discharge the STES needs to reach at least T^{min} degrees to be useable in the district heating loop. The closer the average temperature of the STES is to T^{min}, the slower it can

be discharged. The full calculation can be seen in Appendix B. The constraint becomes:

$$A^\nabla = \frac{\delta T^{\mathrm{max}}}{T^{\mathrm{water}} - T^{\mathrm{min}}}$$

$$B^\nabla = -A^\nabla T^{\mathrm{min}}$$

$$\frac{\Delta_h}{\eta^\Delta c_v} \leq A^\nabla \cdot T_h \cdot V + B^\nabla \cdot V \ \forall h. \tag{3.23}$$

When the STES is at the minimum temperature, it can not be used to cover thermal demand without being charged first.

3.2.2 Model limitations

The STES system has been simplified considerably in an attempt at making a general representation of a STES expressed solely through linear constraints. The simplifications involve ignoring the geometric and geological parameters within the STES, and instead only considering the average temperature of the ground storage, using an estimate for the volumetric heat capacity of the ground.

Larger storage volumes would normally lead to higher storage efficiency, due to the increased volume-to-surface ratio. In this model, the storage heat loss from one hour to the next is a parameter and therefore independent of the final storage volume.

The optimization model also assumes perfect collaboration between the community's consumers. In reality, it is more likely that each consumer would work to minimize their individual cost, as explained in Section 3.2.1. The consumers are also clairvoyant, and have full knowledge of electricity prices, solar production, and electric and thermal demands for the entire year.

3.2.3 Power flow model

After the optimization is preformed, the difference between the cases is investigated from a distribution grid point of view. The optimization model produces aggregated load profiles representing the community, that can be added to a reference distribution grid. How the aggregated peak of the distribution grid is affected by the addition of a given community will be compared. In addition, power flow will be conducted to compare the total line losses.

3.3 Data overview

The following section will give a description of all parameter values, and how they have been estimated. The aim of this thesis is to obtain a general understanding of how a community with a STES will affect the power grid. In reality, most parameters will vary greatly depending on the community's energy demand, STES design, electricity prices, and distribution grid. Most parameter values have been rounded to avoid giving a false sense of accuracy.

3.3.1   Residential load profiles

The residential load profiles used in this analysis are real Norwegian load profiles collected by Hofmann et al. [36]. The profiles cover the period between October 2020 and March 2022, with hourly resolution, and were collected as part of a survey on how consumers responded to the energy crisis in Europe in 2022. The data has been filtered to make it plausibly representative of a community during normal energy conditions. After filtering, 90 load profiles remained for further use. The following filters were applied:

- **Time period:** The analysis requires one year of load profile data, with the period January 2021 to December 2021 being chosen.

- **Location:** The data has to be from a limited area in order for it to be reasonable to assume that the consumers have responded to the same outside temperatures, and had the same space heating needs. In addition, they will have responded to the same electricity prices. Load profiles from the city Oslo, Norway were chosen.

- **Heat source:** The data only contains electric load, and had to be split into thermal and electrical demand based on outside temperature. In order to get an accurate estimate, only profiles that solely relied on electric ovens, or other 1:1 heat sources, to meet their space heating demand were considered.

- **Type of house:** Consumers stating that they lived in the housing category *others* were filtered out, as it would be challenging to estimate thermal and electric demand.

- **Price response:** Only profiles belonging to consumers who stated that they had only taken few, or not taken any, measures to reduce or move power consumption were considered.

3.3.2   Estimation of electric and thermal demands

The consumer load profiles only show total electric energy consumption, and do not make a distinction between energy used for space heating, and energy used for electrical appliances. A STES system can only be used to cover thermal demand, so to evaluate the utility of a STES, the demand data needs to be separated into thermal and electric demand. Since separated load profiles were not available, a method for splitting a single electrical load profile into separate thermal and electric profiles was developed.

On average, two thirds of the total electrical demand of households is used for space heating, but the need for space heating is highly dependent on the outside temperature. Therefore, the developed method makes use of a historic temperature profile, the PROFet tool, and the load profiles.

The temperature profile was downloaded from the Frost API [73]. Since the profiles have been filtered to only contain profiles from Oslo, a temperature profile from Blinderen, Oslo was chosen, for the period from January 1, 2021, to December 31, 2021. There will be a temperature variation within Oslo, but no further details on the locations of individual load profiles were known. It is, however, assumed

that the temperature variation is small enough to be negligible. The temperature profile, which is shown in Figure 3.5, was then used to estimate the ratio between thermal and electric demand each hour of the year, by using the PROFet tool.
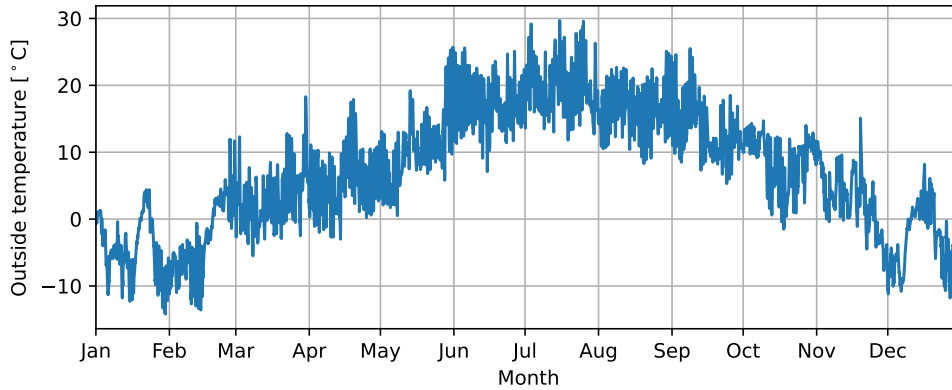
Figure 3.5: The temperature profile used to estimate thermal and electric demand. The temperature data is from a weather station at Blinderen, Oslo [73].

The PROFet tool [74, 75, 76], developed by SINTEF Energy Research, generates demand profiles split into thermal, domestic hot water, and electric demand. It can be given an outside temperature profile to estimate thermal energy demand for a specific year. The profiles have an hourly resolution based on statistical extrapolation, and building characteristics. It is assumed that all buildings have an average building standard, meaning they are below TEK10 standard. Two profiles were generated, one for houses, and one for apartments. These profiles are then used to find the electric-thermal-ratio, defined as

$$r_h = \frac{L_h^{\text{el}} + L_h^{\text{DHW}}}{L_h^{\text{el}} + L_h^{\text{DHW}} + L_h^{\text{th}}}, \tag{3.24}$$

where it is assumed that domestic hot water load L^{DHW} has to be heated by electricity.

Finally, each consumer's load profile is multiplied by this electric-thermal-ratio to find the electric demand of the household for each hour. The rest of the demand is the thermal demand. Figure 3.6 shows the aggregated load profile of 100 profiles, split into electric and thermal demand.
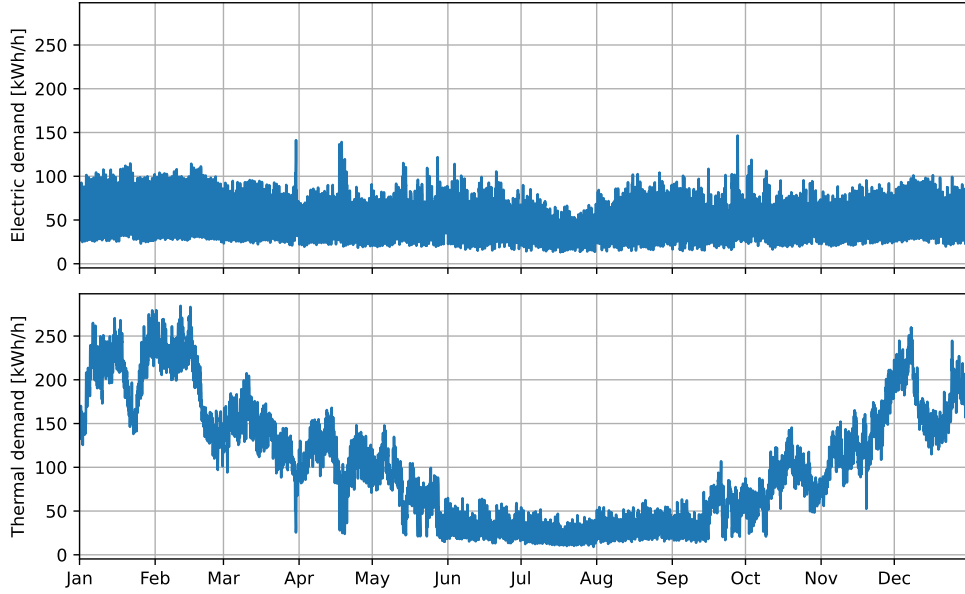
Figure 3.6: Total energy demand of the community, split into electric demand (top) and thermal demand (bottom).

3.3.3 PV production profiles

In order to have local energy production, the consumers can choose to invest in PV systems. Renewables.ninja [37, 38] was used to generate a realistic PV generation profile for a PV system in Oslo in 2014. The year 2014 was chosen because it is the latest year available in CM-SAF, which is the highest quality data set available for Europe. Since the case looks at a newly developed community, it is assumed that all roofs have the same tilt and azimuth, or it could, for example, cover a parking lot. All PV systems in the community therefore use the same PV generation profile, scaled according to each consumer's installed PV capacity. The PV generation profile is shown in Figure 3.7 for a 10 kW$_p$ PV system.
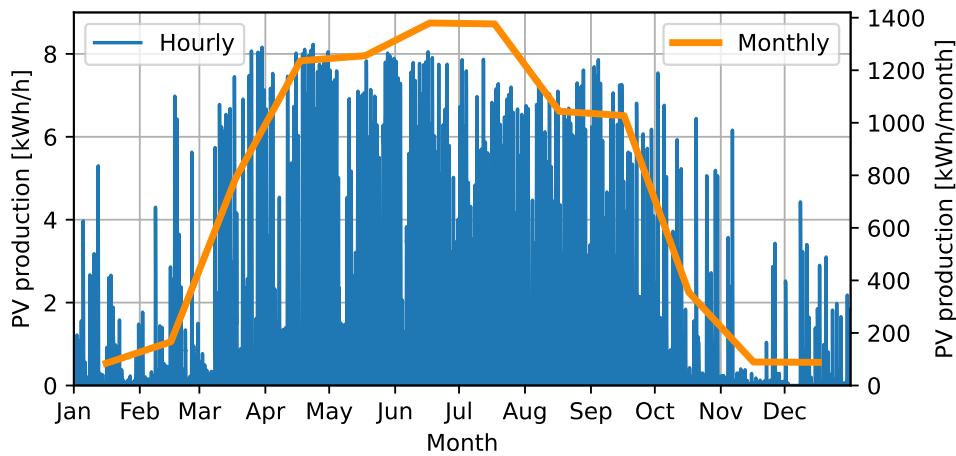
Figure 3.7: The PV production profile used in the model, scaled to a 10 kW$_p$ PV system. The PV profile is based on data from Renewables.ninja [37, 38]

3.3.4 Technical description of the STES system

The modeled STES system is inspired by the relatively new borehole thermal energy storage system at Fjell skole in Drammen, Norway, called GeoTermos. GeoTermos uses 150 m^2 of solar collectors and a heat pump for charging. The heat pump can either be driven by the 1000 m^2 local PV system, or by power imported from the power market [77, 54].

In the model presented in this thesis, the STES system is a borehole thermal energy storage charged by a heat pump only. The heat pump is driven by the shared PV system, or imported power. The system consists of three main components: a heat pump for charging, boreholes and the surrounding ground for storage, and a pump for extracting stored energy from the STES and sending it to the community. The following section will describe each component of the system, as well as the parameters used in the model. Table 3.2 gives an overview of all technical STES parameters.

Table 3.2: Summary of technical STES parameters

Description	Symbol	Value
The fraction of heat retained from one hour to the next	η^{STES}	$0.60^{\frac{1}{8760}}$ h^{-1}
Maximum operating temperature of the STES	T^{max}	60 °C
Minimum operating temperature of the STES	T^{min}	25 °C
Temperature of the water used to charge the STES	T^{water}	80 °C
Maximum temperature change per hour	δT^{max}	0.257 K/h
Temperature of the ground surrounding the STES	T^{BASE}	7 °C
Volumetric heat capacity of the ground	c_v	0.6 kWh/m^{3}K
STES charging efficiency	η^{Δ}	0.99
STES discharge efficiency	η^{∇}	0.99
COP of STES heat pump	COP^{HP}	3
COP of STES pump	COP^{∇}	750

1. Storage

Thermal energy is stored in the ground around the borehole heat exchangers. As previously mentioned, the geometry of the STES, including number of, depth of, and spacing between boreholes, are not included in the model. Instead, the stored energy is based on the storage volume V, state of charge SOC_h, and the heat capacity of the ground c_v. The volume and state of charge are variables in the model, while the heat capacity is a parameter. The bedrock in Oslo mostly consists of gneiss and slate [78]. Both have a volumetric heat capacity c_v of approximately 0.6 kWh/m^{3}K [79], which is used in this model.

The storage also has a heat retainment factor η^{STES} to account for heat loss from one hour to the next. In this model, a constant value is set to give the system

an average storage efficiency of about 60%. This value was chosen because the expected efficiency for a STES providing thermal energy to a community of 100 households is between 40% to 60% [13], but can reach up to 70% if the storage medium has limited thermal conductivity [58]. The efficiency can not be predicted beforehand in the model, as it will depend on how long the energy is stored. Through trial and error, the heat retainment factor was set to $0.60^{\frac{1}{8760}}$ h^{-1}.

2. Temperatures

Storage temperatures vary a lot in existing projects, from as low as $3.4\,^{\circ}\mathrm{C}$, and up to $70\,^{\circ}\mathrm{C}$, depending on the design of the rest of the system [14]. This model will be using the same temperature range as the GeoTermos system, which is from $25\,^{\circ}\mathrm{C}$ to $60\,^{\circ}\mathrm{C}$ [77]. To charge the ground up to $60\,^{\circ}\mathrm{C}$ efficiently, the heat pump heats the water running through the charging loop to $80\,^{\circ}\mathrm{C}$.

The natural temperature of the ground T^{BASE} is assumed to be $7\,^{\circ}\mathrm{C}$, based on measured values from GeoTermos [77]. In reality, there will be a non-constant temperature profile, with seasonal variations in the top layers, and close to constant temperatures deeper underground. This is ignored in the model.

3. Charging and Discharging

The performance of the borehole heat exchangers is limited by the heat conductivity of the ground, and the temperature difference between the water and the ground. This is modeled using the parameter δT^{max}, which limits the rate at which the average STES temperature can change. As charging progresses, the maximum charging rate decreases towards 0, while the maximum discharging rate increases towards δT^{max}. When discharging, it is the opposite. Recall Figure 3.4 for a visual representation of these constraints.

The value of δT^{max} will be highly dependent on the specific STES system, so in this model, a value is chosen such that fully charging the STES is feasible, given the PV generation profile used. The PV profile has about 200 sunny hours from March to October, where sunny is defined as having more than 0.7 kWh of PV production per kW_p of installed capacity. Ignoring heat losses, it is assumed that the STES is designed such that it is possible to charge the STES up to $60\,^{\circ}\mathrm{C}$ by saturating the charging capacity in these hours. The value of δT^{max} becomes $0.257\,\mathrm{K\,h}^{-1}$.

Finally, charging and discharging are associated with a small heat loss, while moving the hot water from the heat pump to the ground. Both η^{Δ} and η^{∇} are set to 0.99, for charging and discharging, respectively. These losses are included when calculating the total losses of the STES. In this model, it is assumed that the vast majority of losses occur in storage, so other losses are left close to 1.

4. Heat pump

S.K Shah et al. found that the annual average COP of a heat pump in existing borehole thermal energy storage systems ranged from 2.84 to 6.2 [80]. The COP will, however, vary throughout operation, as the ambient and fluid temperatures

vary. To simplify the model, a constant and modest COP of 3 was chosen for the COP^{HP} parameter. This parameter is also used for the individual heat pumps.

5. Pump

Following the GeoTermos system, the modeled system discharges the STES by using a regular pump, and pumping cold water into the borehole heat exchangers. In GeoTermos, the maximum discharge rate is 300 kW of heat energy, and the pump consumes about 0.39 kW of electricity to achieve maximum flow, assuming a pump efficiency of 66% [54, 77]. Assuming the electricity needed is proportional to the heat output, the pump can be modelled as a heat pump where

$$COP^{\nabla} = \frac{Q_h}{E_{\text{el}}} = \frac{300 \text{ kW}}{0.39 \text{ kW}} \simeq 750. \tag{3.25}$$

3.3.5   Distribution grid

To evaluate the community's effect on the distribution grid, the Norwegian reference distribution grid from CINELDI is used [69]. The radial grid has 124 nodes, and 123 lines, rated at 22 kV. 54 of the nodes represent existing loads, each with a corresponding hourly load profile spanning one year. The aggregated load profile of the grid is shown in Figure 3.8.
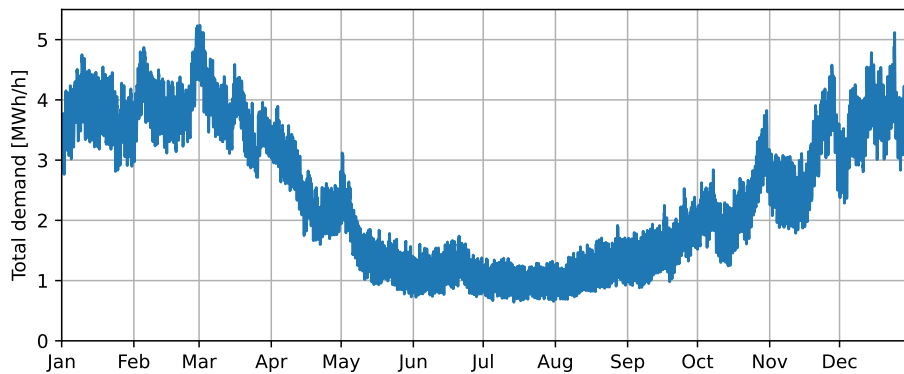
Figure 3.8: The aggregated load profile of all loads in the CINELDI reference distribution grid with hourly resolution.

Some nodes are intended as attachment points for new residential developments, such as local energy communities. Figure 3.9 shows the reference grid, and indicates which nodes already have load, and which nodes are candidates for new developments. The community will be attached to node 89, which is the candidate furthest away from the feeder, indicated as MF, in the radial distribution grid. This will have the most impact on line losses.

When the community load profile is added, it is assumed that the profile gives the active load, and that the community has a constant power factor of 0.95 lagging, like the other loads in the reference grid.

Figure 3.9: The CINELDI reference grid, with load nodes designated for development of local energy communities marked in green. Existing loads are indicated by downward arrows. The figure is adapted from [69] with permission.
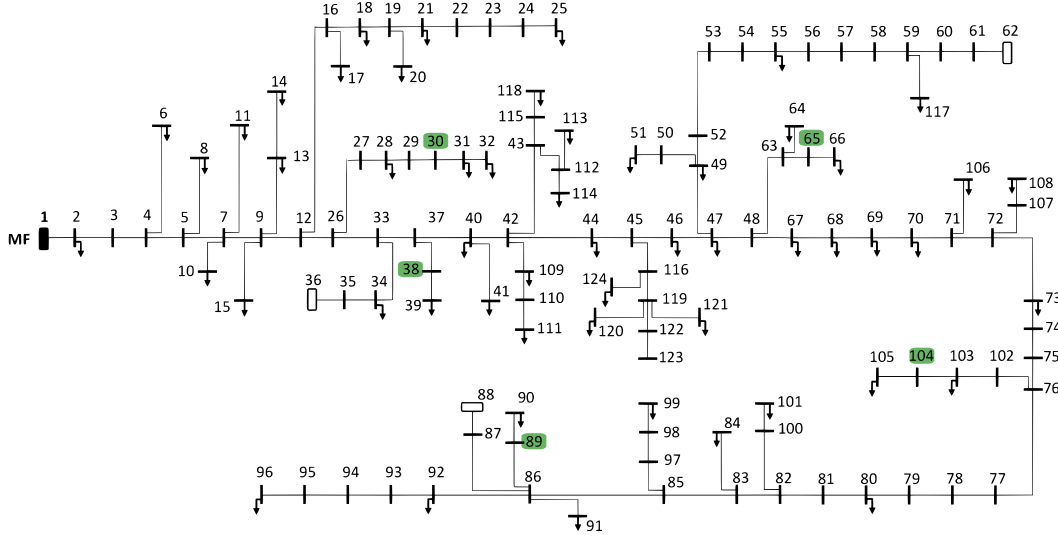
3.3.6   Economic parameters

The model attempts to minimize its yearly costs through investing in local infrastructure, such as a STES and a shared PV system. This section will describe how each of the economic parameters, which are summarized in Table 3.3, are set. All prices have been converted to Euros.[1]

Table 3.3: Summary of investment costs and other economic parameters.

Description	Symbol	Value
Annualized investment cost		
Capacity specific PV investment cost	I_a^{PV}	35 €/kW$_p$
Capacity specific cost of individual heat pump	$I_a^{\text{HP}i}$	40 €/kW$_{\text{th}}$
Capacity specific investment cost of STES	$I_a^{\text{STES,c}}$	1 €/m^3
Base of STES investment cost	$I_a^{\text{STES,b}}$	7200 €
Capacity specific investment cost of heat pump	I_a^{HP}	29 €/kW$_{\text{th}}$
Grid cost		
Capacity grid tariff	cnt	See Figure 3.11
Volumetric grid tariff	vnt	See Table 3.4
Cost of selling power to power market (2020)	snt	-0.44 cents/kWh
Cost of selling power to power market (2030)	snt	0.13 cents/kWh

[1]Exchange rate: 1 NOK = 0.087 EUR, and is considered constant in this thesis.

Annualization and currency

Investments often require large upfront payments to build infrastructure that will last for years. When annualizing the cost into equal yearly payments for the lifetime of the investment, the future payments must be adjusted for the present value of the investment, which gives the equivalent annual cost [81]. Equivalent annual cost is defined as

$$\text{EAC} = \frac{I \cdot r}{1 - (1+r)^{-n}}, \tag{3.26}$$

where I is the investment cost of a given asset, and n is the expected lifetime of the asset. For all assets in this model, the risk adjusted yearly interest rate r is set to 4%, according to Norwegian guidelines for public projects [82]. The equivalent annual cost can also be seen as the yearly payment if the investment is financed with an annuity loan with the given interest and payback period.

Investment cost of PV systems

If the model invests in a PV system for a given household, its annual costs increase by the annualized cost of the PV system, which is proportional to the system's installed capacity. NVE estimates that the capacity specific investment cost of new PV systems in Norway is 7 kNOK/kW$_p$, for PV systems with a capacity between 20 kW$_p$ – 1000 kW$_p$ [83]. The lifetime of the PV installation is assumed to be 30 years. Converted to Euro, the annualized cost I_a^{PV} becomes 35 €/kW$_p$.

Each consumer can invest in a PV capacity between 0 and 20 kW$_p$. Historically, about 9 kW$_p$ has been the average size of residential PV systems [84]. However, since a residential PV system is assumed to be under 20 kW$_p$ [83], 20 kW$_p$ was chosen as the maximum capacity one household could invest in.

Investment cost of individual heat pumps

As with the PV system, the community's annual cost will increase by the annualized cost of the total installed heat pump capacity. The average cost of a residential heat pump is between 20 kNOK and 35 kNOK [85], and the average installed capacity is between 2 kW$_{\text{th}}$ and 7 kW$_{\text{th}}$ [86]. The capacity specific investment cost has been estimated to be

$$I^{\text{HP}_i} = \frac{\text{average price}}{\text{average capacity}} = \frac{25 \text{ kNOK}}{4 \text{ kW}_{\text{th}}} = 6.25 \frac{\text{kNOK}}{\text{kW}_{\text{th}}} \tag{3.27}$$

The lifespan of a heat pump is estimated to be 20 years [87], and with an interest rate of 4%, the annualized capacity specific heat pump cost $I_a^{\text{HP}_i}$ becomes 40 €/kW$_{\text{th}}$.

Investment cost of STES system

STES is not as widespread as either PV systems or heat pumps, which makes it more challenging to estimate the capacity specific investment cost. In order to get a decent estimate, linear regression was done on the STES investment cost data found in [14]. The article gives the total investment cost and storage volume of different existing and simulated systems. A couple of the STES systems were not

considered, due to abnormally low investment cost, as described in the article. As Figure 3.10 shows, this results in a volume specific capacity cost of 10.5 €/m^3, and a base cost of 124 k€. Assuming a life span of 30 years, the annualized capacity specific STES cost $I_a^{\text{STES,c}}$ becomes 1 €/m^3, with an annualized base cost $I_a^{\text{STES,b}}$ of 7200 €. Since the available data was for systems between 18 000 m^3 and 63 000 m^3, the STES system installed by the community in case 3 also has to be within this range.
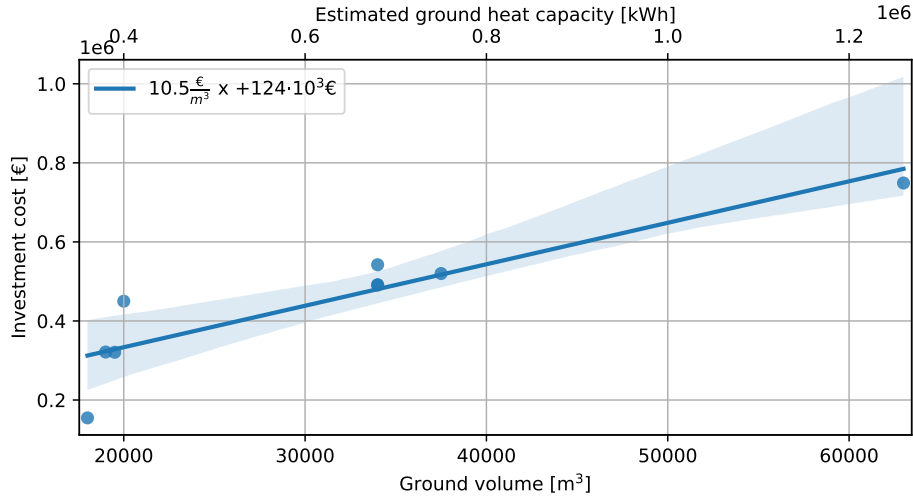

Figure 3.10: Estimated capacity specific investment cost and base cost for a borehole thermal storage system (blue line), based on existing systems (blue dots) [14].

The STES also requires pumps for charging and discharging. This system will be using an air-to-water heat pump for charging, and a regular pump for discharging. Although the cost varies, it has been found that the average capacity specific investment cost of a heat pump with a capacity greater than 100 kW and a COP of 3 is about 400 €/kW$_{\text{th}}$ [88]. The annualized capacity specific cost is therefore 29 €/kW$_{\text{th}}$, when assuming the heat pump has an interest rate of 4%, and a life span of 20 years [87]. The price of the discharging pump and district heating loop is assumed to be a part of the STES cost.

Electricity and grid tariff

Elvia's current grid tariff model is the basis for the grid tariff in the 2020-scenario. The tariff consists of the volumetric grid tariff vnt, shown in Table 3.4, and the capacity grid tariff cnt.

Table 3.4: Elvia's volumetric grid tariff (vnt) from January 1, 2024 [52]. The night prices also apply to weekends and holidays.

Volumetric tariff	Day: 06:00-22:00	Night: 22:00-06:00
January–March	0.034 €/kWh	0.028 €/kWh
April–December	0.042 €/kWh	0.035 €/kWh

The capacity grid tariff is step-based, but for modeling purposes the step model has been converted to a linear one, as shown in Figure 3.11. Notice, that only the first five steps have been used, as Elvia claims that a normal household rarely falls into one of the higher categories [52]. The model will also charge for the one hour with the highest capacity use each month, instead of calculating the average of the three hourly peaks from three distinct days. To make the regression line follow the step model as close as possible, the capacity grid tariff has been split into a base cost of 8.3 € and a capacity specific cost of 2.1 €/kWh/h.
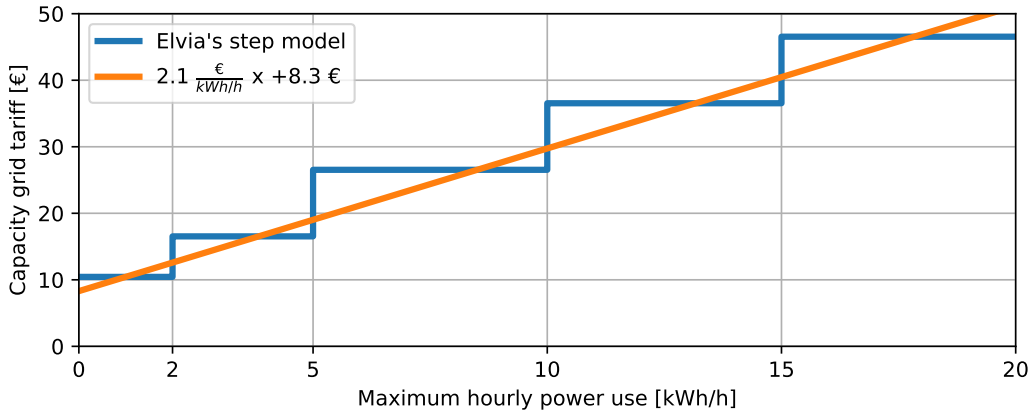
Figure 3.11: Elvia's tariffs for capacity grid cost in 2024 (blue) [52], and the regression line used to linearize the capacity cost in the linear optimization model (orange).

For the electricity prices, historic spot prices for NO1 from 2019 is used. This is because Oslo, where the load profiles are from, is in NO1. 2019 was chosen because it was a more normal year in terms of electricity prices, compared to 2021, when there was an energy crisis in Europe [50]. Figure 3.12 shows the 2019 price profile for NO1 in 2019.

Figure 3.12: Hourly spot prices from NO1 in 2019 [89].

Finally, Elvia pays prosumers a selling grid tariff *snt* of 0.44 cents per kWh exported [52].

Changes in electricity prices and grid tariff model for the 2030-scenario
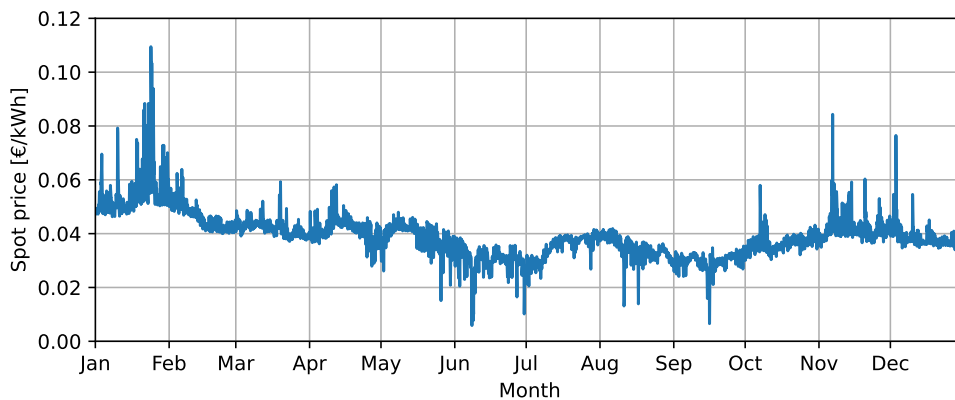
1. 2030 electricity prices

A synthetic 2030 electricity price profile has been made for the 2030-scenario. The price profile is based on NVE's estimates of the average spot prices each week in 2030, shown in Figure 2.6. Hourly variation within each week is based on examples of typical winter and summer weeks [50]. The synthetic 2030 price profile is shown in Figure 3.13.
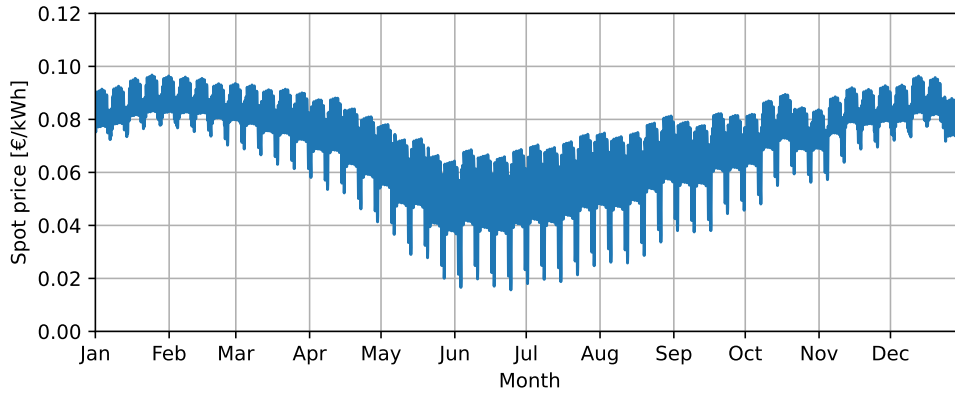

Figure 3.13: The synthetic hourly electricity spot prices used in the 2030-scenario. The profile is based on data from [50].

2. Updated capacity tariff

In the 2030-scenario, the grid tariff's monthly capacity term is calculated based on the community's aggregated peak, instead of the individual peaks. The new tariff is calculated such that the community will continue to pay the same amount in total, for a given representative profile, unless their aggregated capacity demand changes. To accomplish this, the capacity grid tariff has been adjusted as follows:

$$cnt_{\text{agg}} = \frac{cnt_i \cdot \sum_{n=1}^{N} \sum_{m=1}^{M} P_{n,m}^{\text{max,i}}}{\sum_{m=1}^{M} P_m^{\text{max,agg}}} \tag{3.28}$$

The base of the capacity grid tariff, which can be interpreted as the baseline cost for being connected to the grid, remains the same. For the given set of load profiles, the proportional part of the capacity tariff becomes 4.4 €/kWh/h. The adjusted tariff will be different if a different representative load profile is used, as the ratio between individual and aggregated peaks will be different.

In addition to aggregating the capacity tariff, the community will be charged for needed power import capacity and export capacity separately. The same cost per kWh/h is used for both. The suggested grid tariff is meant to incentivize local energy production and consumption better than the current tariff. In the current system, consumers pay nothing for exporting power, as long as they export less than their peak import that month.

3. Changes in selling grid tariff

In the 2020-scenario, the community is paid 0.44 cents per kWh of power export, which is what Elvia pays prosumers. However, once a prosumer has a power export over 100 kW, they are no longer classified as "plusskunde", and a small volume tariff on export is added [90]. In the model, the payment for exporting is removed, and a charge of 0.13 cents per kWh of exported electricity is added. This is based on the current price Elvia charges for exporting electricity to the regional grid [91].

FOUR

RESULTS AND DISCUSSION

This chapter will present the findings from running the model presented in the previous chapter on the three different cases, base, HP, and STES, in the two different scenarios representing 2020 and 2030. The community's aggregated load profile from the optimization model has also been inserted into the CINELDI reference grid, by adding a load corresponding to the community's net power import each hour of the year. Throughout this chapter, cases 1 (base) and 2 (HP) will work as reference cases without a STES, to evaluate the impact the STES has on the grid in case 3 (STES). As described in Section 3.1.1, case 1 is the worst case for electricity demand, as joule heating is the only available source of space heating. Case 2 represents the best case with no energy storage, where every household has the option of investing in a heat pump of the ideal size.

4.1   Load profiles and duration curves

This section discusses the seasonal variations within the three cases in the 2020-scenario, by looking at the community's net power import each hour of the year. In general, less seasonal variation is preferable, as the grid has to be dimensioned to handle peak load, and periods of off-peak load lead to underutilization of this grid capacity.

As a point of reference, Figure 4.1 shows the combined electric and thermal demand of the community, throughout the year. It has a peak demand of 377 kWh/h, and an off-peak demand of 34 kWh/h. Demand is highest in the winter, and lowest in the summer.
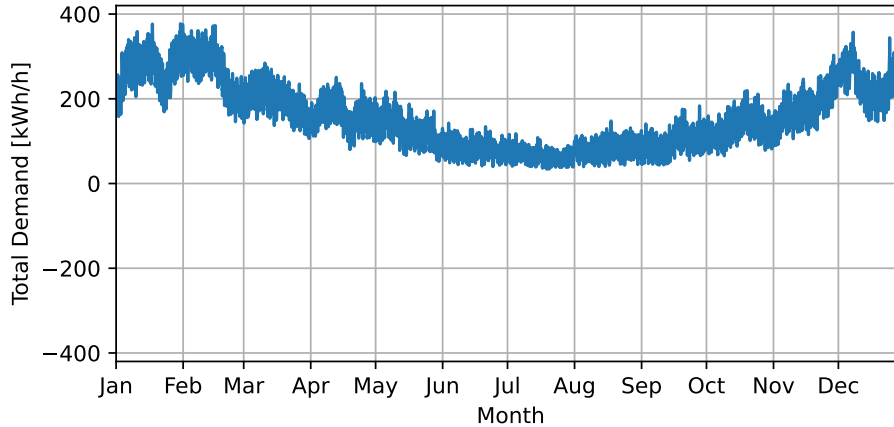
Figure 4.1: The original aggregated load profile of the 100 households, before separating electric and thermal demands.

4.1.1 Seasonal variation and load shifting

Case 1

In case 1, only joule heating is available, so all demand must be met using electricity. The community may, however, invest in a PV system, replacing some power import from the power grid with local energy production. In case 1 of the 2020-scenario, the optimization model ended up installing a PV system with a capacity of 614 kW_p, which resulted in the net power import shown in Figure 4.2.
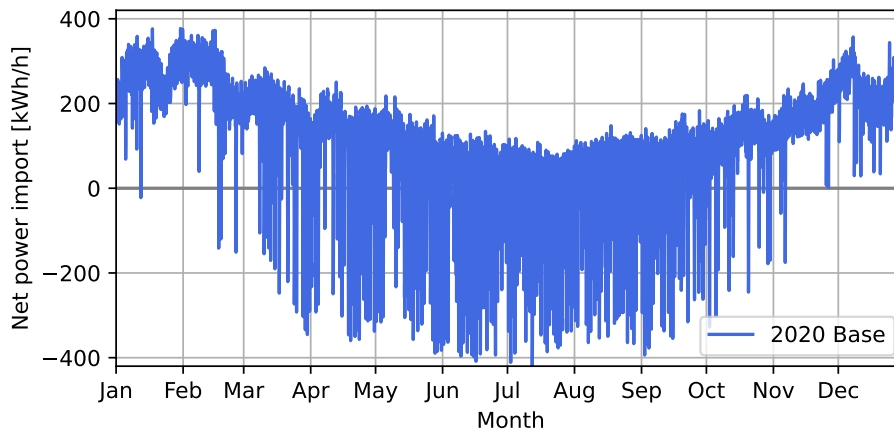
Figure 4.2: The optimization model's aggregated net power import of case 1 in the 2020-scenario.

There are two main takeaways from Figure 4.2:

- The peak load has not been reduced, despite installing a sizeable PV system, because there is little PV production in winter. This is consistent with RME's evaluation of the current energy sharing framework [43].

- During the spring, summer, and fall, PV production often exceeds local demand by a large margin, leading to a net power export up to 422 kWh/h

in some hours. The model installed more PV capacity than the community needs, in order to make a profit from selling surplus power to the power market.

The excess export leads to an increase in the seasonal variation, and the external grid would have to be strong enough to avoid undervoltage in the winter and overvoltage in the summer. Since local energy production was uncommon when most of the power grid was built, undervoltage, which can occur in periods of high demand, was the main design concern. Distribution grids are therefore likely not designed to prevent overvoltage, which can occur during power flow reversal caused by local power export.

Case 2

When given the option to invest in individual heat pumps in case 2, the optimization model installed large enough heat pumps, for each consumer, to cover almost all of their thermal demands. With a COP of 3, the heat pumps reduce the amount of electricity needed to meet thermal demands considerably, as can be seen in the total grid import, shown in Figure 4.3. The PV system is also 26% smaller than in case 1, leading to less export in the summer. Both factors lead to an overall decrease in seasonal variations compared to case 1.
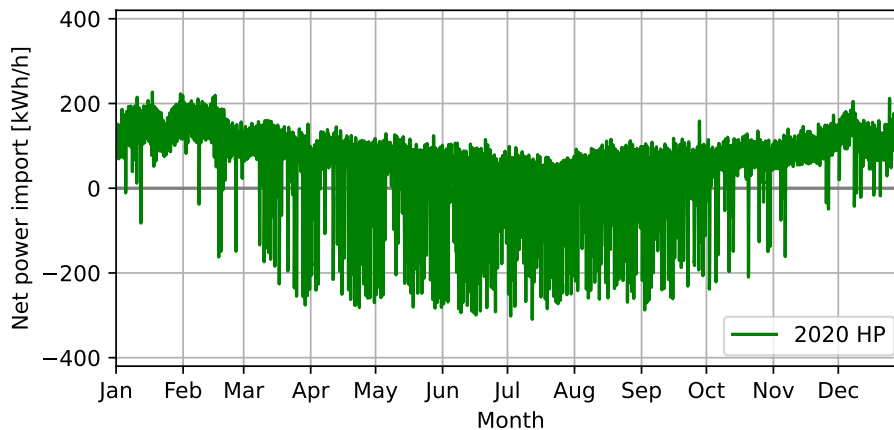
Figure 4.3: The optimization model's aggregated net power import of case 2 in the 2020-scenario.

Compared to case 1, the optimization model led the community to decrease its capacity need, from about 400 kWh/h to 200 kWh/h, by using a more efficient form of space heating. It should be noted that the fixed COP used in the optimization model may result in an unrealistic reduction of peak load, which will be discussed in more detail in Section 4.8.1.

Case 3

In case 3, the individual heat pumps are replaced by a single shared heat pump, connected to a district heating loop and a STES system. The heat pump has the same COP as in case 2, but the addition of thermal energy storage enables some winter demand to be met using stored energy. The STES can be charged

in the summer, when demands are lower, and also make better use of local PV production by storing it instead of exporting it.
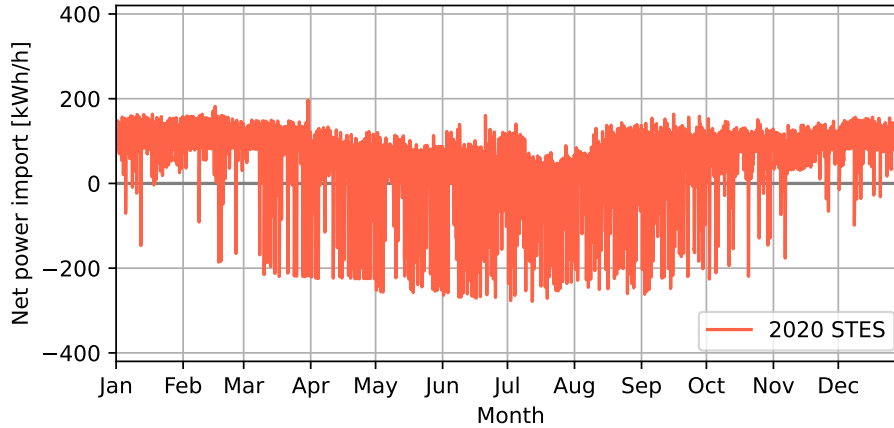

Figure 4.4: The optimization model's aggregated net power import of case 3 in the 2020-scenario.

Figure 4.4 shows that the net power import of case 3 stays below 200 kWh/h, often by a clear margin. Only a single spike in the end of April reaches close to 200 kWh/h. Winter demand is in general lower than in case 2, while the summer demand is a bit higher. Higher demand can only be caused by charging the STES, as there are no other loads that could increase the demand. The increased demand in the summer is the most prominent at the beginning of July and from the second half of August, and experiences a dip towards the end of July. The added demand is inversely correlated with the electricity prices for this period, shown in Figure 3.12.

In hours of high PV production, the net power export is about the same as in case 2. Comparing the load profile to the reference cases, case 3 has a lower seasonal variation than case 1, and a slightly lower variation than case 2. However, there is still a significant amount of power export during the summer, which may cause voltage violations, and instead could have been stored in the STES.

4.1.2 Grid use

Table 4.1 summarizes key figures related to the community's grid use in the three cases. Case 3 has a peak power import that is 48% lower than case 1, and 14% lower than case 2. A case study from Furuset, Norway, found that a STES system decreased the community's peak load by 31%, which is within the range that case 1 and 2 represent [59]. In addition, the total load is 54% and 2.3% lower than in case 1 and 2, respectively. The case study from Furuset had a total load reduction of 26%, indicating that the load reduction from a real community would be somewhere right in the middle of the range given by case 1 and 2.

On the export side, all cases install large PV systems, leading to hours of net power export that are higher than peak import. Case 1 has the highest peak export with 422 kWh/h, and case 3 has the lowest with 278 kWh/h. The model chooses an

Table 4.1: Key figures for grid use and installed PV from the 2020-scenario.

2020-scenario	Peak import [kWh/h]	Peak export [kWh/h]	Total load [MWh]	Installed PV [kW$_p$]
Case 1 (Base)	377	422	842	615
Case 2 (HP)	227	309	400	455
Case 3 (STES)	196	278	391	501

oversized PV system, in order to make a profit from selling surplus power to the power market.

Recall that in the 2020-scenario, each household pays a monthly grid capacity tariff based on the hour of the month with the highest power import or export. This gives the consumers some incentive to keep their peak import and peak export low. In case 1, the consumers have no flexibility beyond the amount of PV they install. In case 2, they have a very small amount of flexibility, in that they may choose to use the less efficient joule heating instead of their heat pump, to export less surplus energy. However, the spot price on the power market is almost always higher than the marginal cost of the export tariff, so the optimization model usually prefers to sell surplus electricity.

In case 3, the model has flexibility through the STES, which can be charged and discharged at any hour. There are two reasons as to why the model may want to charge the STES:

- The spot price is low this hour, so selling surplus electricity is not profitable. It is better to charge the STES, and import less electricity later when meeting future thermal demands. Even if the spot price is the same now and then, selling now and buying later is a net loss, due to the volume grid tariff and electricity taxes. If the current electricity price is low enough, it can even be profitable to import power to charge the STES, as can be seen happening in the summer.

- The consumer is already exporting energy this hour, and any additional export would increase the monthly capacity tariff. The extra energy can be sent to the STES instead to keep the capacity tariff lower.

However, from the power export seen in the load profiles, it is apparent that the optimization model prefers to install larger PV systems than needed and export the excess power, instead of charging the STES, under the current framework.

4.1.3 Duration curves

Figure 4.5 shows the duration curves for each of the three cases, in the 2020-scenario. Around 80% of hours in the year have a positive net power import, in all three cases.

Case 2 and 3 generally import less than case 1, due to having heat sources that are more efficient. In the top 20% hours of power import, case 3 is a bit below case 2. This is because thermal energy from the STES can be used to decrease
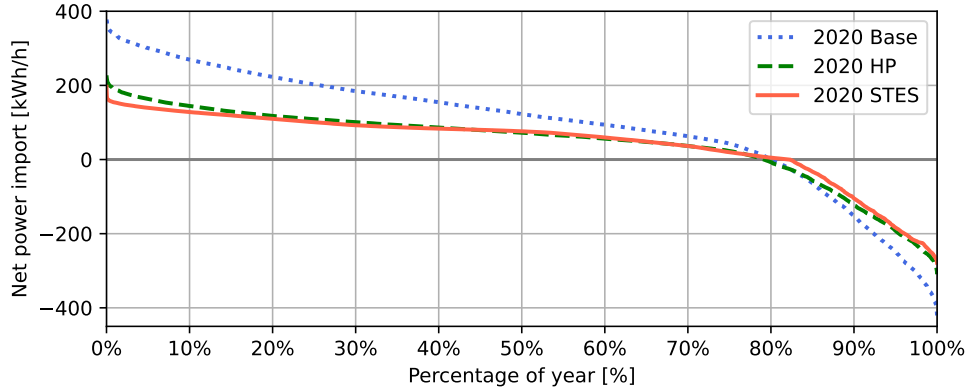
Figure 4.5: Duration curves showing the community's grid use for all cases in the 2020-scenario.

the need for electric space heating in the coldest winter hours, when electricity demands peak in case 1 and 2. On the export side, case 1 will in about 5% of hours export more energy than case 2 or 3 exports in a single hour ever.

The duration curves show a potential issue with the load profile, from the perspective of the power grid. In all cases, peak export is larger than peak import. The capacity demand has therefore increased, compared to having no PV system, and is now largely determined by the community's peak export. In addition, the grid has to be dimensioned to handle power flow reversal, which happens in about 20% of hours. This can potentially lead to overvoltage. Both of these factors have been identified as potential issues with distributed energy production and prosumers [5].

4.2 Utilization of local PV production

One interesting result from Table 4.1 is that case 3 installs a PV system that is about 50 kW_p larger than in case 2, yet has a peak export that is about 30 kWh/h lower. This indicates that adding a STES enables having more local PV production, without placing additional strain on the power grid in hours of high production.

The results from Section 4.1 show how the optimization model minimizes total costs by investing in a large PV system. The model allows each household to own up to a 20 kW_p share of the system, giving a theoretical maximum size of 2000 kW_p. Even though the optimization model only led to installing about a quarter of this at most, peak export surpasses peak import in all cases. In reality, a community is probably not likely to build a system this large, since they also value practical considerations that the model ignores, such as available area. It does, however, show that current day grid tariffs might not incentivize local consumption well, which can cause issues in a future with higher penetration of local energy production.

In the 2020-scenario, the optimization model's DSO *pays* the community 0.44 cents per kWh of exported energy, just like Elvia currently does. This makes

sense when one assumes that exported power is used by close neighbors who are not prosumers, who still pay electricity tariff as if the energy came from a power plant far away. The DSO can pay the prosumer some of the money it saves from reduced line losses. If a substantial share of consumers become prosumers, this assumption stops being true. PV systems that are geographically close will have similar production profiles, potentially leading to high aggregated power export on sunny days, which needs to be transported far. In a grid with a high penetration of PV production, it no longer makes sense for the DSO to incentivize exporting.

The model does not include a mechanism for enforcing curtailment of PV production, but there could in practice be an agreement between the community and the DSO that limits maximum power export. This would incentivize the optimization model to purchase a smaller PV system, as it is less profitable. With the addition of a STES, curtailment can be replaced by sending the surplus energy to the storage.

As with all flexibility and storage options, the socioeconomic value of a STES system should be considered on a case by case basis. If the surrounding grid is over-dimensioned, and there is a lot of available capacity, there is no need to implement expensive methods to reduce peaks. On the other hand, if the alternative is to reinforce several lines in the grid, storage and flexibility may be the better alternative.

It is also important to note that STES systems alone are not enough to solve all the challenges that come with more local renewable energy production. Short-term flexibility and storage systems that can output electric energy are still valuable tools for peak reduction. However, STES systems specifically offer a way of lowering seasonal variations, as local energy production in the summer can be stored until the winter, reducing grid strain in both seasons, as Table 4.1 shows.

4.3 Power grid analysis

The results outlined above indicate that using a STES can help reduce power import peaks, by enabling load shifting from winter to summer. Reducing the community's peak is in general beneficial to the power grid, as it reduces transportation losses. However, costs associated with line losses are low compared to grid reinforcement costs. The need for grid reinforcements can be reduced if the community has reduced its demand when the grid's aggregated demand peaks. In order to assess the total strain on the grid, the community's contribution to the aggregated peak of the grid must be considered. Even if the community's peak load is not reduced significantly, the strain on the grid can still be eased if the community is able to shift load away from the grid's aggregated peak load hour.

The CINELDI reference grid has an aggregated peak load of 5.23 MWh/h, that occurs on February 28 [69]. The peak load will increase when adding the community of 100 household to the grid. However, since the aggregated peak hour is in the winter, seasonal load shifting may keep the aggregated peak increase to a minimum. Table 4.2 shows how total load and peak load is affected by adding the community in each of the three cases.

Table 4.2: Change in the total load and peak load in the CINELDI reference grid by adding the aggregated load profile of the community as a load, for each case in the 2020-scenario.

2020-scenario	Total load [MWh]	Peak load [MWh/h]
Case 1 (Base)	23.5 (+3.9%)	5.46 (+4.3%)
Case 2 (HP)	23.0 (+1.9%)	5.36 (+2.3%)
Case 3 (STES)	23.0 (+1.9%)	5.34 (+2.1%)

The load is calculated as the sum of each node's active load for each hour. This means that power export, which is a negative load in the model, contributes to lowering the total load. Even though case 1 had the highest total power export, case 2 and 3 both contributed less to the distributions grid's total load and peak load. Case 1 and 2 contribute the same amount to the total load. However, case 3 contributed less to the peak load than case 2 did, indicating that STES can be more beneficial to the grid than heat pumps alone, in terms of capacity demand.

4.4   Line losses

As mentioned in Section 2.3.3, distributed PV systems are believed to contribute to reducing line losses, despite not reducing the peak power demand. To assess this claim, and give an overall evaluation of the community's grid strain, the line losses in the CINELDI reference distribution grid have been investigated.

Figures 4.6 to 4.8 show how much the total line losses in the reference grid are affected by adding the community to load node 89 (see Figure 3.9). One characteristic of the loss profiles is that case 3 adds about 10 kWh/h of line losses at most, compared to about 25 kWh/h and 15 kWh/h in cases 1 and 2, respectively. This is not surprising, as the lower losses in case 3 correspond to the reduction in demand discussed in Section 4.1.1, and it is known that lower demands lead to lower line losses.
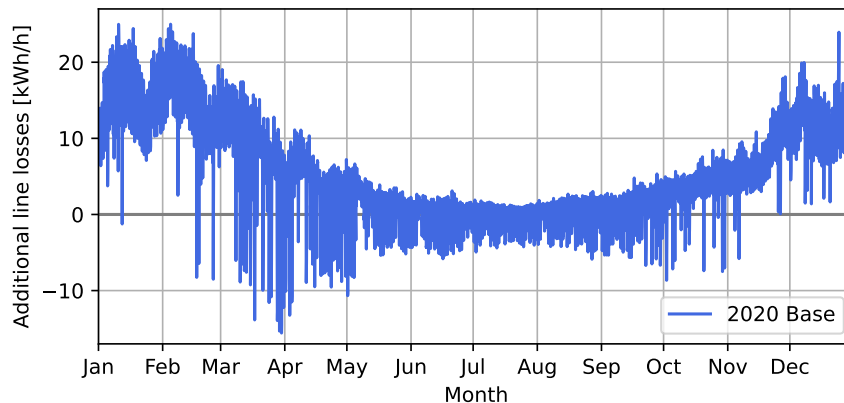

Figure 4.6: Difference in total line losses each hour from adding the case 1 community in the 2020-scenario to the CINELDI reference grid.

Another characteristic of the line loss profiles is that adding the community reduces

the total losses in the reference grid in some hours. The reduction of line losses is at its highest in the months of March and April, while the effect is less prominent between May and September, despite PV production being higher in these months. The loads in the CINELDI reference grid are in general higher in spring than in summer, as can be seen in Figure 3.8, so surplus power from the community PV goes directly to nearby load nodes. In the summer, however, the total demand of the distribution grid is lower, so the community's shared PV system produces enough power to cover more than the demand of the closest load nodes. The rest of the surplus power therefore has to meet the demand of load nodes further away from the community's node, and has to be transported further. The result is that the reduction in line losses diminish in the summer, when PV production is at its highest. PV production could even cause losses in the distribution grid to increase, if enough nodes have a local PV system.

Figure 4.7: Difference in total line losses each hour from adding the case 2 community in the 2020-scenario to the CINELDI reference grid.
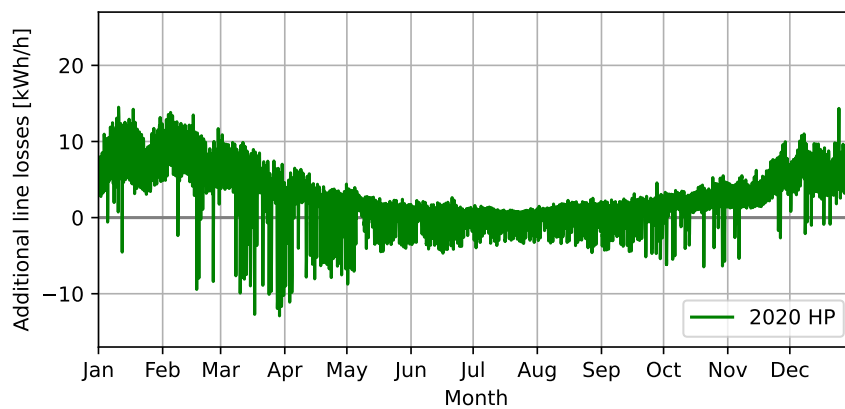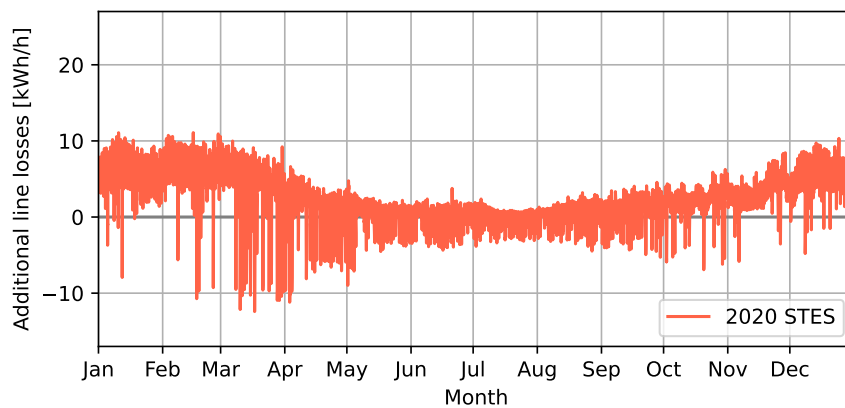

Figure 4.8: Difference in total line losses each hour from adding the case 3 community in the 2020-scenario to the CINELDI reference grid.

4.5   2030-scenario

This section will evaluate the results from the 2030-scenario, mainly by comparing case 3 in the 2030-scenario to case 3 in the 2020-scenario. Load and line loss profiles

for case 1 and 2 in the 2030-scenario can be found in Appendices C.1 and C.2. The 2030-scenario is described in more detail in Section 3.1.2. One of the main differences is that a synthetic electricity price profile for 2030 is used instead of the 2019 price profile. The grid rent has also been adjusted to try to incentivize local consumption of locally produced energy. The grid capacity tariff is divided into separate capacity tariffs for import and export, and is no longer calculated per household, but instead based on the aggregated load profile of the community. Finally, the DSO no longer incentivizes local export by paying prosumers for power export, and instead charges a small volumetric fee.

4.5.1   Seasonal variations in demand

In the 2030-scenario, the net power load profile of case 3 is flatter than in the 2020-scenario, as shown in Figure 4.9.
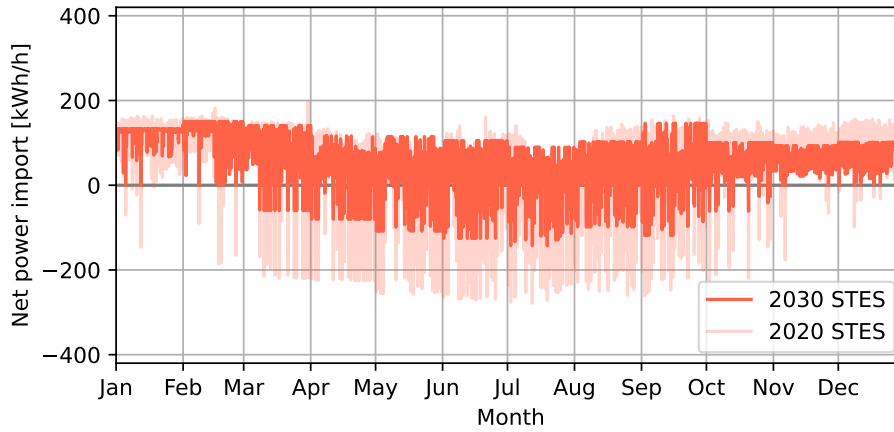

Figure 4.9: Net power import of case 3 in the 2030-scenario, with the same profile from the 2020-scenario in the background.

The net power import stays below 150 kWh/h at all times, which is a reduction of 23% from the 2020-scenario. The 2030-scenario incentivizes this in two ways:

- In the 2030-scenario, the spot prices are higher in the winter, incentivizing the model to import less energy in what is usually the peak import period.

- The new import grid tariff is calculated based on the aggregate import, instead of individually per household. In the 2020-scenario, the optimization model can pick off-peak houses strategically to import power from the power market without paying any additional capacity tariffs. This circumvention of the capacity tariff is no longer possible when the community has a shared capacity tariff.

The optimization model is able to respond to these incentives by using the STES. In hours with high demand, a lot of the demand is thermal. This demand can be covered by using the STES pump to discharge stored energy from the STES, instead of using a heat pump to convert electricity to heat. Since the discharging pump uses way less electric energy than the heat pump to deliver the same amount

of thermal energy, net power import is reduced. The 2030-scenario thus indirectly incentivizes the optimization model to use the STES more.

The load profile also shows that total power export has been reduced. That is a result of installing a smaller PV system, as well as using more of the surplus production to charge the STES, which has some losses. Peak export has also been reduced to below 150 kWh/h. The new grid tariff incentivizes lowering peak power export, and using the STES more, so charging the STES instead of selling surplus PV generation becomes more lucrative to the optimization model. In total, the difference between peak import and export has been reduced, leading to a more even load profile, with less seasonal variation than the same case in the 2020-scenario.

Notably, in the 2030-scenario, the optimization model led to import peaking in September, due to charging the STES with imported power. September is the last month before thermal demands start increasing, so the model charges the STES as close to winter as possible to keep heat losses to a minimum. September also has less PV production than the summer months, so electricity is imported from the grid instead.

4.5.2 Grid use and PV production in 2030

The seasonal load variation of all cases is reduced in the 2030-sceanrio, compared to the corresponding case in the 2020-scenario, which can be seen in Figures 4.9 and C.1. The main reason for the reduction, is that less PV capacity is installed in all three cases. However, while case 1 and 2 installed 309 kW$_p$ and 236 kW$_p$ less PV capacity in the 2030-scenario, respectively, case 3 reduced the installed PV capacity by just 114 kW$_p$, as Table 4.3 shows.

Table 4.3: Key figures from grid use and PV capacity in the 2030-scenario. Numbers in parentheses describe the relative difference compared to the corresponding case in the 2020-scenario.

2030-scenario	Peak import [kWh/h]	Peak export [kWh/h]	Total load [MWh]	Installed PV [kW$_p$]
Case 1 (Base)	377 (-0%)	179 (-58%)	1115 (+32%)	306 (-50%)
Case 2 (HP)	220 (-3%)	110 (-64%)	606 (+51%)	219 (-28%)
Case 3 (STES)	150 (-23%)	142 (-49%)	502 (+28%)	387 (-23%)

Table 4.3 also shows that case 3 is the only case that decreased peak import considerably. It is also the only case where the community has substantial flexibility in how thermal demands can be met. The results indicate that local energy communities with a STES have a potential for reducing peak load, if incentivized properly. To get the optimization model to use this potential, the 2030-scenario added indirect economical incentives in the form of new grid tariffs, and more variable electricity prices.

In the 2030-scenario, case 3 has a higher peak export than case 2. However, it must be taken into account that case 3 also has the highest installed PV capacity.

Case 3 has 168 kW$_p$ more PV capacity, but only 32 kWh/h higher peak export than case 2. Just like in the 2020-scenario, peak export is kept lower by having the option of sending surplus PV production to the STES, ultimately allowing more PV to be installed while using less capacity, and without any PV curtailment.

In addition to not having a significantly higher peak export, the total exported power is also comparable to case 2, even though the installed PV capacity is a lot higher. This can be seen by comparing the area on the export side in Figure 4.10. On the import side, the duration curve of case 3 is below case 1 and 2 at all times, which means that both peak imported power and total imported power is lower.
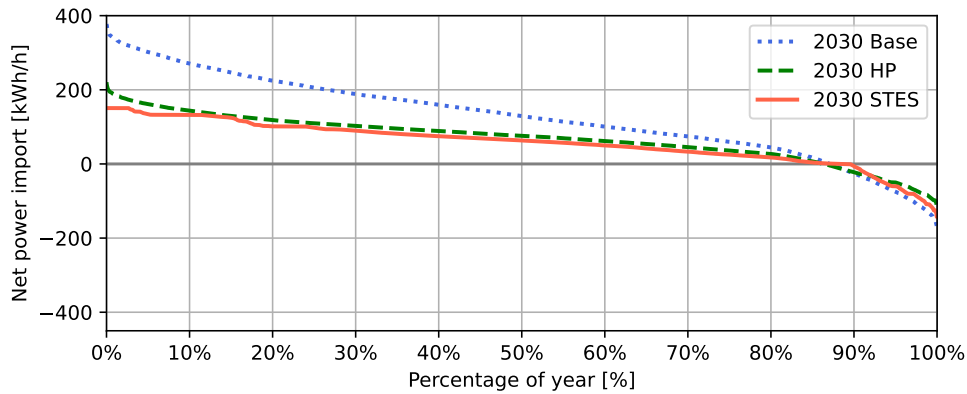

Figure 4.10: Duration curves showing the community's grid use for all cases in the 2030-scenario.

4.5.3   Load in the distribution grid in 2030

Table 4.4 shows how the total load and peak load in the CINELDI reference grid is affected by adding the community in each case, optimized for the 2030-scenario. While case 3 increased the peak load by 2.1% in the 2020-scenario, it only increases peak load by 1.5% in the 2030-scenario. The new incentives in the 2030-scenario did not only lead the optimization model to reduce the STES community's peak, it also leads to load reduction when the distribution grid experiences peak load. This is what is ultimately important when reducing the transmission capacity needed from the grid [48].

Table 4.4: Total load and peak load in the CINELDI reference grid after adding the aggregated load profile of the community as a load, for each case in the 2030-scenario. The numbers in parentheses show the change relative to the reference grid without the added community.

2030-scenario	Total load [MWh]	Peak load [MWh/h]
Case 1 (Base)	23.8 (+5.2%)	5.47 (+4.4%)
Case 2 (HP)	23.2 (+2.8%)	5.36 (+2.3%)
Case 3 (STES)	23.1 (+2.3%)	5.32 (+1.5%)

The total load column in Table 4.4 has higher values in all cases in the 2030-scenario, which is explained by the fact that the optimization model led to less

PV capacity being installed.

It is important to remember that the optimization model only minimizes its own costs, and does not care about the cost of operating the distribution grid. These costs should not be completely disregarded, as the grid tariff ultimately needs to cover the cost of grid reinforcements. In reality, it might be more socioeconomically efficient to regard the STES as a general load shifting tool, and not just a way of minimizing tariff payments. By participating in flexibility markets, the community could receive direct financial compensation for operating a STES in a grid friendly manner.

4.5.4   Line losses in 2030

The main difference between case 3 in the 2020- and 2030-scenario, in terms of line losses, is that line losses are reduced less in spring in the 2030-scenario, as shown i Figure 4.11. Since the 2030-scenario exports less surplus PV production, this change is to be expected. In the reference distribution grid, the community is the only load that acts as a prosumer. If there were more local production in the rest of the grid, the loss reduction in the 2020-scenario would probably not be as large.
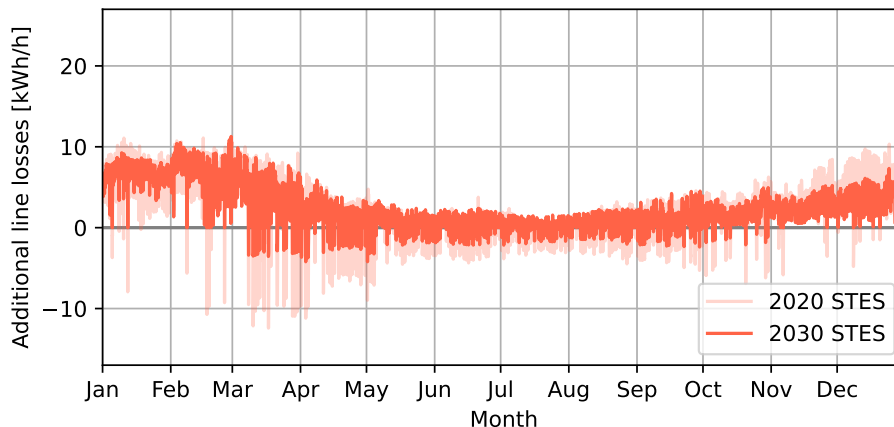

Figure 4.11: Difference in total line losses each hour after adding the case 3 community in the 2030-scenario to the CINELDI reference grid. The corresponding profile from the 2020-scenario is in the background.

Figure 4.11 also shows that the months of November and December experience a reduction in line losses, which corresponds to the reduction in power import caused by using more stored energy from the STES in these months.

One of the changes made in the 2030-scenario, is the removal of the 0.44 cents/kWh reward for exporting power paid by the DSO. The reward is based on the assumption that local production leads to reduced line losses. As can be seen in Figure 4.11, the reduction in losses is not substantial, so the removal of the reward makes sense. Instead, the 2030-scenario has a small volumetric tariff of 0.13 cents/kWh on export, in addition to the capacity tariff.

4.6 STES usage in 2020 and 2030

This section will compare how the STES is used to cover thermal demands in the 2020-scenario and the 2030-scenario. It is also a general discussion around the charging and discharging patterns observed. Figure 4.12 shows how much each thermal energy source contributes to the total thermal demand of the community each week of the year. The total height of each bar is identical in both scenarios, as they share thermal demand profiles. Appendix C.3 contains the corresponding plots for the other cases.
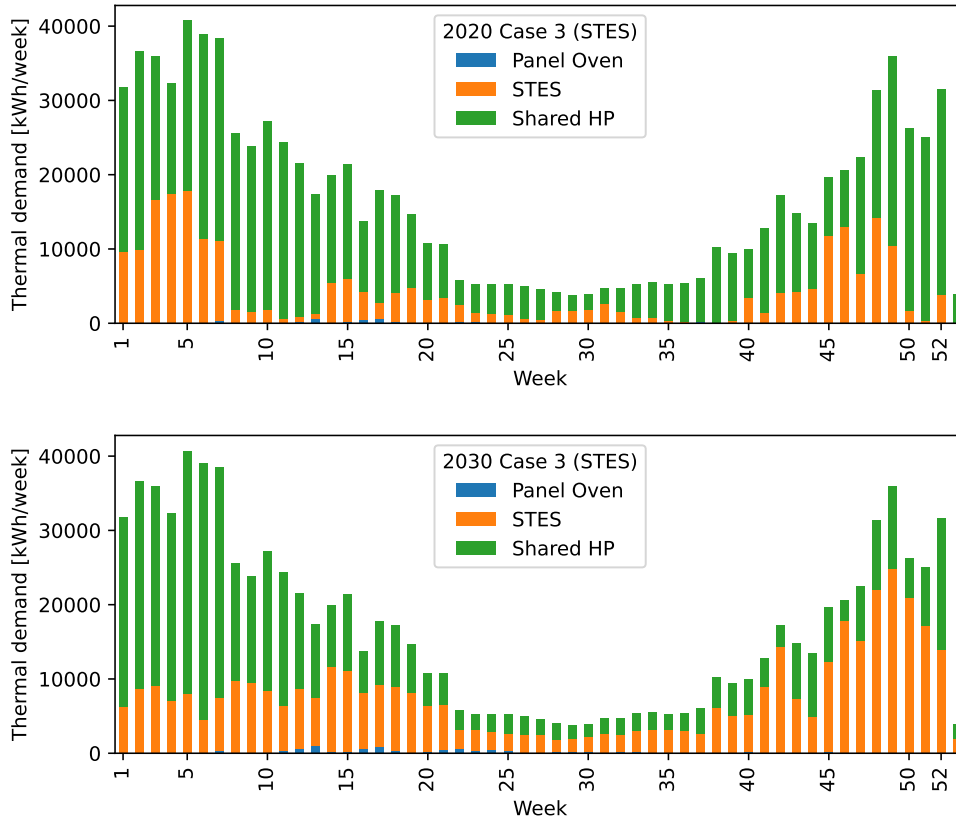

Figure 4.12: Sources of thermal energy meeting the thermal energy demand each week for case 3 in the 2020-scenario (top) and 2030-scenario (bottom).

The STES part of each bar represents the thermal energy that is discharged from the STES each week. The green part is thermal energy that goes directly from the shared heat pump to the district heating loop, without passing through the boreholes. The first observation is that the optimization model invests in a shared heat pump that is large enough to cover all thermal demands. In the 2020-scenario, the heat pump has a maximum output of 165 kW_{th}, while the 2030-scenario has a maximum output of 299 kW_{th}. The 2030-scenario has a larger heat pump to be able to charge the STES faster when there is a lot of surplus PV production, or the electricity price is low. Recall that the 2030-scenario has 23% less installed PV, but 49% lower peak export, than the 2020-scenario.

The only reason the panel oven is ever used, is to purposefully avoid exporting all surplus PV production, in a few hours of high production in March and May,

to avoid paying a higher export tariff those months. Normally, surplus power can be sent to the STES to limit export, but not if the borehole heat exchangers are already transferring heat to the surrounding ground at their maximum rate, according to Equation (3.22).

Another observation is that the 2030-scenario uses the STES a lot more, not just to store energy from summer to winter, but also to store daytime PV production to cover nighttime thermal demands during the entire summer. This is likely due to both the added export tariff in the 2030-scenario, but also the new price profile used. The 2030 electricity price profile has much larger variation between day and night prices, incentivizing intraday load shifting.

Another difference between the 2020-scenario and the 2030-scenario is that the first one prefers to use much of the stored energy in the middle of winter, while the latter uses more stored energy in the fall and early winter. This can be explained by the 2020-scenario having higher electricity prices at the beginning of the year. In the 2030-scenario, the prices are about the same all winter, which incentivizes discharging the STES earlier, as thermal losses increase when the STES is kept at higher temperatures for longer periods of time.

Figure 4.13 shows the state of charge in the STES each hour of the year, in the 2020- and 2030-scenarios. The relationship between state of charge and average temperature is linear, as indicated by the y-axis on the right-hand side of the plots.
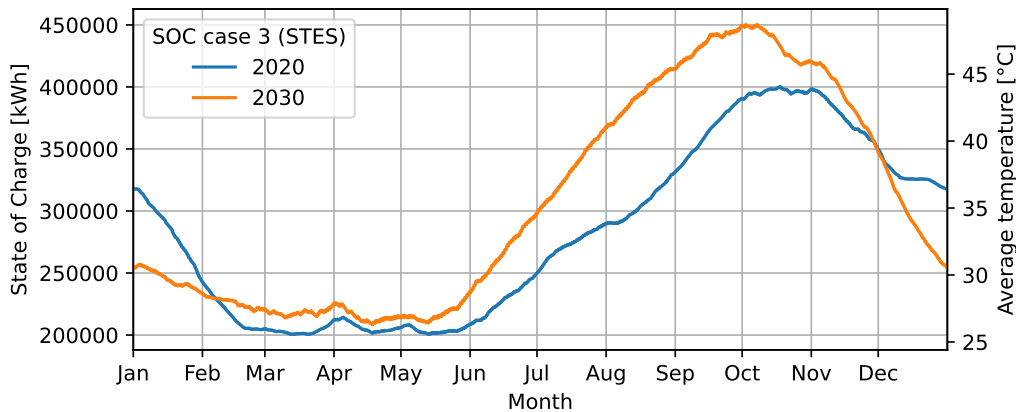

Figure 4.13: State of charge in the STES throughout the year in the 2020-scenario (blue) and 2030-scenario (orange).

The state of charge plot shows the seasonal trends in charging and discharging, but short term charging and discharging barely shows up, despite clearly occurring in Figure 4.12. The seasonal trends are however close to what is expected from a STES, with charging starting in June, charging up to a maximum temperature in October, and discharging in the winter. The plots show how the 2030-scenario charges their STES more, reaching almost $50\,°C$, while the 2020-scenario only reaches $45\,°C$. This is despite the fact that the 2030-scenario installed less PV. The changes made in the 2030-scenario have changed how the optimization model prioritizes energy usage to prioritize using energy storage more.

The maximum temperature of the STES was set to 60 °C, which the model reaches in neither scenario. This is because the optimization model has to pick a STES volume within a specified range. The smallest possible volume was 18 000 m^3, which was chosen in both scenarios. If given the chance, the model would have picked a smaller size, but all the STES systems used to estimate the volumetric cost of a borehole thermal energy storage system were at least that volume. This artificial limitation on volume only affects the price of the STES. During operation, volume only affects the relationship between state of charge and temperature. The model is not advanced enough to let volume affect losses, which means there is no incentive to having a larger STES, beyond having more storage capacity. In reality, increasing the volume of a STES system increases its efficiency, as relative heat losses decrease.

4.7   Energy sharing framework and STES

The load profiles shown in Figures 4.2 and 4.3 show that peak load is not reduced by communities investing in a shared PV system. In case 1, the peak load is the same as the peak energy demand without any PV. In case 2, peak load is reduced purely as a consequence of increased energy-efficiency from the heat pumps[1]. The shared PV system, enabled by the energy sharing framework, has no effect on peak load. This is consistent with a recent evaluation made by RME, which reports that the energy sharing framework does not reduce grid investment costs. Since the investment cost is covered by grid rent, and the energy sharing framework does not reduce the need for grid investments, it mainly results in moving costs from the group of consumers sharing a PV system, to other consumers [43].

The report highlights that DSOs and other actors think that the current energy sharing framework is a step in the right direction. There is, however, a need for more comprehensive solutions, for example in the form of local energy communities [43]. The results from the model demonstrate that prosumers alone are not a feasible solution for reducing the need for grid investments, as most prosumers have PV systems, that do little to reduce peaks. However, [5] argues that prosumers, with the addition of local energy storage systems, may play an important role in the future power grid system. It also highlights the importance of using thermal energy carriers when possible, instead of solely relying on electric energy.

A STES system fits this description, as it includes both local energy storage and the use of thermal energy to meet thermal demand. The STES enables local consumption of surplus PV production in summer, and uses the stored energy to reduce electric demands in winter. In the 2020-scenario, representing the current framework and grid rent model, the optimization model led to investing in large PV systems and selling a lot of surplus power, instead of storing the energy and using it to reduce peaks in winter as much as possible. In the 2030-scenario, with the added capacity tariff for export, the model installed less PV, but also used the STES more, as shown in the previous section, which means that the community's

---

[1]The peak reducing effect of heat pumps might be overestimated by the current model, as the heap pump's COP is not adjusted for colder outside temperatures in winter, as covered in Section 4.8.1.

self-consumption increased. The 2030-scenario's grid rent model is not meant as a suggestion for a new grid rent model, but rather an example to demonstrate how the community reacts when incentivized to sell less power. Alternatives to separate import and export tariffs can be static export limits, or dynamic limits based on the grid's instantaneous power balance. Some DSOs RME spoke with want the state of the local grid to be a factor when energy sharing is considered, as there is large variation in how well a given grid is equipped to handle local power export [43].

Adding an export tariff alone would only penalize local production, so a new framework should also contribute to the possibility and feasibility of implementing shared local energy storage. The current framework forces consumers to divide the shared resource into static percentages [43], and does not allow selling surplus to, and buying from, a shared storage system. This thesis has not considered how energy and costs should be divided among the consumers, but recognizes that a fair sharing scheme must be implemented in practice. A framework for local energy communities should be developed, that enables the legal entity to own and operate local energy production and local energy storage, and share the production and stored energy among the consumers in the community.

4.8   Model evaluation

This section will evaluate the assumptions made while constructing the model, and what effects they may have had on the final results. The results of the optimized objective functions will also be presented.

4.8.1   Consequences of fixed heat pump COP

Both the individual heat pumps in case 2, and the shared heat pump is case 3, have been given a fixed COP of 3 in the optimization model. In reality, the COP varies, depending on the temperature of the cold storage; i.e., the outside temperature. Heat pumps that use air as their cold storage generally have a low COP when the outside temperature is low, and may not work at all when the outside temperature reaches below $-25\,°\mathrm{C}$. Since the thermal demand increases when the outside temperature decreases, heat pumps might be unable to reduce peak demand in regions that experience these temperatures [5].

By using a fixed COP of 3, the optimization model in case 2 and 3 might need less electricity to meet thermal demands in winter, than real heat pumps would. This in turn causes the results to overestimate the reduction in peak load achieved by using a heat pump. However, as can be seen from Figure 3.5, the temperature never went below $-15\,°\mathrm{C}$, which means that peak load would still be reduced when using the heat pump.

When the STES is available, stored energy can be used for space heating. The STES discharging pump is not affected by the outside temperature, and uses way less electricity to deliver the same amount of thermal energy to the district heating loop, compared to the heat pump. If the heat pumps had been modeled with a variable COP, the energy storage might have been used more. High COP

in summer, and lower COP in winter, incentivizes load shifting, and can make up for some heat loss in the STES. Using a variable COP in the optimization model could have reduced peak load in case 3 further, and increased the difference between case 2 and case 3.

In order to better assess the peak reduction potential of heat pumps, with or without STES, the COP should have been a function of the outside temperature. Since the COP and the outside temperature are parameters, and not variables, the optimization model would remain linear, even if the relationship between COP and outside temperature is non-linear.

Finally, the model does not consider the use of heat pumps for space cooling in the summer, which is a popular use case for home air conditioning units. The GeoTermos installation at Fjell elementary school in Drammen, Norway, can choose to extract heat from the school building to both charge the STES and provide a more comfortable indoor climate at the same time [54].

4.8.2   Total cost of the community

As stated in the model description, the aim of the model is not to evaluate whether a STES is a profitable investment. The economic effect of having a STES system depends on several case specific factors, that the model only attempts to find plausible estimates for. Nevertheless, the optimization model attempts to minimize electricity costs by investing, so it is important that the cost of electricity and of the investments are realistic. These prices directly affect the amount of investments made, and how they are operated, and therefore affect the load profiles produced by the model. As this thesis primarily focuses on the community's grid use, these costs need to be realistic for the optimization model to produce plausible investment and operation behaviors.

Figure 4.14 shows the optimized yearly costs of the community in each case and scenario. The cost terms have been grouped into electricity costs, grid tariffs, and annualized investment costs for PV, individual heat pumps, and STES system. A breakdown of all objective terms can be found in Appendix D. As a point of reference, the electricity bills of Norwegian households typically add up to about 10 – 20 kNOK per year, depending on the type of building [92]. For a community with 100 households, this adds up to 87 – 174 k€.

The 2020-scenario cases install a lot of PV, which they sell to keep their electricity costs low. Grid tariffs are, however, not lowered by selling, and might even increase in months when peak export is higher than peak import. Thus, grid tariffs end up being a large part of the total costs. The combined electricity and grid tariff cost is a bit lower than the average cost for Norwegian households, but this can be explained by the optimization model community selling surplus PV power, which is subtracted from the electricity cost.

One investment cost that does not affect the demand profile, is the cost of building the STES. For both scenarios, the optimization model led to building the smallest possible STES available, as discussed in Section 4.8.3, which in practice means the STES is a fixed cost. This is in some ways good for the results, as the price of the STES is hard to estimate based on the limited amount of borehole STES
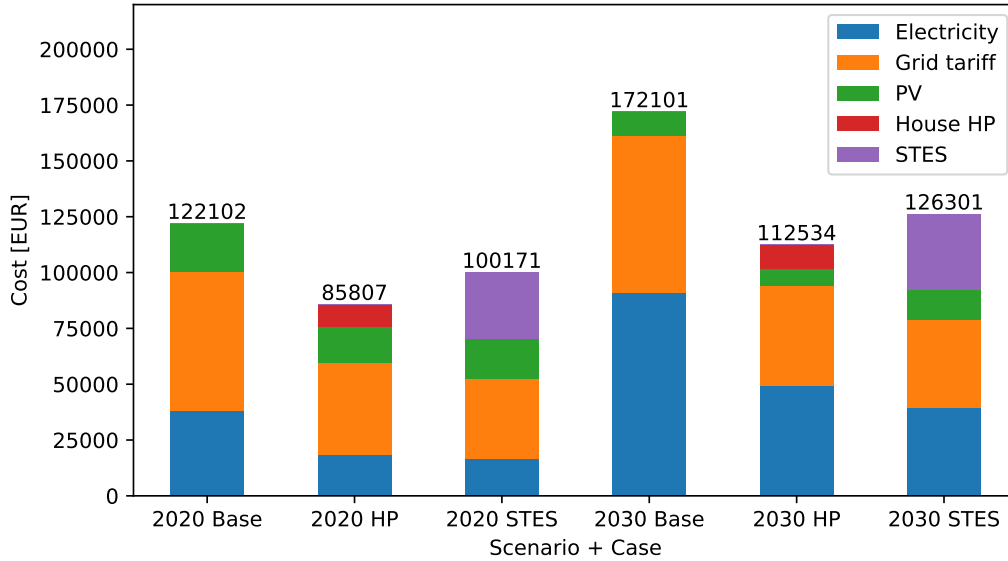
Figure 4.14: The annual cost of all cases in both scenarios, split into the objective terms. STES costs consists of cost of storage and heat pump, and grid tariff consists of capacity cost, volume cost, and taxes.

systems currently in operation, and lack of public operational data. The optimization model is ultimately not affected by the price of the STES, and can instead demonstrate how a community would minimize its costs, given that a STES is already available.

One cost that has not been included, is the cost of the district heating loop in case 3. This cost would be determined by the number and types of households, which means it would not affect the optimization model, other than adding a fixed cost on top of the total cost in case 3. Figure 4.14 shows that the total cost of building and operating a STES is somewhat higher than using only individual heat pumps, and lower than using only joule heating. Keeping in mind that total costs is not the primary output of the model, it is still interesting to compare these results to other studies. The case study from Furuset found that the alternative with a STES system was 3% more expensive than only using electricity for space heating. In the optimization models, case 3 ended up being 17% more expensive than case 2, which represents the best case for electric heating [59]. The results are thus somewhat comparable to the findings from that case study.

4.8.3 STES evaluation

In both the 2020-scenario and 2030-scenario, the case 3 community installs the smallest STES it is allowed to. Figure 4.13 shows that the maximum average temperature reached is $50 \, °C$, despite up to $60 \, °C$ being possible. This indicates that the community does not need a larger STES, no matter how cheap it would be to increase the STES volume. It is important to note that the model does not include the reduction in heat losses associated with a larger STES, which could affect this result. If the seasonal differences in temperature or electricity prices were higher, STES losses were lower, or the heat pump COP followed the outside

temperatures better, the STES might have seen more use.

It should be noted that some results discussed in this chapter only apply for STES systems that use PV driven heat pumps for charging. One advantage of using a PV driven heat pump is that the PV system can be used to meet electric demand in the summer, and that the heat pump can be charged with imported power. This increases the flexibility of the system, as it potentially could be used to avoid overvoltage if there is a lot of local PV production nearby. Historically, however, STES systems have often been charged by using either solar thermal collectors or waste heat, and these alternatives will not give the same results in regard to exported power during the summer. The reduction of peak load during the winter will, however, be the same regardless of the energy source being used to charge the STES initially.

4.8.4   Evaluation of assumptions

This section will evaluate some assumptions made in the model, and the impact they could have had on the results. The assumption expected to have the greatest impact on the final results, is the fixed COP, that has already been discussed in detail in Section 4.8.1.

Clairvoyant community

The optimization model is clairvoyant, and knows the electricity prices, electric demand, and thermal demand for each hour of the year. In reality, the electricity prices for consumers paying spot price is set the one day in advance, while electric demand is somewhat stable, and thermal demand depends on the outside temperature. The outside temperature is also unknown many months in advance, except from an expected seasonal variation.

To improve the optimization model, it would be more realistic to give it expected values for outside temperature and electricity prices, based on previous years. The model could use historic information, and exact electricity prices and temperatures for one day, and optimize one day at a time.

In addition, the model assumes perfect collaboration between the consumers. This would involve consumers having insight into their neighbors' energy demand, which would violate privacy considerations. It is also more realistic to assume that consumers would act in their own self-interest, and only minimize their own cost, which would require making a complementarity model, as discussed in Section 3.2.1.

Linear capacity tariff

The capacity tariff used in the model is linear, and charges consumers for the hour with the highest consumption each month. The capacity tariff this is based on is actually a stepped tariff, as shown in Figure 3.11, and consumers are charged for the mean capacity consumption of the three hours with the highest consumption from three separate days. This means that there is more leeway in the real tariff, than the one used in the model. However, since the optimization model acts like

perfect consumers, the stricter tariff should not cause a significant difference in the results. The model is designed to give a rough estimate of grid usage, and it is assumed that other parameters, such as the load profiles, electricity prices, and PV system prices, have a greater impact on the results than modeling the capacity tariff rules perfectly.

Load flexibility

Limited load flexibility is offered to the optimization model to reduce peak load or make better use of available PV production in case 1 and 2. Case 1 has virtually no flexibility, and case 2 can only choose to use less efficient heating when there is surplus PV production. Real consumers would have at least some choices that the consumers in the model do not get, such as when to turn on the dishwasher, or charge an electric vehicle.

Since only case 3 is given any substantial flexibility, the ability to respond to price signals is skewed in favor of case 3. It is, however, realistic to assume that a shared STES with intelligent control mechanisms is more capable of optimizing charging and discharging based on price signals, or other incentives like local flexibility markets, compared to individual consumers, as explained in Section 2.3.2.

STES operates in steady state

One of the constraints in the optimization model, is that the STES SOC at the beginning of the year must be the same as the SOC at the end of the year. This constraint means that the STES operates in steady state in the simulated year. In reality, it normally takes 3 – 5 years for a STES system to reach steady state. During the first few years, heat losses are high, as the temperature of the surrounding ground is low, and only small amounts of stored energy can be extracted to cover thermal demands [13]. This charging period must be taken into account when calculating the total investment cost of a STES system.

Methods for shortening the initial starting period are being developed, and some have managed to reach steady state within 1 – 2 years [13]. When building new residential communities, the STES can be built first, and begin charging while the rest of the buildings in the community that it belongs to is being built.

FIVE

CONCLUSION

The aim of this thesis was to evaluate the load shifting potential of a local energy community with a shared seasonal thermal energy storage (STES), compared to similar communities without a STES. A linear optimization model was developed to represent a community with 100 households, and their hourly demands for electric and thermal energy for one year. Two reference cases were also developed, representing the same community without a STES system. One case could invest in individual heat pumps, while the other had to use joule heating. These reference cases represent the best case and worst case for grid use without energy storage, respectively. All cases could invest in a shared local PV system for local energy production. The optimization model outputs aggregated load profiles for the community, that were added to CINELDI's reference distribution grid to evaluate the community's grid use in a broader context.

The results showed that when the STES was available, power import was reduced in the winter and increased in the summer, which resulted in a reduction of peak power import, compared to both reference cases. The peak reduction was high compared to the case using joule heating, but less prevalent compared to the case with heat pumps. The STES case showed a slight improvement from the heat pump case, which was caused by using stored thermal energy in the STES. When the load profiles were added to the distribution grid, the STES case increased the grid's peak load the least. The heat pump case and the STES case had the same total load, but the STES case shifted more load away from the distribution grid's aggregated peak load hours.

By moving power import away from peak load hours in the grid, the STES case showed slightly lower line losses in winter than heat pumps alone. By using stored thermal energy, the heat pump can be used less in the winter, lowering electric demands. The STES case installed more PV capacity than the heat pump case, but it also used more of the PV production locally, instead of selling it to the power market. Peak power export is thus lower in the STES case. Exporting local power production may lead to a reduction in line losses, as it did for all cases in April and May. However, there was minimal reduction in line losses in

during the summer months, even though export rates were high. This indicates that with enough local production, it becomes more beneficial for the power grid that the energy is used locally or stored for later, instead of being exported, as power export can increase the likelihood of voltage violations occurring.

To investigate how the model responds to different price signals and tariffs, a 2030-scenario was developed, with a synthetic 2030 electricity price profile, and grid tariffs incentivizing exporting less power. With these incentives, the STES community shifts more load away from both the community's and the grid's peak, reducing seasonal variations further. These incentives could also be added in the form of flexibility markets, or agreements with the DSO, instead of through added grid tariffs. In the 2030-scenario, with incentives to export less power, all cases installed smaller PV systems. However, the STES community reduced its installed PV capacity the least, as it could use surplus PV production to charge the STES, while reducing its total power export. This means that even though the local energy production was reduced, the consumption of local energy increased.

5.1   Future work

To obtain a better understanding of the socioeconomic effects of local energy communities with STES, the following factors should be subjects in future work.

The change in grid strain of existing STES systems, such as the GeoTermos as Fjell should be estimated. It is currently difficult to evaluate the accuracy of simulated results, as there is little information from real systems. Obtaining this information would make it easier to make models that can predict the grid impact of implementing a STES system in different grids.

Models should also use a heat pump COP that varies with the outside temperature in order to obtain more realistic comparisons regarding the peak reduction potential and optimal STES use.

It is also interesting to explore STES systems in the context of local flexibility markets. STES systems' potential role as aggregators in flexibility markets should be investigated further, and compared to other flexibility and load shifting methods, such as batteries. These evaluations should focus on cold climate countries with high seasonal variations, as STES systems will be most relevant in these areas.

Grid tariff models with better incentive compatibility between consumers and system operators should be developed, to incentivize socioeconomically efficient and grid friendly local energy production and grid use.

[1]   Miljødirektoratet. "Miljømål 5.1." Miljøstatus. Apr. 9, 2024. URL: https://miljostatus.miljodirektoratet.no/miljomal/klima/miljomal-5.1 (visited on 04/20/2024).

[2]   Lars Sørgard et al. "Mer av alt - raskere - Energikommisjonens rapport." NOU 2023:3. ISBN: 978-82-583-1537-4. Feb. 1, 2023.

[3]   *Act relating to Norway's climate targets (Climate Change Act)*. June 16, 2017.

[4]   Hanne Birgitte Laird. "Klimakur 2030: Tiltak og virkemidler mot 2030." URL: https://www.miljodirektoratet.no/klimakur. 2020.

[5]   Nils Kristian Nakstad et al. "Nett i tide – om utvikling av strømnettet." Utredning NOU 2022:6. ISBN: 978-82-583-1501-5. Oslo: Strømnettutvalget, June 14, 2022, p. 220.

[6]   Rita Kleven and Eivind Aabakken. "Sliter med å bygge nok strømnett: 450 bedrifter står i kø." NRK. Oct. 9, 2023. URL: https://www.nrk.no/trondelag/sliter-med-a-bygge-nok-stromnett_-450-bedrifter-star-i-ko-1.16573562 (visited on 05/06/2024).

[7]   "Documenting a Decade of Cost Declines for PV Systems." NREL. URL: https://www.nrel.gov/news/program/2021/documenting-a-decade-of-cost-declines-for-pv-systems.html (visited on 04/25/2024).

[8]   "Plusskunder - NVE." URL: https://www.nve.no/reguleringsmyndigheten/regulering/nettvirksomhet/nettleie/tariffer-for-produksjon/plusskunder/ (visited on 04/01/2024).

[9]   Janne Hirvonen, Hassam ur Rehman, and Kai Sirén. "Techno-economic optimization and analysis of a high latitude solar district heating system with seasonal storage, considering different community sizes." In: *Solar Energy* 162 (Mar. 1, 2018), pp. 472–488. DOI: 10.1016/j.solener.2018.01.052.

[10] Martin Lillebo, Henrik Kirkeby, and Thor Holm. "Prosumenters innvirkning på lavspente distribusjonsnett." ISBN: 978-82-410-2086-5. RME, Sept. 2020.

[11] Michael Lanahan and Paulo Cesar Tabares-Velasco. "Seasonal Thermal-Energy Storage: A Critical Review on BTES Systems, Modeling, and System Design for Higher System Efficiency." In: *Energies* 10.6 (June 2017), p. 743. DOI: 10.3390/en10060743.

[12] Martin Skancke et al. "The transition to low emissions Climate policy choices towards 2050." NOU 2023:25. Ministry of Climate and Environment, Oct. 27, 2023.

[13] Fang Guo et al. "Large-scale living laboratory of seasonal borehole thermal energy storage system for urban district heating." In: *Applied Energy* 264 (Apr. 15, 2020), p. 114763. DOI: 10.1016/j.apenergy.2020.114763.

[14] Tianrun Yang et al. "Seasonal thermal energy storage: A techno-economic literature review." In: *Renewable and Sustainable Energy Reviews* 139 (Apr. 1, 2021), p. 110732. DOI: 10.1016/j.rser.2021.110732.

[15] J. Xu, R. Z. Wang, and Y. Li. "A review of available technologies for seasonal thermal energy storage." In: *Solar Energy* 103 (May 1, 2014), pp. 610–638. DOI: 10.1016/j.solener.2013.06.006.

[16] Harry Mahon et al. "A review of thermal energy storage technologies for seasonal loops." In: *Energy* 239 (Jan. 15, 2022), p. 122207. DOI: 10.1016/j.energy.2021.122207.

[17] Frida Berglund, James Lam, and Kjersti Aarrestad. "Lagringsteknologier for fleksibilitet i energisystemet." DNV, Nov. 20, 2020.

[18] Hanne Kauko et al. "Assessing the potential of seasonal thermal storage for local energy systems: Case study for a neighborhood in Norway." In: *Smart Energy* 6 (May 1, 2022), p. 100075. DOI: 10.1016/j.segy.2022.100075.

[19] A. Lyden et al. "Seasonal thermal energy storage in smart energy systems: District-level applications and modelling approaches." In: *Renewable and Sustainable Energy Reviews* 167 (Oct. 1, 2022), p. 112760. DOI: 10.1016/j.rser.2022.112760.

[20] "The electricity grid." Norwegian Energy. URL: https://energifaktanorge.no/en/norsk-energiforsyning/kraftnett/ (visited on 04/02/2024).

[21] "Security of electricity supply." Norwegian Energy. URL: https://energifaktanorge.no/en/norsk-energiforsyning/forsyningssikkerhet/ (visited on 04/02/2024).

[22] "Ny nettleie (fra 1. juli 2022) - NVE." NVE. URL: https://www.nve.no/reguleringsmyndigheten/kunde/nett/ny-nettleie-fra-1-juli-2022/ (visited on 05/06/2024).

[23] "Last ned grunndata." Statnett. Mar. 21, 2024. URL: https://www.statnett.no/for-aktorer-i-kraftbransjen/tall-og-data-fra-kraftsystemet/last-ned-grunndata/ (visited on 03/27/2024).

[24] "Joule heating." Encyclopedia Britannica. Mar. 1, 2024. URL: https://www.britannica.com/science/Joules-law (visited on 04/22/2024).

[25] "How a heat pump works – The Future of Heat Pumps – Analysis." IEA. URL: https://www.iea.org/reports/the-future-of-heat-pumps/how-a-heat-pump-works (visited on 04/22/2024).

[26] Paul A. Tipler and Gene Mosca. *Physics for Scientists and Engineers with Modern Physics*. 6th. ISBN: 9781319155988. W.H. Freeman & Company, 2017.

[27] "Generation of Electricity and District heating - Technology descriptions and projections for long-term energy system planning." ISBN: 978-87-94447-08-9. Copenhagen, Denmark: Danish Energy Agency, Aug. 2016.

[28] Karen Byskov Lindberg, Synne Krekling Lien, and Arnkell Jonas Petersen. "Samtidighet og sammenlagring COFACTOR-rapport Begrepsforklaring og case-studie." ISBN: 978-82-14-07584-7. SINTEF Community, Oct. 25, 2022.

[29] Swati Sharda, Mukhtiar Singh, and Kapil Sharma. "Demand side management through load shifting in IoT based HEMS: Overview, challenges and opportunities." In: *Sustainable Cities and Society* 65 (Feb. 1, 2021), p. 102517. DOI: 10.1016/j.scs.2020.102517.

[30] Jørgen Bjørndalen et al. "Fra brettet til det smarte nettet - Ansvar for driftskoordinering i kraftsystemet." RME, May 7, 2020.

[31] Ove Wolfgang et al. "Prosumers' role in the future energy system." ISBN: 978-82-93198-27-7. Nov. 13, 2018.

[32] Tor Håkon Jackson Inderberg, Kerstin Tews, and Britta Turner. "Is there a Prosumer Pathway? Exploring household solar energy development in Germany, Norway, and the United Kingdom." In: *Energy Research & Social Science* 42 (Aug. 1, 2018), pp. 258–269. DOI: 10.1016/j.erss.2018.04.006.

[33] "Solkraft - NVE." URL: https://www.nve.no/energi/energisystem/solkraft/ (visited on 04/23/2024).

[34] Oda Andrea Hjelme et al. "Norsk solkraft 2022 – innenlands og eksport." Multiconsult, 2022.

[35] Amine Allouhi et al. "Up-to-date literature review on Solar PV systems: Technology progress, market status and R&D." In: *Journal of Cleaner Production* 362 (Aug. 15, 2022), p. 132339. DOI: 10.1016/j.jclepro.2022.132339.

[36] Matthias Hofmann, Sigurd Bjarghov, and Stian Nessa. "Norwegian hourly residential electricity demand data with consumer characteristics during the European energy crisis." In: *Data in Brief* 51 (Dec. 1, 2023), p. 109687. DOI: 10.1016/j.dib.2023.109687.

[37] Iain Staffell and Stefan Pfenninger. "Using bias-corrected reanalysis to simulate current and future wind power output." In: *Energy* 114 (Nov. 1, 2016), pp. 1224–1239. DOI: 10.1016/j.energy.2016.08.068.

[38] Stefan Pfenninger and Iain Staffell. "Long-term patterns of European PV output using 30 years of validated hourly reanalysis and satellite data." In: *Energy* 114 (Nov. 1, 2016), pp. 1251–1265. DOI: 10.1016/j.energy.2016.08.060.

[39] "Hvordan får solkraft fra Norges hustak inn i kraftsystemet?" Fornybar Norge. URL: https://www.fornybarnorge.no/solenergi/rapport-2022/ (visited on 05/06/2024).

[40] "NVEs svar på oppdrag om solkraft og annen lokal energiproduksjon." NVE, Feb. 5, 2024.

[41] Hanne Sæle et al. "Assessment of flexibility in different ancillary services for the power system." In: Sept. 2020, pp. 1–6. DOI: 10.1109/EEM49802.2020.9221996.

[42] Åsmund Jenssen et al. "Aggregatorrollen, fleksibilitetsmarkeder og forretningsmodeller i energisystemet." 2017-20. ISBN: 978-82-8368-017-1. July 12, 2017.

[43] Bjørnar Araberg Fladen et al. "Deling av overskuddsproduksjon - Utredning for Energidepartementet." Utredning for Energidepartementet 1. RME, Jan. 2024.

[44] Bjørnar Araberg Fladen et al. "Ordning for deling av fornybar kraftproduksjon - Forslag til endringer i forskrift om kontroll av nettvirksomhet og forskrift om kraftomsetning og nettjenester." RME, Aug. 2021.

[45] Andreas Uihlein and Aura Caramizaru. *Energy communities: an overview of energy and social innovation.* ISBN: 978-92-76-10713-2. Publications Office of the European Union, 2020.

[46] Andrei Z. Morch. "Scenarios for implementation of Energy Communities in Norway." SINTEF. URL: https://www.sintef.no/en/projects/2020/fine/scenarier-for-implementering-av-energisamfunn-i-norge/scenarier-for-implementering-av-energisamfunn-i-norge/ (visited on 04/24/2024).

[47] Directorate-General for Energy. "In focus: Energy communities to transform the EU's energy system." Dec. 13, 2022. URL: https://energy.ec.europa.eu/news/focus-energy-communities-transform-eus-energy-system-2022-12-13_en (visited on 04/24/2024).

[48] Julian Hentschel et al. "Descriptive study of Local Energy Communities." 1-2019. ISBN: 978-82-8368-039-3. Jan. 2019.

[49] "The power market." Energy Facts Norway. URL: https://energifaktanorge.no/en/norsk-energiforsyning/kraftmarkedet/ (visited on 05/06/2024).

[50] Jon Gustav Kirkerud et al. "NVE Rapport nr. 25/2023: Langsiktig kraftmarkedsanalyse 2023 : energiomstillingen – en balansegang." ISBN: 978-82-410-2285-2. Nov. 2023.

[51] Energidepartementet. *Forskrift om økonomisk og teknisk rapportering, inntektsramme for nettvirksomheten og tariffer.* Jan. 22, 2024.

[52] "Grid rent prices for private customers." Elvia. Jan. 16, 2024. URL: https://www.elvia.no/hva-er-elvia/elvia-transports-the-electricity-to-your-home/grid-rent-prices-for-private-customers/ (visited on 03/21/2024).

[53] Kjell Rune Verlo et al. "Oppsummering av høring og anbefaling til endringer i nettleiestrukturen." 6/2020. ISBN: 978-82-410-2059-9. Oslo, Norway: RME, Sept. 2020.

[54] Enova. "GeoTermos, Fjell2020 | Støttet prosjekt." Enova. URL: https://www.enova.no/om-enova/om-organisasjonen/teknologiportefoljen/geotermos-fjell2020/ (visited on 02/15/2024).

[55] M. Aldubyan and A. Chiasson. "Thermal Study of Hybrid Photovoltaic-Thermal (PVT) Solar Collectors Combined with Borehole Thermal Energy Storage Systems." In: *Energy Procedia*. Power and Energy Systems Engineering 141 (Dec. 1, 2017), pp. 102–108. DOI: 10.1016/j.egypro.2017.11.020.

[56] Thomas Schmidt et al. "Design Aspects for Large-scale Pit and Aquifer Thermal Energy Storage for District Heating and Cooling." In: *Energy Procedia* 149 (Sept. 1, 2018), pp. 585–594. DOI: 10.1016/j.egypro.2018.08.223.

[57] S. Bespalko, A. Miranda, and O. Halychyi. "Overview of the existing heat storage technologies: sensible heat." In: *Acta Innovations* 28 (2018), pp. 82–113.

[58] Farzin M. Rad and Alan S. Fung. "Solar community heating and cooling system with borehole thermal energy storage – Review of systems." In: *Renewable and Sustainable Energy Reviews* 60 (July 1, 2016), pp. 1550–1561. DOI: 10.1016/j.rser.2016.03.025.

[59] Hanne Kauko. "Sesonglagring av varme for lokale energisystem – analyse av potensialet på Furuset." In: 35 (2021).

[60] "Nyhavna i Trondheim – pilottester for høytemperatur sesongvarmelager (HT-BTES) og integrering i fjernvarmesystemet for styrket fleksibilitet." Enova. URL: https://www.enova.no/om-enova/om-organisasjonen/teknologiportefoljen/nyhavna-i-trondheim--pilottester-for-hoytemperatur-sesongvarmelager-ht-btes-og-integrering-i-fjernvarmesystemet-for-styrket-fleksibilitet/ (visited on 05/07/2024).

[61] Bastian Welsch. "Technical, Environmental and Economic Assessment of Medium Deep Borehole Thermal Energy Storage Systems." Doktor-Ingenieur. Darmstadt: Technische Universität Darmstadt, 2019.

[62] D. Bauer et al. "German central solar heating plants with seasonal heat storage." In: *Solar Energy*. International Conference CISBAT 2007 84.4 (Apr. 1, 2010), pp. 612–623. DOI: 10.1016/j.solener.2009.05.013.

[63] M. Jradi, C. Veje, and B. N. Jørgensen. "Performance analysis of a soil-based thermal energy storage system using solar-driven air-source heat pump for Danish buildings sector." In: *Applied Thermal Engineering* 114 (Mar. 5, 2017), pp. 360–373. DOI: 10.1016/j.applthermaleng.2016.12.005.

[64] Arefeh Hesaraki, Sture Holmberg, and Fariborz Haghighat. "Seasonal thermal energy storage with heat pumps and low temperatures in building projects—A comparative review." In: *Renewable and Sustainable Energy Reviews* 43 (Mar. 1, 2015), pp. 1199–1213. DOI: 10.1016/j.rser.2014.12.002.

[65] Etienne Saloux and José A. Candanedo. "Model-based predictive control to minimize primary energy use in a solar district heating system with seasonal thermal energy storage." In: *Applied Energy* 291 (June 2021), p. 116840. DOI: 10.1016/j.apenergy.2021.116840.

[66] Helge Skarphagen et al. "Design Considerations for Borehole Thermal Energy Storage (BTES): A Review with Emphasis on Convective Heat Transfer." In: *Geofluids* 2019 (Apr. 22, 2019). Publisher: Hindawi, e4961781. DOI: 10.1155/2019/4961781.

[67] Bruce Sibbitt et al. "The Performance of a High Solar Fraction Seasonal Storage District Heating System – Five Years of Operation." In: *Energy Procedia* 30 (Dec. 31, 2012), pp. 856–865. DOI: `10.1016/j.egypro.2012.11.097`.

[68] Alejandro Pena-Bello et al. "Balancing DSO interests and PV system economics with alternative tariffs." In: *Energy Policy* 183 (Dec. 1, 2023), p. 113828. DOI: `10.1016/j.enpol.2023.113828`.

[69] Iver Bakken Sperstad et al. "Reference data set for a Norwegian medium voltage power distribution system." In: *Data in Brief* 47 (Apr. 1, 2023), p. 109025. DOI: `10.1016/j.dib.2023.109025`.

[70] Lill Mari Engan. "LillMari/LoadShiftSTES." URL: `https://github.com/LillMari/LoadShiftSTES` (visited on 05/10/2024).

[71] *Python*. Version 3.11.4. URL: `https://www.python.org`. June 7, 2023.

[72] *Gurobi*. Version 11.0. URL: `https://www.gurobi.com/`.

[73] Meteorologisk institutt. "Frost API." https://frost.met.no/index.html.

[74] Kamilla Heimar Andersen et al. "Further development and validation of the "PROFet" energy demand load profiles estimator." In: 2021 Building Simulation Conference. Sept. 1, 2021. DOI: `10.26868/25222708.2021.30159`.

[75] K. B. Lindberg, S. J. Bakker, and I. Sartori. "Modelling electric and heat load profiles of non-residential buildings for use in long-term aggregate load forecasts." In: *Utilities Policy* 58 (June 1, 2019), pp. 63–88. DOI: `10.1016/j.jup.2019.03.004`.

[76] "Flexibility Suite API." https://flexibilitysuite.byggforsk.no/index.html. URL: `https://flexibilitysuite.byggforsk.no/index.html` (visited on 03/29/2024).

[77] Randi Kalskin Ramstad et al. "Sluttrapport Fjell2020 konseptutredning miljøløsninger." Oct. 17, 2017, p. 28.

[78] "Geologi – Oslo byleksikon." oslobyleksikon. URL: `https://oslobyleksikon.no/side/Geologi` (visited on 04/15/2024).

[79] David Banks. *An Introduction to Thermogeology: Ground Source Heating and Cooling*. Jan. 30, 2009.

[80] Sheikh Khaleduzzaman Shah, Lu Aye, and Behzad Rismanchi. "Seasonal thermal energy storage system for cold climate zones: A review of recent developments." In: *Renewable and Sustainable Energy Reviews* 97 (Dec. 1, 2018), pp. 38–49. DOI: `10.1016/j.rser.2018.08.025`.

[81] E. Audsley and J. Wheeler. "The annual cost of machinery calculated using actual cash flows." In: *Journal of Agricultural Engineering Research* 23.2 (1978), pp. 189–201. DOI: `10.1016/0021-8634(78)90048-3`.

[82] Kåre P. Hagen et al. "Samfunnsøkonomiske analyser." 2012: 16. ISBN: 978-82-583-1153-6. Oslo, Norway: Departementenes servicesenter Informasjonsforvaltning, Oct. 3, 2012, p. 169.

[83] "Kostnader for kraftproduksjon - NVE." URL: https://www.nve.no/energi/analyser-og-statistikk/kostnader-for-kraftproduksjon/ (visited on 04/05/2024).

[84] "Forbruk, produksjon og installert effekt." Elhub. URL: https://elhub.no/data/forbruk-og-produksjon/ (visited on 05/07/2024).

[85] "Pris varmepumpe og installasjon – Varmepumpeforeningen." Varmepumpe-info.no. URL: https://www.varmepumpeinfo.no/pris-pa-varmepumpe-og-installasjon (visited on 04/16/2024).

[86] Thomas Leypoldt Marthinsen. "Hvor stor varmepumpe trenger jeg? | TjenesteTorget." Oct. 21, 2019. URL: https://tjenestetorget.no/blogg/hvor-stor-varmepumpe-trenger-jeg (visited on 04/16/2024).

[87] Florian Knobloch et al. "FTT:Heat — A simulation model for technological change in the European residential heating sector." In: *Energy Policy* 153 (June 1, 2021), p. 112249. DOI: 10.1016/j.enpol.2021.112249.

[88] Steven Meyers, Bastian Schmitt, and Klaus Vajen. "The future of low carbon industrial process heat: A comparison between solar thermal and heat pumps." In: *Solar Energy* 173 (Oct. 1, 2018), pp. 893–904. DOI: 10.1016/j.solener.2018.08.011.

[89] Jan Pecinovsky and Frank Boerman. *entsoe-py*. URL: original-date:2017-07-12T13:17:39Z. Apr. 16, 2024.

[90] "Plusskunder - NVE." Nov. 2, 2023. URL: https://www.nve.no/reguleringsmyndigheten/regulering/nettvirksomhet/nettleie/tariffer-for-produksjon/plusskunder/ (visited on 05/07/2024).

[91] "Nettleiepriser for regionalnett." URL: https://www.elvia.no/nettleie/alt-om-nettleiepriser/nettleiepriser-for-regionalnett/ (visited on 05/07/2024).

[92] "Gjennomsnittlig årsforbruk av strøm fordeler seg slik." Strømtest.no. URL: https://www.xn--strmtest-74a.no/calculator/stromforbruk/ (visited on 05/05/2024).

DERIVATION OF STES PUMP ENERGY RELATIONS

The following section will derive the expressions used for thermal energy delivered from the STES and electric energy consumed by the STES discharging pump.

A.1 Thermal energy delivered from STES

The thermal energy delivered from the boreholes heat exchangers can be expressed as follows:

$$Q_h = \frac{\nabla_h \cdot \text{COP}^\nabla}{\text{COP}^\nabla - 1}. \tag{A.1}$$

When modelling the STES pump, it is taken into account that the pump needs some electric energy E_{el} to move energy from the boreholes Q_c to the district heating loop Q_h:

$$Q_h = Q_c + E_{\text{el}}. \tag{A.2}$$

The coefficient of performance COP^∇ of the pump is defined as

$$COP^\nabla = \frac{Q_h}{E_{\text{el}}} \tag{A.3}$$

By solving Equation (A.3) for E_{el}, and using the expression in Equation (A.2) we get

$$Q_h = Q_c + \frac{Q_h}{COP^\nabla}. \tag{A.4}$$

Which can be solved for Q_h:

$$Q_h = Q_c + \frac{Q_h}{COP^\nabla}$$

$$Q_h - \frac{Q_h}{COP^\nabla} = Q_c$$

$$Q_h \left(1 - \frac{1}{COP^\nabla}\right) = Q_c$$

$$Q_h(COP^\nabla - 1) = Q_c COP^\nabla$$

$$Q_h = \frac{Q_c COP^\nabla}{COP^\nabla - 1}$$

In this thesis, ∇_h is used instead of Q_c for thermal energy discharged from the STES, which gives us the final expression

$$Q_h = \frac{\nabla_h COP^\nabla}{COP^\nabla - 1}. \tag{A.5}$$

A.2 Electricity delivered to STES pump

The electric power consumption of the heat pump can be expressed as

$$E_{\text{el}} = \frac{\nabla_h}{COP^\nabla - 1} \tag{A.6}$$

In order to derive this expression, we begin with Equations (A.2) and (A.3) again. This time, we solve Equation (A.3) for Q_h, which gives us

$$Q_h = E_{\text{el}} COP^\nabla. \tag{A.7}$$

Equation (A.7) can now substitute Q_h in Equation (A.2):

$$E_{\text{el}} COP^\nabla = Q_c + E_{\text{el}}. \tag{A.8}$$

Solving Equation (A.8) for E$_{\text{el}}$ gives us:

$$E_{\text{el}}(COP^\nabla - 1) = Q_c$$

$$E_{\text{el}} = \frac{Q_c}{COP^\nabla - 1}.$$

Again, ∇_h is used in place of Q_c, which gives us the expression used in this thesis:

$$E_{\text{el}} = \frac{\nabla_h}{COP^\nabla - 1}. \tag{A.9}$$

STES CHARGING AND DISCHARGING CONSTRAINTS

The constraints (3.22) and (3.23) limit how quickly the average temperature of the STES may change at a given hour. This section will derive the coefficients in the linear equations that limit the maximum change in temperature when charging and discharging the STES.

B.1   Charging constraint coefficients

When the STES is close to fully charged, the temperature difference between the ground and the water is low, slowing down the possible transfer of heat into the ground. This is modeled using a constraint based on Figure B.1.

Expressing this constraint as a linear combination of variables is made more difficult by the fact that average ground temperature in hour h, T_h, is not a variable. Instead, it is given by the formula

$$T_h = T^{\text{BASE}} + \frac{\text{SOC}_h}{V c_v}, \tag{B.1}$$

which is not linear, since one of the terms has the variable V in the denominator. By multiplying (B.1) by V, a linear expression is found:

$$T_h V = T^{\text{BASE}} V + \frac{\text{SOC}_h}{c_v}. \tag{B.2}$$

The increase in average temperature δT_h due to charging the STES in a given hour h can be expressed as

$$\delta T_h = \frac{\eta^\Delta \Delta_h}{V c_v}, \tag{B.3}$$

where $\eta^\Delta \Delta_h$ is the thermal energy supplied to the storage after considering transportation losses, V is the storage volume, and c_v is the volumetric heat capacity of the storage medium.
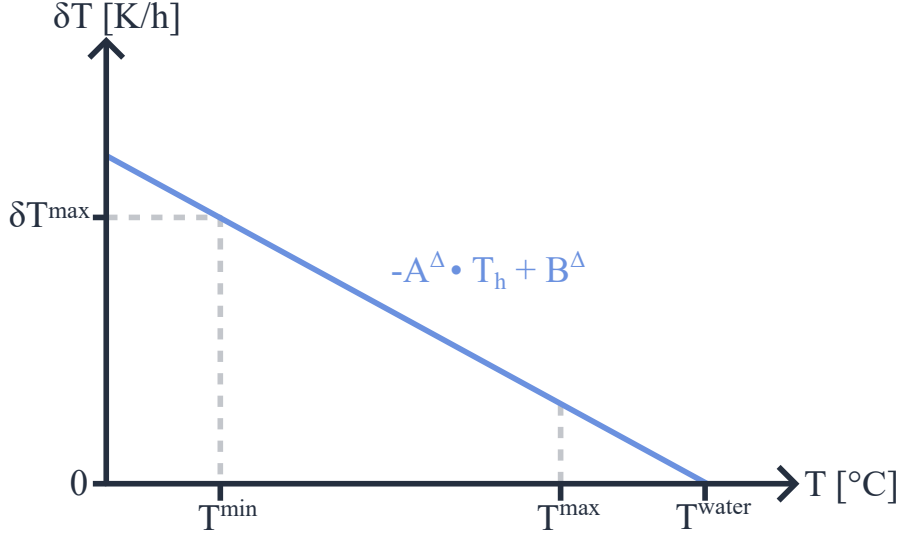
Figure B.1: Constraint (3.22) shown in a plot where the x-axis is the current temperature, and the y-axis is the maximum possible increase in temperature this hour. The constraint forces the rate of charging to be below the blue line. T^{min} and T^{max} is the operating range of the STES. T^{water} is the temperature of the water used to heat the STES.

As illustrated in Figure B.1, the change in temperature δT_h has to be less than or equal to the blue line limiting the maximum temperature increase:

$$\delta T_h \leq -A^\Delta T_h + B^\Delta. \tag{B.4}$$

Substituting the expression in Equation (B.3) for δT_h gives us

$$\frac{\eta^\Delta \Delta_h}{V c_v} \leq -A^\Delta T_h + B^\Delta. \tag{B.5}$$

To make the expression linear, it is multiplied by the volume V:

$$\frac{\eta^\Delta \Delta_h}{c_v} \leq -A^\Delta T_h V + B^\Delta V. \tag{B.6}$$

As shown in Equation (B.2), the expression $T_h V$ is a linear combination of variables, making this inequality a fully linear constraint.

To find the coefficients A^Δ and B^Δ, the function must be evaluated in two points. The first point is where the storage temperature is the same as the water temperature. When the storage has reached this temperature, the water is not able to raise the temperature further:

$$-A^\Delta T^{\text{water}} + B^\Delta = 0 \tag{B.7}$$

Solving Equation (B.7) for B^Δ yields:

$$B^\Delta = A^\Delta T^{\text{water}}. \tag{B.8}$$

The maximum increase in temperature, which is a parameter that has been calculated separately, is only possible when the storage temperature is at its lowest, T^{min}:

$$-A^\Delta T^{\text{min}} + B^\Delta = \delta T^{\text{max}}. \tag{B.9}$$

Substituting the expression found in Equation (B.8) for B^Δ in Equation (B.9) yields:

$$A^\Delta(T^{\text{water}} - T^{\text{min}}) = \delta T^{\text{max}}. \tag{B.10}$$

Solving for A^Δ yields:

$$A^\Delta = \frac{\delta T^{\text{max}}}{(T^{\text{water}} - T^{\text{min}})}. \tag{B.11}$$

B.2   Discharging constraint coefficients

The constraint limiting the rate of discharging the STES are derived similarly to the charging constraint. However, since $-\delta T_h$ is now defined as the decrease in average temperature due to discharging in hour h, given as:

$$-\delta T_h = \frac{\nabla_h}{\eta^\nabla V c_v}. \tag{B.12}$$

The maximum discharging rate slows down when the temperature decreases. Temperature change is therefore limited according to:

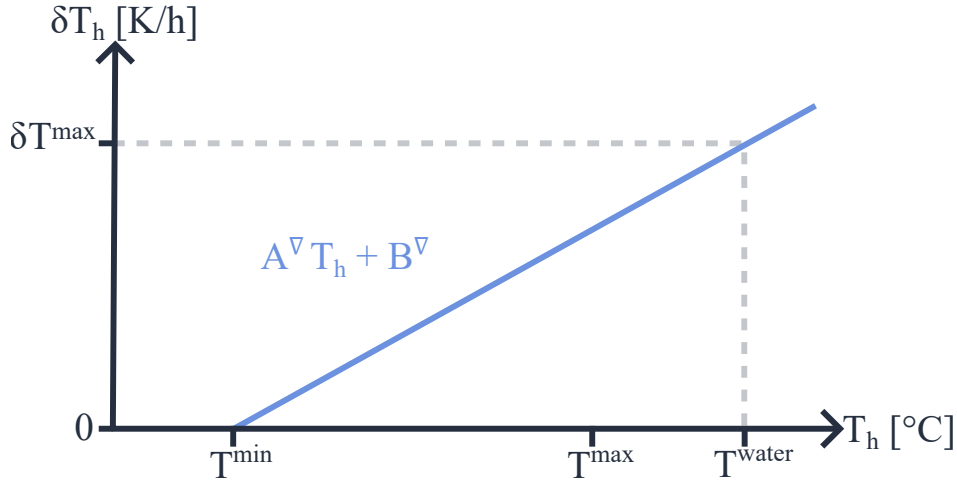$$-\delta T_h \leq A^\nabla T_h + B^\nabla, \tag{B.13}$$

as shown in Figure B.2

Figure B.2: Illustration of discharging constraint.

To find A^∇ and B^∇, Equation (B.13) is first evaluated at the minimum temperature. When the temperature is at the minimum operation temperature, the STES can not be discharged further:

$$A^\nabla T^{\text{min}} + B^\nabla = 0, \tag{B.14}$$

which solved for B^∇ yields

$$B^\nabla = -A^\nabla T^{\text{min}}. \tag{B.15}$$

To make the line limiting charging and discharging have the same slope, the other point on the line becomes $(T^{\text{water}}, \delta T^{\text{max}})$. Substituting this into the equation for the line gives

$$A^\nabla T^{\text{water}} + B^\nabla = \delta T^{\text{max}}. \tag{B.16}$$

Equation (B.15) is inserted into Equation (B.16), and solved for A^∇, yielding

$$A^\nabla = \frac{\delta T^{\text{max}}}{T^{\text{water}} - T^{\text{min}}} \tag{B.17}$$

By inserting Equation (B.12) into Equation (B.13) and multiplying by V, the final linear constraint becomes

$$\frac{\nabla_h}{\eta^\nabla c_v} \leq A^\nabla T_h V + B^\nabla V. \tag{B.18}$$

ADDITIONAL RESULTS FOR CASE 1 AND 2

C.1 Net grid import

Net grid import of case 1 and 2 in the 2030-sceanrio is shown in Figure C.1, with the corresponding case from the 2020-scenario in the background.
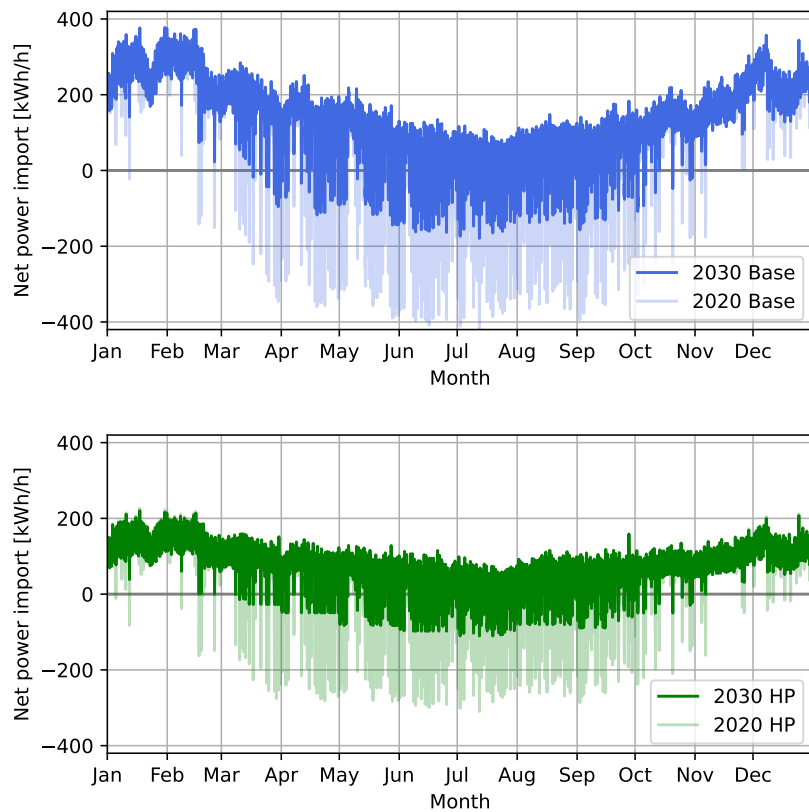

Figure C.1: Net power import of case 1 (top) and 2 (bottom) in the 2030-scenario, with the same profile from the 2020-scenario in the background.

Export has been considerably reduced because less PV has been installed in both cases. Peak import, on the other hand, has seen almost no changes compared to the 2020-scenario.

C.2   Additional line losses

The change in line total losses after adding the aggregated load profile from the optimization model to the CINELDI reference grid in case 1 and 2 for the 2030-scenario, are shown in Figure C.2.
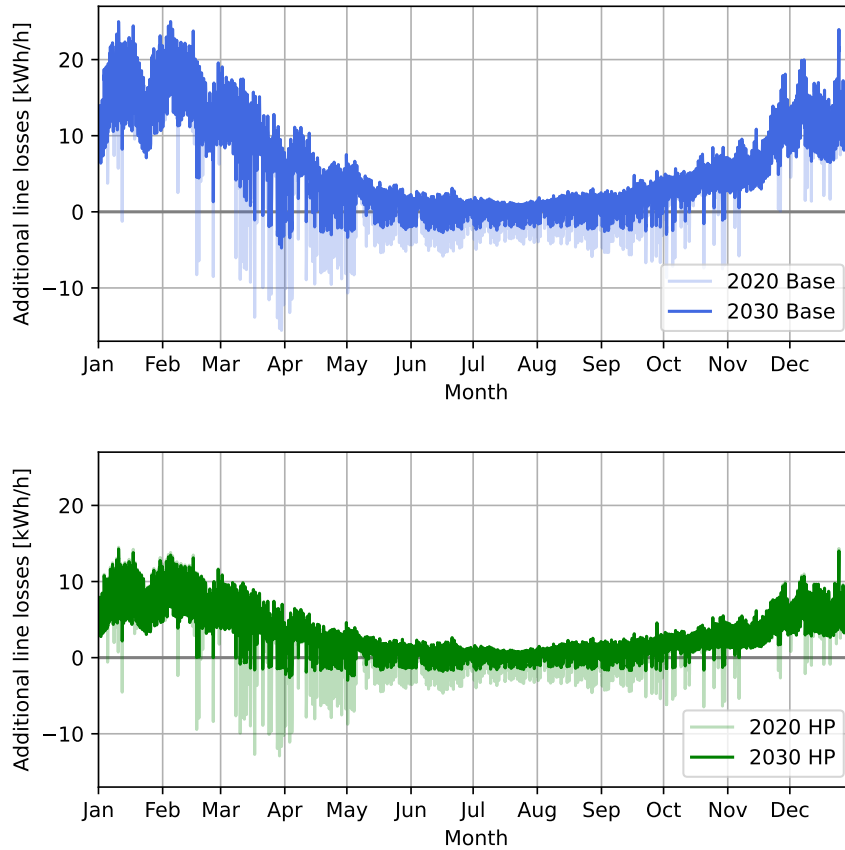

Figure C.2: Difference in total line losses each hour after adding the case 1 (top) and 2 (bottom) community in the 2030-scenario to the CINELDI reference grid. The corresponding profile from the 2020-scenario is in the background.

The corresponding change for the 2020-scenario is shown in the background, showing that the biggest change from the 2020-scenario is that line losses in March and April are reduced less in the 2030-scenario as a consequence of having less PV.

C.3   Space heating sources for case 2 in 2020 and 2023

Space heating sources for case 2 in the 2020-scenario and the 2030-scenario are shown in Figure C.3. The optimization model led to most of the household's installing a heat pump with high enough capacity to cover most of the thermal demand in both scenarios.
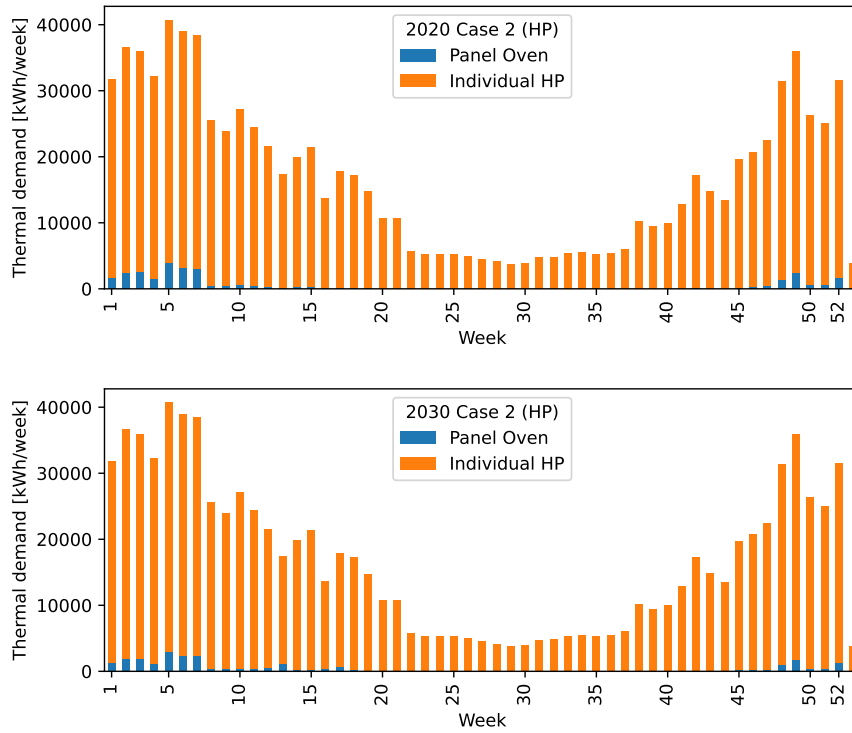

Figure C.3: Sources of thermal energy meeting the thermal energy demand each week for case 2 in the 2020-scenario (top) and 2030-scenario (bottom).

The space heating sources for case 1 are not shown, as case 1 has no options other than joule heating (panel ovens), which means all bars will be blue.

COMPREHENSIVE OVERVIEW OF COST TERMS

The cost of the individual cost terms of the optimization model's objective function are shown in Tables D.1 and D.2 for the 2020- and 2030-scenario, respectively.

Table D.1: Overview of the cost terms from the objective function of the optimization model for the 2020-scenario.

2020-scenario	Symbol	Case 1 (Base)	Case 2 (HP)	Case 3 (STES)
Electricity	C^{SP}	38318	18549	16789
Taxes	C^{T}	13435	7549	7084
Volume tariff	C^{V}	25548	13964	12749
Capacity tariff	C^{C}	23293	19589	16034
PV investment	C^{PV}	21507	15918	17542
HP investment	C^{HP}	0	10235	0
STES investment	C^{STES}	0	0	29970

Table D.2: Overview of the cost terms from the objective function of the optimization model for the 2030-scenario.

2030-scenario	Symbol	Case 1 (Base)	Case 2 (HP)	Case 3 (STES)
Electricity	C^{SP}	90682	49199	39591
Taxes	C^{T}	14232	8036	6557
Grid volume tariff	C^{V}	28566	16008	13155
Capacity grid tariff	C^{C}	27893	20764	19617
PV investment	C^{PV}	10725	7659	13535
HP investment	C^{HP}	0	10865	0
STES investment	C^{STES}	0	0	33844